FAKULTÄT FÜR INFORMATIK
Faculty of Informatics

# Real Time Processing and Synchronization in Hybrid Hippocampal Microcircuits

DIPLOMARBEIT

zur Erlangung des akademischen Grades

**Diplom-Ingenieur**

im Rahmen des Studiums

**Medizinische Informatik**

eingereicht von

**Markus Michael Hilscher, BSc.**
Matrikelnummer 0727932

an der
Fakultät für Informatik der Technischen Universität Wien

Betreuer: DDDr. Frank Rattay
Institut für Analysis und Scientific Computing, Technische Universität Wien
Co-Betreuer: Dr. Richardson Naves Leão
Neurodynamics Lab, Department of Neuroscience, Uppsala University

Wien, 03.09.2012

(Unterschrift Verfasser) (Unterschrift Betreuer)

Technische Universität Wien
A-1040 Wien ▪ Karlsplatz 13 ▪ Tel. +43-1-58801-0 ▪ www.tuwien.ac.at

Die approbierte gedruckte Originalversion dieser Diplomarbeit ist an der TU Wien Bibliothek verfügbar
The approved original version of this thesis is available in print at TU Wien Bibliothek.
TU Bibliothek Your knowledge hub WIEN

TU WIEN Bibliothek Your knowledge hub
Die approbierte gedruckte Originalversion dieser Diplomarbeit ist an der TU Wien Bibliothek verfügbar
The approved original version of this thesis is available in print at TU Wien Bibliothek.

# Erklärung zur Verfassung der Arbeit

Markus Michael Hilscher, BSc.
[redacted]

Hiermit erkläre ich, dass ich diese Arbeit selbständig verfasst habe, dass ich die verwendeten Quellen und Hilfsmittel vollständig angegeben habe und dass ich die Stellen der Arbeit - einschließlich Tabellen, Karten und Abbildungen -, die anderen Werken oder dem Internet im Wortlaut oder dem Sinn nach entnommen sind, auf jeden Fall unter Angabe der Quelle als Entlehnung kenntlich gemacht habe.

(Ort, Datum) (Unterschrift Verfasser)



Die approbierte gedruckte Originalversion dieser Diplomarbeit ist an der TU Wien Bibliothek verfügbar
The approved original version of this thesis is available in print at TU Wien Bibliothek.
TU Bibliothek Your knowledge hub WIEN

TU WIEN Bibliothek Your knowledge hub
Die approbierte gedruckte Originalversion dieser Diplomarbeit ist an der TU Wien Bibliothek verfügbar
The approved original version of this thesis is available in print at TU Wien Bibliothek.

# Acknowledgements

I would like to express my sincere gratitude to everyone who guided and supported me during my studies and especially during my diploma thesis.

First and foremost, I want to thank my supervisor Professor DDDr. Frank Rattay from the Vienna University of Technology, who I got to know at the very beginning of my studies and who supported me continuously during my diploma thesis with a lot of patience, motivation and enthusiasm. I met Professor Rattay as a very competent person, who I could discuss all my scientific and personal questions with. After I expressed my wish of going abroad for research and writing my diploma thesis, he arranged that I got an invitation from the University of Uppsala.

There I got to know Professor Dr. Richardson Naves Leão, who introduced me to scientific experiments and supervised my first research paper and this thesis. I got involved in exciting projects and state-of-the-art research. In addition to that he offered me to study in Brazil at the Federal University of Rio Grande do Norte. The time in Uppsala and in Natal was definitely life-changing and important for making the first steps in my starting career as a neuroscientist.

I also want to thank the International Office of the Vienna University of Technology for supporting me with a grant which made it easy for me to stay in Sweden.

Furthermore, I am happy that I made a lot of new international friends who helped me to feel welcome in their countries and who I can share interests in research with. We had a lot of exciting adventures and I will never forget all the fun we had together.

Finally, I want to thank my parents Silvia and Wilfried as well as my brother Bernhard who have an essential contribution to my academic success. They kept me always free of problems and took every pressure away to support me in my studies.



Die approbierte gedruckte Originalversion dieser Diplomarbeit ist an der TU Wien Bibliothek verfügbar
The approved original version of this thesis is available in print at TU Wien Bibliothek.
TU Bibliothek Your knowledge hub WIEN

TU WIEN Bibliothek Your knowledge hub
Die approbierte gedruckte Originalversion dieser Diplomarbeit ist an der TU Wien Bibliothek verfügbar
The approved original version of this thesis is available in print at TU Wien Bibliothek.

# Abstract

**Objectives:** Synchronization among neurons is thought to arise from the interplay between excitation and inhibition but the connectivity rules that contribute to synchronization are unknown. Neuronal networks are extremely complex, not only because of the huge amount of cells involved but also because of the variety of different actions contributing to network activities. We studied this problem by investigating hippocampal microcircuits in CA1 using the multi channel patch clamp technique and real-time computing.

**Methods:** The real-time system in combination with the patch clamp technique which is often referred to as *dynamic clamp*, allowed us to build hybrid neuronal networks containing both biological and artificial (modeled) cells. We were able to introduce the synaptic responses from other cells to patched neurons during network activity. By connecting a model interneuron with two pyramidal cells (PC), we were able to test the role of different connection rules in synchronizing pyramidal cell activity.

**Results:** Our experiments demonstrated that eliminating the feedback from PCs to the interneuron produced the greatest level of synchronization. We investigated several aspects of interneuron-PC-PC communication and studied the synchrony level of the two patched pyramidal cells by simulating different biological realistic hippocampal microcircuits. Moreover we investigated the role of intrinsic membrane mechanisms contributing to synchronization. Application of the hyperpolarization-activated cyclic-nucleotide (HCN) cation channel current (Ih) blocker ZD7288 dramatically impaired PC synchronization and altered the connection pattern that produced the largest synchronization index.

**Conclusion:** Our results shed light on how hippocampal microcircuits can synchronize and generate oscillatory activity. Additionally, we suggest how hippocampal neurons are connected and how these connections alter the way these circuits process information. We also demonstrate that changes in the conductance of HCN channels, by blocking them pharmacologically, can modulate hippocampal network synchronization.



Die approbierte gedruckte Originalversion dieser Diplomarbeit ist an der TU Wien Bibliothek verfügbar
The approved original version of this thesis is available in print at TU Wien Bibliothek.
TU Bibliothek Your knowledge hub WIEN

TU WIEN Bibliothek Your knowledge hub
Die approbierte gedruckte Originalversion dieser Diplomarbeit ist an der TU Wien Bibliothek verfügbar
The approved original version of this thesis is available in print at TU Wien Bibliothek.

# Kurzfassung

**Motivation:** Heutzutage wird vermutet, dass sowohl synaptische Erregung als auch Inhibierung zur Synchronisation zwischen Neuronen führt. Die zugrundeliegenden Mechanismen sind aber immer noch weitgehend unbekannt. Neuronale Netze sind äußerst komplex, nicht nur wegen der enormen Anzahl an Zellen, sondern auch wegen der Vielfalt der verschiedenen Netzwerkaktivitäten. Wir studierten dieses Problem indem wir neuronale Netze der CA1 Region des Hippocampus untersuchten und Multi-Channel-Patch-Clamp und Real-Time Methoden anwandten.

**Methoden:** Das Real-Time System in Kombination mit Patch-Clamp, das oft als *Dynamic-Clamp* bezeichnet wird, ermöglichte es uns hybride neuronale Netzwerke, bestehend aus biologischen und modellierten Zellen, aufzubauen. Wir konnten lebenden, gepatchten Neuronen synaptische Aktivitäten anderer Zellen während angehender Netzwerkaktivitäten zuführen. Durch das Verbinden eines Model-Interneurons mit zwei Pyramidenzellen, konnten wir die Auswirkungen von unterschiedlichen Verbindungsregeln auf die Synchronisation dieser Pyramidenzellen testen.

**Ergebnisse:** Unsere Experimente zeigten, dass die Eliminierung der Feedback-Verbindungen von Pyramidenzellen zum Interneuron die größte Synchronität hervorrufte. Durch die Simulation von verschiedenen biologischen neuronalen Netzen im Hippocampus konnten wir eine Vielzahl an Aspekten der Interneuron-Pyramidenzellen-Pyramidenzellen-Kommunikation untersuchen und die Synchronität der beiden gepatchten Pyramidenzellen studieren. Darüber hinaus untersuchten wir die Auswirkungen von spezifischen Membranmechanismen auf diese Synchronisation. Das Anwenden des hyperpolarization-activated cyclic-nucleotide cation (HCN) channel current (Ih) Blocker ZD7288 beeinträchtigte drastisch die Pyramidenzellen-Synchronisation und veränderte die Eigenschaften des neuronalen Netzes, das zum größten Synchronisationsindex führte.

**Fazit:** Unsere Ergebnisse erläutern, wie sich neuronale Netze im Hippocampus synchronisieren und Oszillationen erzeugen können. Darüber hinaus berichten wir, wie Neuronen im Hippocampus verbunden sind und wie diese Verbindungen Auswirkungen auf die Signalweiterleitung haben. Außerdem zeigen wir, dass Änderungen in der Leitfähigkeit der HCN-Kanäle die Synchronisation neuronaler Netze verändern können, wenn sie pharmakologisch geblockt werden.



Die approbierte gedruckte Originalversion dieser Diplomarbeit ist an der TU Wien Bibliothek verfügbar
The approved original version of this thesis is available in print at TU Wien Bibliothek.
TU Bibliothek Your knowledge hub WIEN

TU WIEN Bibliothek Your knowledge hub
Die approbierte gedruckte Originalversion dieser Diplomarbeit ist an der TU Wien Bibliothek verfügbar
The approved original version of this thesis is available in print at TU Wien Bibliothek.

# Contents

**Abstract** v

**1 Introduction** 1
- 1.1 Motivation . . . 1
- 1.2 Intention of the Approach . . . 2
- 1.3 Organizational and Ethical Issues . . . 4
- 1.4 Structure of this Thesis . . . 4

**2 From the Hippocampus to the Cell** 5
- 2.1 The Hippocampal Location . . . 5
- 2.2 The Anatomical Structure and Its Nomenclature . . . 6
- 2.3 The Principal Cell . . . 8
- 2.4 The Huge Variety of Interneurons . . . 10
- 2.5 Action Potentials - The Fingerprint of a Cell . . . 10
- 2.6 Excitatory and Inhibitory Postsynaptic Potentials . . . 13

**3 Hippocampal Activities** 15
- 3.1 The Agile Hippocampus . . . 15
- 3.2 Hippocampal Microcircuits . . . 16
- 3.3 Circuit Connectivity . . . 17
- 3.4 The Phenomenon of Synchronization . . . 18
- 3.5 Hybrid Neuronal Networks . . . 20

**4 The Real-Time System** 23
- 4.1 Fast - Faster - Real Time . . . 23
- 4.2 Control and Measurement Device Interface . . . 23
- 4.3 Real Time Application Interface . . . 24
- 4.4 Hardware . . . 25
- 4.5 Installation and Configuration . . . 26

**5 The Artificial Neuron** 31
- 5.1 Mathematical modeling . . . 31
- 5.2 Fast-spiking Interneuron . . . 31
- 5.3 Pyramidal Cell . . . 33



Die approbierte gedruckte Originalversion dieser Diplomarbeit ist an der TU Wien Bibliothek verfügbar
The approved original version of this thesis is available in print at TU Wien Bibliothek.
TU Bibliothek Your knowledge hub WIEN

**6 The Real-Time Neuron** **37**
6.1 Real-Time Implementation . . . . . 37
6.2 Performance . . . . . 40

**7 The Experimental Setup** **43**
7.1 Tissue Preparation . . . . . 43
7.2 Electrophysiological Recordings . . . . . 43
7.3 Data Analysis . . . . . 44

**8 Results** **47**
8.1 Synchronization in Hybrid Networks . . . . . 47
8.2 Synchronization Depends on the Network Connectivity . . . . . 48
8.3 Excitatory Connections Mobilize Neurons . . . . . 50
8.4 Feedback Connections in the Network . . . . . 50
8.5 Membrane Mechanisms of a Neuron . . . . . 52
8.6 The Effects of Ih . . . . . 52

**9 Discussion** **55**

**A Abbreviations** **59**

**B Source Code** **61**

**Bibliography** **79**



Die approbierte gedruckte Originalversion dieser Diplomarbeit ist an der TU Wien Bibliothek verfügbar
The approved original version of this thesis is available in print at TU Wien Bibliothek.
TU Bibliothek Your knowledge hub WIEN

# List of Tables

4.1 Required Software Packages . . . . . 26

# List of Figures

1.1 Experimental Setup . . . . . 3

2.1 Location of the Hippocampus . . . . . 6
2.2 Neuronal Circuit of the Hippocampus . . . . . 7
2.3 Layers of the Hippocampus . . . . . 8
2.4 Hippocampal Pyramidal Cell and Interneuron . . . . . 9
2.5 The Patch Clamp Technique . . . . . 11
2.6 The Action Potential . . . . . 12
2.7 Summation of Potentials . . . . . 14

3.1 Hippocampal Microcircuit . . . . . 16
3.2 Circuit Connectivity Patterns . . . . . 18
3.3 Neuronal Network Configurations . . . . . 21

4.1 Real Time Application Interface Components . . . . . 25

5.1 Fast-spiking Interneuron . . . . . 33
5.2 Synaptic Current of a Fast-spiking Interneuron . . . . . 34
5.3 Synaptic Current of a Fast-spiking Interneuron prepared for Real-time . . . . . 34
5.4 Hippocampal Pyramidal Cell . . . . . 35
5.5 Synaptic Current of a Pyramidal Cell prepared for Real-time . . . . . 35

6.1 Dynamic Clamp Operating Principle . . . . . 38
6.2 Performance of the Real-time System . . . . . 40



Die approbierte gedruckte Originalversion dieser Diplomarbeit ist an der TU Wien Bibliothek verfügbar
The approved original version of this thesis is available in print at TU Wien Bibliothek.
TU Bibliothek Your knowledge hub WIEN

6.3 Performance of the Improved Real-time System used for the Experiments . . . . . 41

7.1 Synchrony Index . . . . . 45

8.1 Synchronization in Neuronal Networks . . . . . 49
8.2 Various Neuronal Networks . . . . . 51
8.3 ZD7288 Disrupts Synchronization in Neuronal Networks . . . . . 53

Die approbierte gedruckte Originalversion dieser Diplomarbeit ist an der TU Wien Bibliothek verfügbar
The approved original version of this thesis is available in print at TU Wien Bibliothek.

Die approbierte gedruckte Originalversion dieser Diplomarbeit ist an der TU Wien Bibliothek verfügbar
The approved original version of this thesis is available in print at TU Wien Bibliothek.

CHAPTER 1

# Introduction

## 1.1 Motivation

The hippocampus is a seahorse-shaped brain structure of both humans and other vertebrates, located in the medial temporal lobe, bilaterally. It plays a crucial role in the formation of long-term memory and spatial navigation. Nowadays it is known that dysfunctions of the hippocampus are associated with memory disorders, Alzheimer's disease, schizophrenia or even epilepsy. However, little is known about which functions of the hippocampal cells are affected by these diseases and how they can be influenced in order to achieve healing. Looking at specific networks, so-called microcircuits, and their connectivities can help us to understand the mechanisms underlying neuronal activities such as synchronization and oscillations, which are important brain phenomena. In this study we want to gain insight into the complex connectivity patterns in the hippocampus and in consequence understand how they contribute to brain activities.

Human brains oscillate during sleep, exploration, learning and also when we remember events in our surroundings. These rhythmic activities in the brain are well described and named after the frequency band in which they oscillate, such as theta, gamma or ripple oscillations [ Fisahn et al., (2005) ]. Theta oscillations (4 - 12 $Hz$) have been related to exploratory behavior, rapid eye movement sleep (REM sleep) and cognitive functions such as attention, memory and learning [ Bland and Oddie, (2001) ]. They are regular rhythmic activities and can be observed in several species [ Mehta, (2005) ]. Gamma oscillations (slow gamma: 30 - 60 $Hz$, fast gamma: 60 - 100 $Hz$) which can also be observed in vitro [ Fisahn et al., (1998) ], are assumed to be the pacemaker for temporal encoding. They have been related to the transformation of sensory inputs into coherent information and to memory [ Fries et al., (2007) ]. Finally, ripple oscillations (100 - 200 $Hz$) are fast oscillatory patterns which have been associated to the process leading to memory storage, related to the migration from the hippocampus to the neocortex [ Buzsáki, (1989) ]. Other observed brain rhythms are delta oscillations (1 - 4 $Hz$), beta oscillations (12 - 30 $Hz$), alpha oscillations (9 - 11 $Hz$) and spindling (11 - 15 $Hz$).

All of these rhythmic phenomena suggest an indication that neuronal rhythms are able to shape communication in multi-scale brain networks. Nevertheless, our knowledge about the contribution of different cell populations to brain rhythms and neuronal information processing is sparse.

A common approach for studying brain activities is by recording the activities of single neurons. A typical neuron in rest has a transmembrane voltage (called membrane potential in the following) of approximately -60 $mV$ which rapidly raises to approximately +40 $mV$ when it gets stimulated and quickly returns to approximately -60 $mV$ after complex ion channel mechanisms took place. This type of cell activity following a specific trajectory is meant when physiologists talk about *cell firing* and *action potentials*. Studying temporal coding, which relies on the precise timing of neuronal action potentials, as well as rate coding, considering their frequency, are common ways to investigate neuronal information signaling. For example, it is believed that large-scale oscillations are generated by a group of interacting neurons which become synchronized. Studies show that these oscillatory activities generally arise from feedback connections and subsequently synchronous firing between their neurons [ Kopell et al., (2000) ]. However, the mechanisms behind neuronal synchronization are still not completely known, since there are numerous different activities involved. Neuronal synchronization may be achieved through direct synaptic coupling between cells or through inputs from a common presynaptic pacemaking cell or whole cell assemblies. [ Hansel et al., (1995) ][ Tort et al., (2007) ]

## 1.2 Intention of the Approach

There are several in vitro preparations that permit the study of neuronal activities in the hippocampus. Mouse brain tissue, for example, can be dissected out and gently sliced into thin sections that, under the right conditions, can survive up to six hours under the microscope. Moreover, they are able to maintain several aspects of network activity that are observed in the brain [ Fisahn et al., (2005) ]. One of the most common electrophysiological techniques is known as *patch clamp*. It permits the study of single cell activities by contacting the cell's membrane with a micropipette and offers very stable recordings of their electrical properties.

Using real-time programming and data acquisition (DAQ) such as Linux RTAI[1] combined with patch clamp and intracellular recordings, we are able to introduce to specific neurons the synaptic response from other cells during network activity. Selected living cells are touched with an electrode and their membrane potentials are amplified and fed into a real-time computer. The computer contains equations for synaptic conductances or more advanced a model of a specific neuron and simulates synaptic currents, which are inserted in the living cells again. Such a system is called *dynamic clamp*. It gives us the possibility of building hybrid neuronal networks by connecting biological and modeled cells. Moreover, it allows us to resolve important issues concerning the contribution of different cell types to network activities. We are able to study different network configurations and show their effects on network synchronization. [ Sharp et al., (1993a) ][ Sharp et al., (1993b) ][ Dorval et al., (2001) ]

[1] http://www.rtai.org



Die approbierte gedruckte Originalversion dieser Diplomarbeit ist an der TU Wien Bibliothek verfügbar
The approved original version of this thesis is available in print at TU Wien Bibliothek.
TU Bibliothek Your knowledge hub WIEN

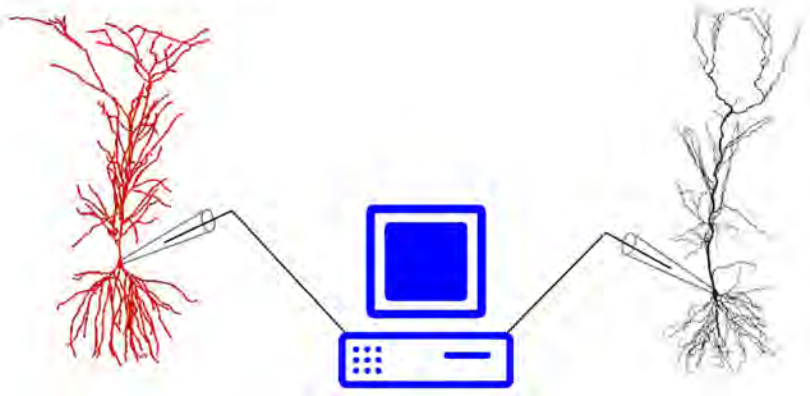


**Figure 1.1:** Experimental setup of the hybrid network. Two living hippocampal pyramidal cells are patched and connected to an interneuron which is simulated on a computer. Reconstructions of pyramidal cells are taken from [ Spruston, (2008) ] and [ Cutsuridis et al., (2010) ].

In our particular case, two pyramidal cells (PC), which are the main excitatory cells in the hippocampus, are contacted (*patched*) with two different microelectrodes. Their membrane potentials are measured, amplified and fed through a DAQ card into the dynamic clamp computer. The computer simulates a fast-spiking interneuron, another type of neuron in the hippocampus which is believed to strongly influence the firing properties of pyramidal cells. This artificial interneuron is described through differential equations and computed in real-time (see chapters 5 and 6). It receives synaptic inputs from the patched cells and outputs its own synaptic currents, which in turn are applied to the living cells in order to build a hybrid neuronal network. Thus, the hybrid neuronal network consists of three main communicating players, two living excitatory cells and one modeled inhibitory interneuron. To understand the dynamic mechanisms in a functional neuronal network consisting of defined populations, one has to understand the involved cells and their synaptic properties. Hybrid neuronal networks are designed to investigate particular functions by looking at specific neurons rather than all cells present in this region, which is not affordable by now. Therefore, this approach does not cover the locally distributed representation of information present in a neuronal network, but acquires neuronal signals directly from cells at a high spatial and especially temporal resolution (see chapter 3).

By testing various network configurations (i.e. connectivity patterns), we study how the two patched pyramidal cells are affected by several different inputs from the model interneuron. Also firing frequencies of the artificial cell are varied and studied in order to understand the role of interneurons in pyramidal cell synchronization. This approach helps us to explore the importance of local pacemakers to the global rhythm of brain networks, as well as the importance of excitation, inhibition and intrinsic currents. Furthermore, we determine the role of intrinsic membrane mechanisms contributing to synchronization by concentrating our investigations on a specific ion channel, the so-called hyperpolarization-activated cyclic-nucleotide (HCN) cation



Die approbierte gedruckte Originalversion dieser Diplomarbeit ist an der TU Wien Bibliothek verfügbar
The approved original version of this thesis is available in print at TU Wien Bibliothek.

channel. Its current, the HCN channel current (Ih) is often referred to as a pacemaker current due to its role in pacing rhythms of neuronal networks. Therefore, pharmacological manipulation with the Ih channel blocker ZD7288 (10 $\mu m$) is performed to study the role of HCN channels on the synchronization of neuronal activity.

The challenge which must be overcome by our real-time approach is that the procedure of measuring the membrane potential, calculating the equations and injecting the current, needs to be completed faster than the fastest dynamic process in the system. Besides adequate hardware (including real-time Linux, fast high definition DAQ and differential amplifier), efficient modeling techniques and mathematical methods for the simulation of the artificial neuron are needed. We use Hodgkin–Huxley (HH) type models [ Hodgkin and Huxley, (1952) ] to describe the biophysical characteristics of cell membranes and their dynamical behaviors. These models consist of nonlinear ordinary differential equations which approximate the electrical characteristics of neurons and are suitable for our approach.

## 1.3 Organizational and Ethical Issues

This diploma thesis results from a cooperation between the Institute for Analysis and Scientific Computing, Vienna University of Technology, Vienna, Austria and the Neurodynamics Lab, Department of Neuroscience, Uppsala University, Uppsala, Sweden. It covers both computational neuroscience aspects including mathematical modeling of neurons as well as electrophysiological recordings of hippocampal slices of mice. All animal experiments have been approved by Swedish Animal Welfare authorities and follow Uppsala University guidelines for the care and usage of laboratory animals.

## 1.4 Structure of this Thesis

The chapters of this diploma thesis are organized as follows. Chapter 2 gives an introduction to the hippocampus by explaining anatomical and physiological properties. Chapter 3 describes hippocampal activities and how to study them by investigating specific microcircuits. Chapter 4 contains the preliminaries for this work including required software, hardware and computational aspects for building hybrid neuronal networks. Chapter 5 describes the used models including simulations whereas chapter 6 contains the description and implementation for the real-time system. The remaining chapters 7, 8 and 9 present methods, results and a discussion.



Die approbierte gedruckte Originalversion dieser Diplomarbeit ist an der TU Wien Bibliothek verfügbar
The approved original version of this thesis is available in print at TU Wien Bibliothek.
TU Bibliothek Your knowledge hub WIEN

CHAPTER 2

# From the Hippocampus to the Cell

This chapter introduces the hippocampus, its anatomical location and the microcircuitry of this important component of humans and other vertebrates which is often called the brains "memory card". This chapter also presents the main pathways of the hippocampus and describes the different layers, in which it is organized. Furthermore, it informs about the various cell types in the hippocampus and explains the generation of action potentials as well as postsynaptic mechanisms.

## 2.1 The Hippocampal Location

The hippocampus is a bilateral structure, part of the forebrain and located under the medial temporal lobe in human brains. It plays an essential role in the formation of long-term memory and spatial navigation and has a significant influence on cognition as well as diseases, such as Alzheimer's disease, schizophrenia or epilepsy. This nucleus is also present in other vertebrates, which makes it possible to study hippocampal activities on animal models. Most studies of the hippocampus are done in rodents, such as mice and rats, which are the most commonly used ones in neuroscience. It is important to know that the brains of all mammals have basically the same anatomical parts, types of cells and neuronal pathways as human brains. Most of the various brain nuclei found in mice can also be identified in human brains. However, the size and sometimes the location of nuclei varies between mice and humans, which requires deep anatomical studies in order to avoid uncertainty when dealing with animal models. Figure 2.1 A shows a comparison of a human brain and a mouse brain where the main anatomical regions are similar. Figure 2.1 B illustrates coronal sections with stained cells of brains of the both species. Despite the different size and the location, it is notably that the arrangement of the mouse hippocampus is inverted compared to the human hippocampus. Nevertheless, the basic regions of the hippocampus and its cells remain the same.



Die approbierte gedruckte Originalversion dieser Diplomarbeit ist an der TU Wien Bibliothek verfügbar
The approved original version of this thesis is available in print at TU Wien Bibliothek.
TU Bibliothek Your knowledge hub WIEN

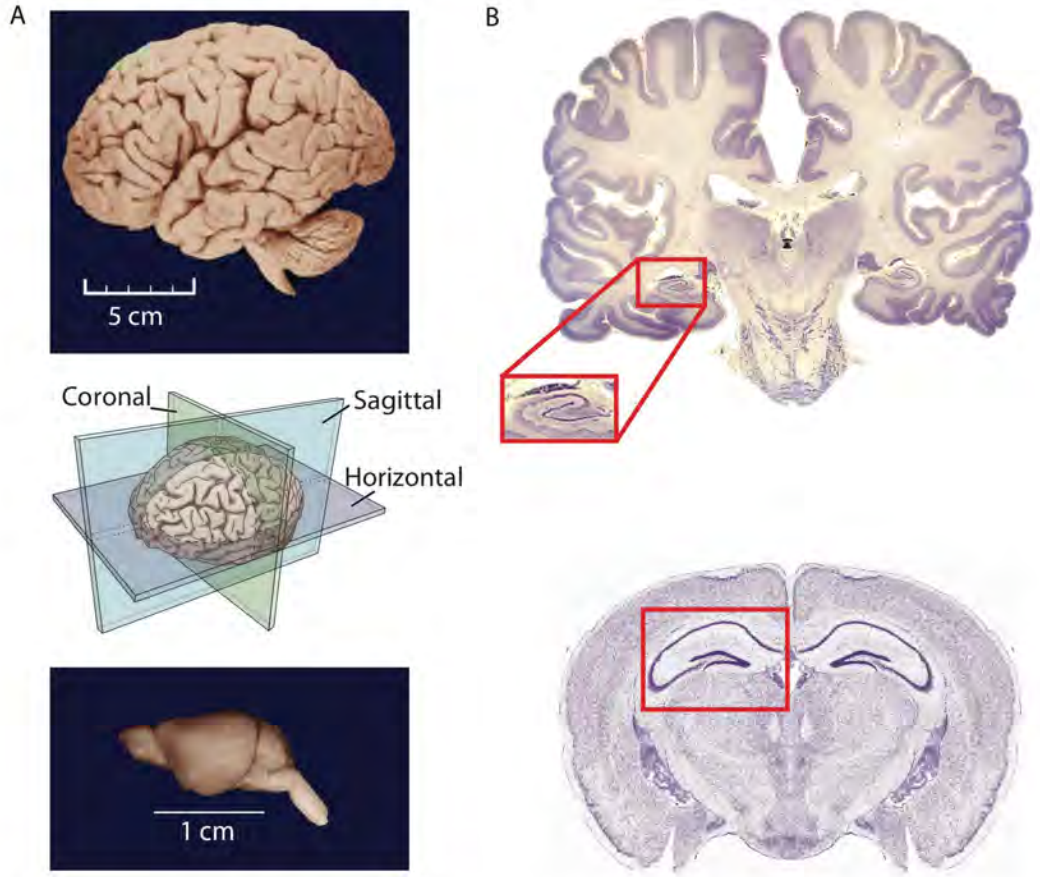



**Figure 2.1:** Location of the hippocampus in brains of humans and mice. A: The top panel shows the side view of a human brain (homo sapiens), the bottom panel the side view of a mouse brain (Mus musculus). The middle panel shows the major planes of section for brains. B: The top panel includes a coronal section of the human brain and denotes the location of the hippocampus, which is enlarged in the red rectangle. The bottom panel shows a coronal section of the mouse brain. Note that the arrangement of the mouse hippocampus is inverted compared to the human hippocampus. [ Purves et al., (2004) ][ Comparative Mammalian Brain Collections ][ Allen Institute for Brain Science ]

## 2.2 The Anatomical Structure and Its Nomenclature

The hippocampal formation consists of the main structures dentate gyrus (DG), subiculum (Sub), presubiculum, parasubiculum and cornu ammonis (CA), whose subdivisions are called CA1 to CA4. There is some debate whether CA4 is an own region or belongs to the DG. Also for CA2 it is difficult to define its borders, hence it is very little studied. However, the most functionally relevant regions are CA1 and CA3, which contain excitatory pyramidal cells and various



Die approbierte gedruckte Originalversion dieser Diplomarbeit ist an der TU Wien Bibliothek verfügbar
The approved original version of this thesis is available in print at TU Wien Bibliothek.
TU Bibliothek Your knowledge hub WIEN

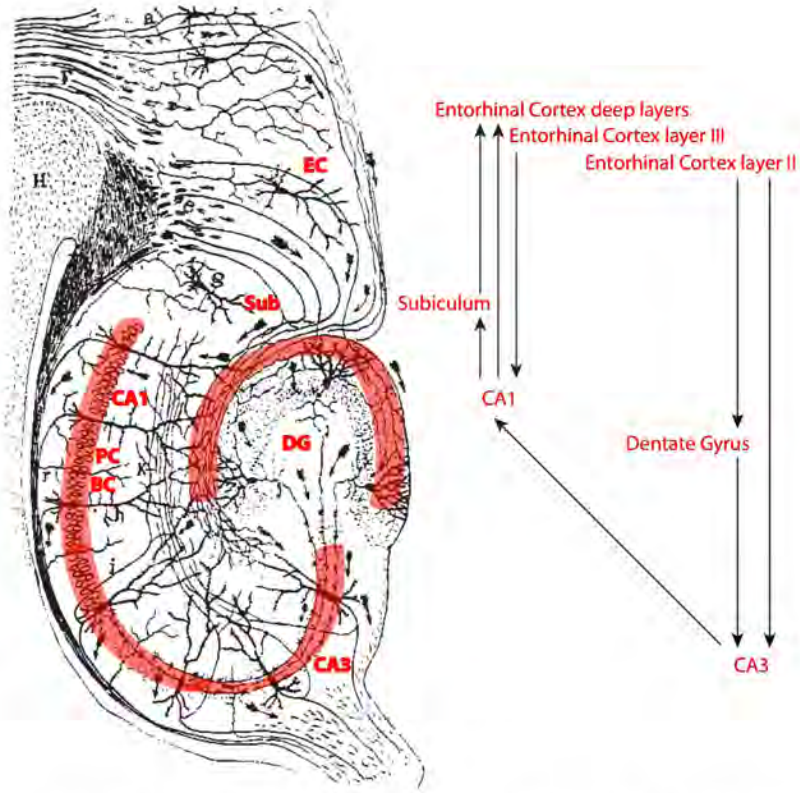



**Figure 2.2:** Neuronal circuit of the hippocampus. The left panel shows a modified drawing of the neuronal circuit of the rodent hippocampus, from Santiago Ramón y Cajal, Histologie du Systeme Nerveux de l'Homme et des Vertebres (Maloine, Paris, 1911), chap. II. Abbreviations: DG - dentate gyrus, Sub - subiculum, EC - entorhinal cortex [ Marín-Padilla M., (1998) ]. The right panel shows a schematic drawing of the main pathways in the hippocampal formation.

types of inhibitory interneurons [ Freund and Buzsáki, (1996) ][ Somogyi and Klausberger, (2005) ][ Klausberger and Somogyi, (2008) ]. As Fig. 2.2 demonstrates, the dentate gyrus receives excitatory inputs from the entorhinal cortex, another brain region, and activates pyramidal cells in the CA3 region. From CA3, via the so-called Schaffer collaterals, CA1 pyramidal cells are activated which in turn project to the subiculum and back to the entorhinal cortex. [ Andersen et al., (2006) ][ Axmacher et al., (2006) ]

The CA regions are further structured depth-wise in clearly defined layers in which the cells are tightly aligned and their cell bodies form *strata* (see Fig. 2.3).

- Alveus (alv.), which is the deepest layer of the hippocampus,
- Stratum oriens (ori.),



Die approbierte gedruckte Originalversion dieser Diplomarbeit ist an der TU Wien Bibliothek verfügbar
The approved original version of this thesis is available in print at TU Wien Bibliothek.
TU Bibliothek Your knowledge hub WIEN

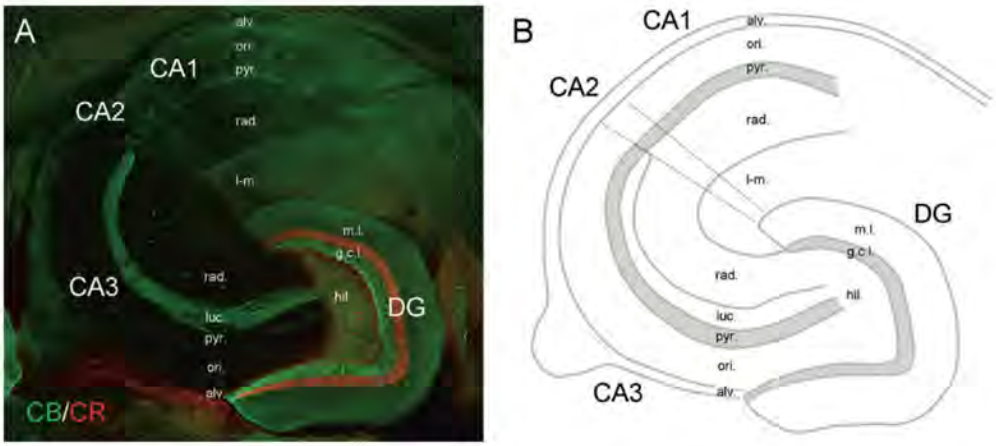



**Figure 2.3:** Layers of the hippocampus. A: Section of the hippocampus of a mouse immunostained for the calcium-binding proteins calbindin (CB, green) and calretinin (CR, red). The CA1 area shows the labeling of pyramidal cell bodies. B: Schematic drawing of the areas and layers of the hippocampus. Abbreviations: alv. - alveus, ori. - stratum oriens, pyr. - stratum pyramidale, rad. - stratum radiatum, l-m. - stratum lacunosum-moleculare, g.c.l. - granule cell layer of the dentate gyrus. The borders between the CA areas are indicated by dashed lines [ Cutsuridis et al., (2010) ].

- Stratum pyramidale (pyr.),
- Stratum lucidum (luc.),
- Stratum radiatum (rad.),
- Stratum lacunosum-moleculare (l-m.) and
- Hilus (hil.), which separates the CA region from the dentate gyrus.

## 2.3 The Principal Cell

One can easily imagine that the hippocampus consists of a multitude of different cell types. Among the different neuronal types in the hippocampus, one can distinguish two main types: excitatory and inhibitory cells. The first type of neurons usually releases the neurotransmitter glutamate for sending signals to other cells across synapses and increases the membrane potential of postsynaptic cells, whereas the latter decreases the postsynaptic membrane potential by releasing the neurotransmitter gamma-aminobutyric acid (GABA). Principal cells of the hippocampus are primarily excitatory and their cell bodies are aligned in well-defined layers. The principal cells of the CA regions are called pyramidal cells.



Die approbierte gedruckte Originalversion dieser Diplomarbeit ist an der TU Wien Bibliothek verfügbar
The approved original version of this thesis is available in print at TU Wien Bibliothek.
TU Bibliothek Your knowledge hub WIEN

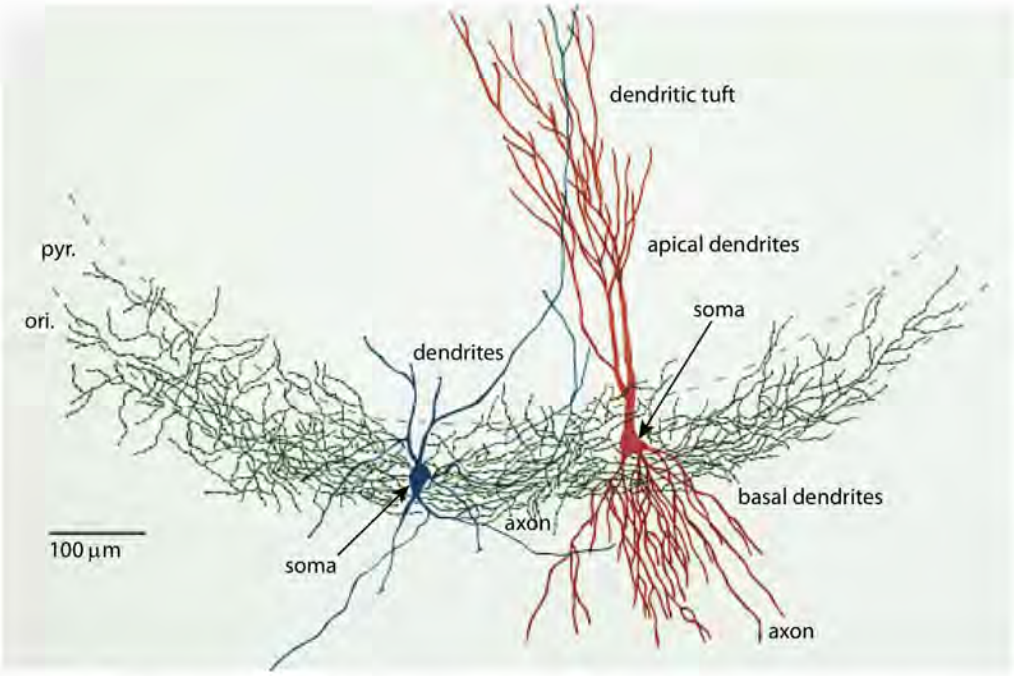



**Figure 2.4:** Reconstruction of a hippocampal pyramidal cell (red) and an interneuron (blue). The soma of the pyramidal cell is located in the stratum pyramidale and its dendrites show long projections to other layers. The soma of the basket cell is also located in the stratum pyramidale, its dendrites are oriented radially to the cell body. Abbreviations: ori. - stratum oriens, pyr. - stratum pyramidale [ Miles et al., (1996) ].

**Pyramidal cells** (Fig. 2.4, shown in red) are typically excitatory and use glutamate as their main neurotransmitter. They usually have a triangular shaped cell body (*soma*), large apical dendrites, several basal dendrites, dendritic spines and are situated in the pyramidal cell layer (stratum pyramidale) of the hippocampus. The apical dendrites, which emerge from the apex of the pyramidal cell soma, typically end in the stratum radiatum and form a dendritic tuft in the stratum lacunosum-moleculare. The basal dendrites arise from the base of the cell body and their branches reach up to the alveus. The dendritic spines are small membranous protrusions and serve as postsynaptic targets for glutamatergic terminals. Their large number on PCs indicates a high amount of excitatory synaptic inputs to these cells. The somata of PCs are usually free of excitatory synapses but receive many inhibitory inputs, which come from another type of synapses. The axon of PCs typically originates from the base of the soma and reaches the alveus where it gives inputs to the subiculum and the entorhinal cortex. Also axon collaterals are present, which provide the main excitatory input to interneurons, a second important cell type in the hippocampus. The collaterals form synapses to neighboring PCs, although this type of connectivity in the CA1 is very rare. [ Deuchars and Thomson, (1996) ][ Megías et al., (2001) ]



Die approbierte gedruckte Originalversion dieser Diplomarbeit ist an der TU Wien Bibliothek verfügbar
The approved original version of this thesis is available in print at TU Wien Bibliothek.
TU Bibliothek Your knowledge hub WIEN

## 2.4 The Huge Variety of Interneurons

Interneurons have an extensive local axonal arborization and are usually inhibitory, i.e. they use GABA or glycine as their main neurotransmitters. Interneurons can form synapses to both principal cells and other interneurons. There is still some controversy regarding the terminology and identification of the different types of interneurons. Nowadays two main classes can be distinguished, namely interneurons forming synapses to the soma and proximal dendrites (perisomatic inhibitory cells) or to the distal dendrites (dendritic inhibitory cells) of other cells. There is a huge diversity of interneuron types, reaching the number of at least 16 by now. [ Klausberger and Somogyi, (2008) ][ Sik et al., (1995) ][ Hájos et al., (2004) ][ Oren and Kullmann, (2012) ] The following are the most studied ones:

**Basket cells** (BC, Fig. 2.4, shown in blue) are inhibitory GABAergic interneurons which target the cell bodies and proximal dendrites of pyramidal cells as well as other neurons. Therefore, BCs belong to the group of perisomatic inhibitory interneurons. BCs of the hippocampus are usually strongly interconnected by mutual inhibitory synapses. Furthermore, they are fast-spiking and most of them express the calcium-binding protein parvalbumin. Cell bodies of parvalbumin positive BCs are usually located in the stratum pyramidale or the stratum oriens, but can also be found in the stratum radiatum. The dendrites of basket cells are typically radially orientated and reach various layers whereas the axons are mainly found in the cell body layer.

Other perisomatic interneurons are cholecystokinin expressing basket cells and so-called axo-axonic cells which innervate principal cells on their axon initial segments, a part of the axon in the vicinity of the soma where spikes are initiated because of a high sodium channel density.

**Oriens lacunosum-moleculare** (O-LM) cells are dendritic inhibitory interneurons and got their name because of their anatomical structure. O-LM cells develop their dendritic tree in the stratum oriens and have axonal projections into the stratum lacunosum-moleculare. In contrast to other interneurons, O-LM cells have a lot of long and thin spines on their dendrites. Interneurons with similar structure and properties but different locations are the pyramidale lacunosum-moleculare (P-LM) cells, with their somata in the stratum pyramidale and the radiatum lacunosum-moleculare (R-LM) cells, with their somata in the stratum radiatum respectively.

Other dendritic inhibitory interneurons are bistratified cells, ivy interneurons and interneuron-selective cells. [ Cutsuridis et al., (2010) ]

## 2.5 Action Potentials - The Fingerprint of a Cell

Neurons generate electrical signals to transmit information. The most common way to measure these signals is to use an intracellular microelectrode. A patch clamp microelectrode is glass pipette with a relatively big tip diameter, in order to pull a small piece of the cell's membrane by gentle suction into the pipette, which allows us to study the electrical activity of the patched neuron. This leads to the formation of a high resistance seal (*gigaseal*) between the glass tip



Die approbierte gedruckte Originalversion dieser Diplomarbeit ist an der TU Wien Bibliothek verfügbar
The approved original version of this thesis is available in print at TU Wien Bibliothek.
TU Bibliothek Your knowledge hub WIEN

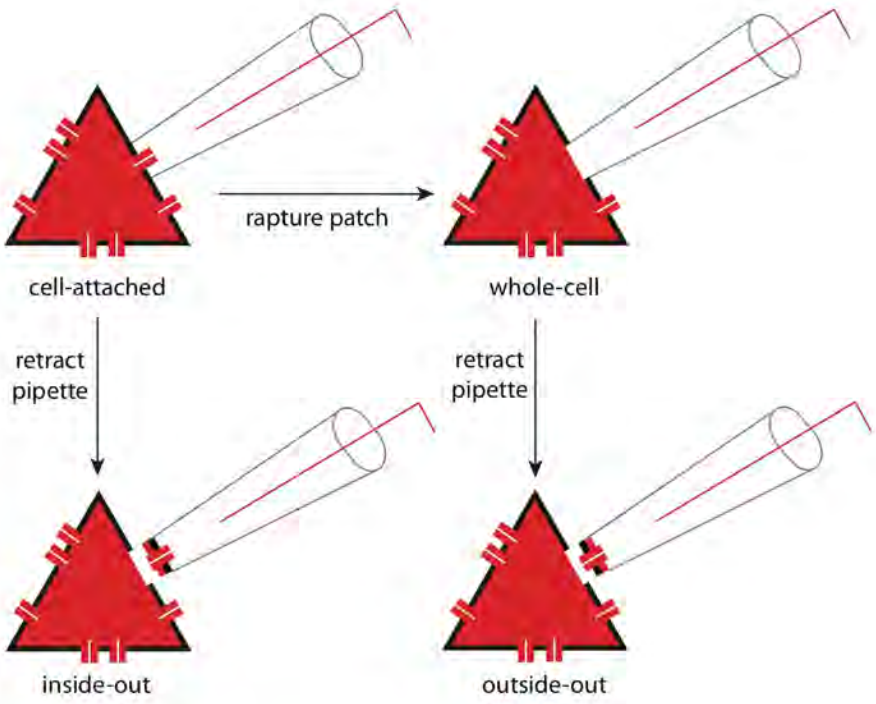



**Figure 2.5:** Different modes of patch clamp. A cell-attached patch is a simple form of patch clamp, where the cell is contacted with a micropipette. Retracting the pipette yields to an inside-out patch, having the intracellular side of the membrane exposed to the extracellular medium. A whole-cell patch is performed, if the glass pipette stays sealed with the cell and the cell's membrane is ruptured by a gentle suction. Retracting the pipette leads to an outside-out patch, where the outside of the cell's membrane is exposed to the extracellular medium.

and the cell membrane. Such a *patch* is called *cell-attached*. An *inside-out patch* is performed if the electrode is quickly retracted from the cell, causing the intracellular side of membrane facing outward from the micropipette. On the other hand, leaving the pipette sealed to the rest of the cell, a *whole-cell patch* can be achieved by rupturing the cell's membrane through a gentle suction and accessing its intracellular medium. Using antibiotic molecules in the electrode solution instead of a suction to rupture the cell's membrane, a *perforated patch* is made. Finally, an *outside-out patch* is performed, if the electrode is slowly withdrawn from the cell and the outside of the membrane is exposed to the extracellular medium. Figure 2.5 summarizes the different patch clamp configurations. We use the whole-cell patch technique, which allows stable single cell recordings of neurons.

Patching the cell, a negative potential is usually measured. This potential is called *resting membrane potential* and varies between different neurons. It is typically between -40 $mV$ and -90 $mV$ and represents the voltage between the inside and the outside of a cell in rest. If the cell



Die approbierte gedruckte Originalversion dieser Diplomarbeit ist an der TU Wien Bibliothek verfügbar
The approved original version of this thesis is available in print at TU Wien Bibliothek.
TU Bibliothek Your knowledge hub WIEN

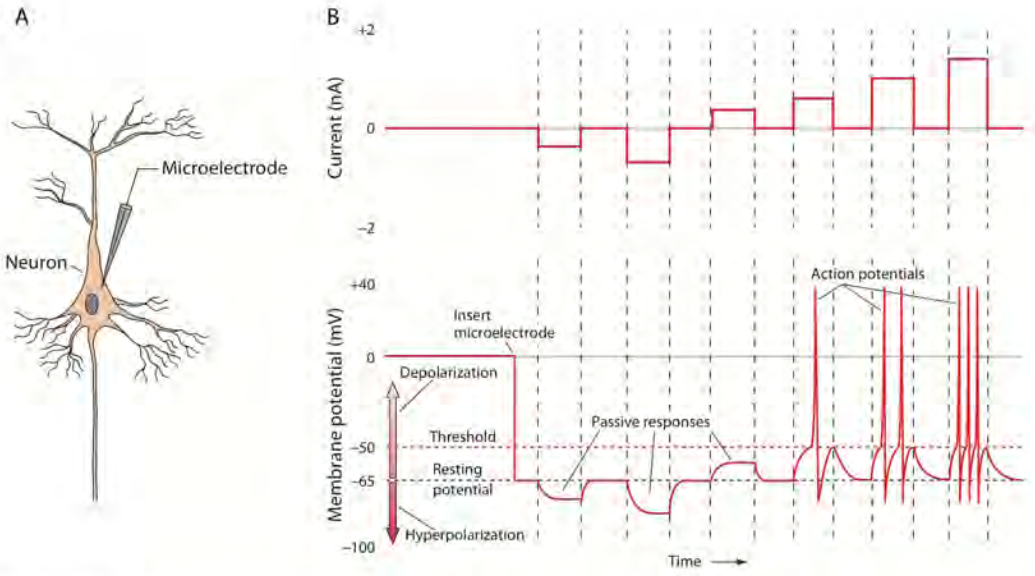



**Figure 2.6:** Electrical responses of a neuron. A: Schematic representation of a patched neuron in the soma. B: Current and voltage traces when measuring a cell's activity. Inserting the microelectrode into the cell shows the cell's resting membrane potential. Injecting hyperpolarizing currents into the neuron causes passive changes in the membrane potential whereas injecting depolarizing currents, which are able to lift the membrane potential over the cell's threshold potential, generate action potentials. The figure is taken and modified from [ Purves et al., (2004) ].

receives an appropriate stimulus, it changes its resting transmembrane voltage and generates an electrical signal. This stimulus can be applied artificially through the electrode or can be achieved by the input of other neurons through *synaptic potentials*. These signals, which activate receptors in synapses, are involved in the transmission of information between neurons. If a neuron wants to send information to another neuron, it sends an electrical signal via its axon. Axons are typically quite long, hence they are quite bad electrical conductors for transferring signals. To overcome this drawback, neurons have a mechanism, which allows them to conduct electrical signals over long distances, despite their poor electrical properties. This mechanism for sending electrical signals produces *action potentials*, which are also referred to as *spikes*.

To initiate such an action potential (AP), one can use the electrode and inject a certain current. A negative current *hyperpolarizes* the cell, which means that its membrane potential becomes more negative. Turing off the current injection, the cell usually stabilizes and goes back to its resting membrane potential. On the other hand, injecting a current which makes the neuron more positive than the resting membrane potential is called *depolarization*. If the increasing membrane potential reaches a certain *threshold*, an AP occurs.



Die approbierte gedruckte Originalversion dieser Diplomarbeit ist an der TU Wien Bibliothek verfügbar
The approved original version of this thesis is available in print at TU Wien Bibliothek.

The AP is a quick change from a negative (approximately -60 $mV$) to a positive (approximately + 40 $mV$) membrane potential and has typical characteristics for specific cells. It does not change its amplitude if larger currents are applied and follows the so-called *all-or-none principle*, i.e. it either occurs if the stimulation is high enough or it does not occur if the stimulation is too low. Higher current amplitude of the stimulus leads to higher spiking frequency of the neuron as seen in Fig. 2.6. However, one should know that, besides all the electrical mechanisms involved in the generation of APs, there are also chemical processes taking place, i.e. multiple activities of channels, that permit the flow of different ions with different charges, leading to differences in the membrane voltage. [ Purves et al., (2004) ]

## 2.6 Excitatory and Inhibitory Postsynaptic Potentials

Neuronal networks consist of various cells and cell types, which are connected to each other by synapses and signal information between one another. The sending neuron is the presynaptic cell, whereas the receiving neuron is called postsynaptic cell. Transmitting information between cells is done by synapses where positively or negatively charged ions flow into the postsynaptic cell. This causes *postsynaptic potentials*. Excitatory postsynaptic potentials (EPSP) increase the probability of postsynaptic APs, while inhibitory postsynaptic potentials (IPSP) decrease their probability. The flow of ions that causes an EPSP or an IPSP is an excitatory postsynaptic current (EPSC) or an inhibitory postsynaptic current (IPSC) respectively.

Both EPSPs and IPSPs arise from the binding of neurotransmitters to specific receptors on the postsynaptic neuron and open or close their ion channels. Most neurons receive both excitatory and inhibitory inputs. The differences between EPSPs and IPSPs are because of their different types of channels and their reversal potentials. The reversal potential is the membrane potential at which a given neurotransmitter causes no flow of ions through the ionic channels of that specific neurotransmitter receptor. An EPSP has a reversal potential more positive than the AP threshold in order to depolarize the cell above the threshold and cause the cell to spike. On the other hand, an IPSP has a reversal potential more negative than the threshold in order to prevent the cell from spiking.

EPSPs and IPSPs are usually very small and single postsynaptic potentials are not able to dramatically change a cell's membrane potential. Therefore, a multitude of synaptic inputs is needed to initiate an AP. Figure 2.7 shows a simplified construction of a neuron receiving two excitatory inputs and one inhibitory input. Neither the first nor the second EPSP alone is able to reach the cell's threshold potential. Only if both EPSPs occur at about the same time, they sum together and depolarize the cell strongly enough to result in an AP. In the same way, an IPSP can sum with an EPSP and can reduce its amplitude in order to prevent the production of an AP. To summarize, if the sum of all EPSPs and IPSPs together sufficiently depolarizes the neuron above its threshold, an AP is generated [ Purves et al., (2004) ].



Die approbierte gedruckte Originalversion dieser Diplomarbeit ist an der TU Wien Bibliothek verfügbar
The approved original version of this thesis is available in print at TU Wien Bibliothek.
TU Bibliothek Your knowledge hub WIEN

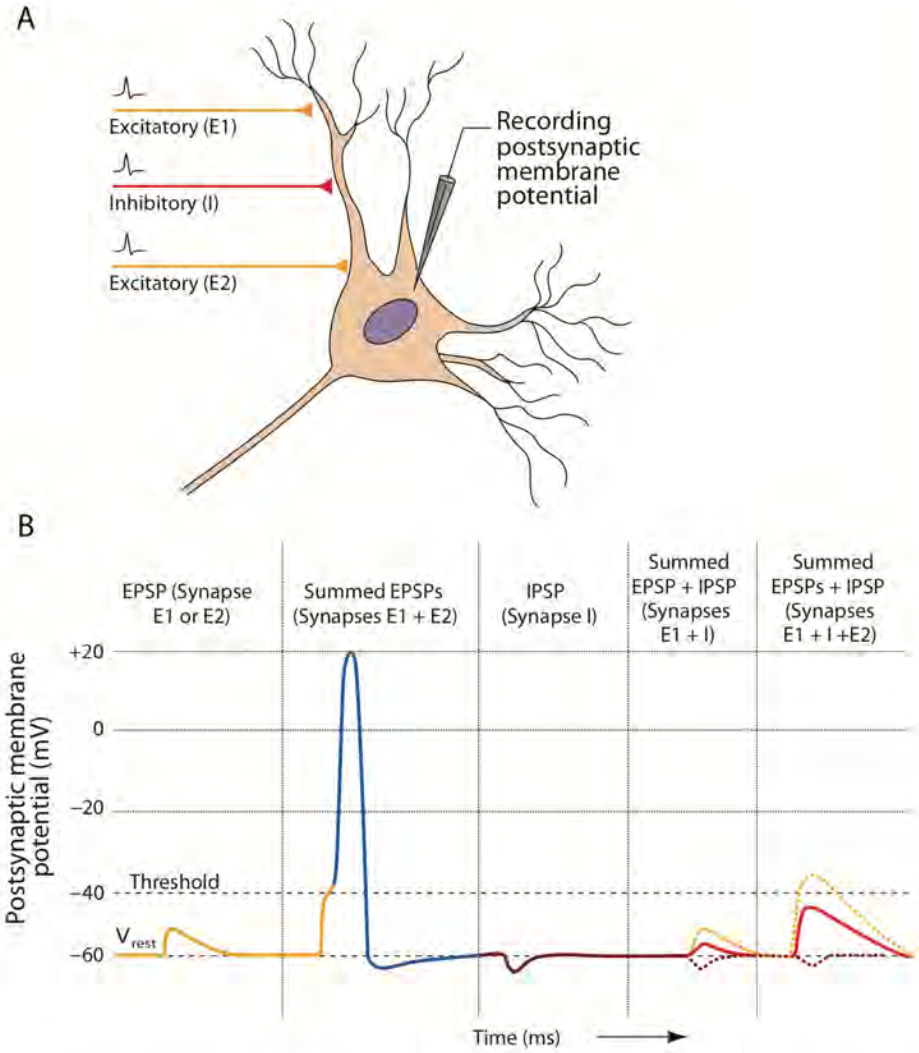



**Figure 2.7:** Summation of EPSPs and IPSPs. A: Schematic representation of a cell with a recording electrode which monitors the output of two excitatory synapses (E1 and E2) and an inhibitory synapse (I). B: Inputs from either the excitatory synapse E1 or the excitatory synapse E2 alone do not depolarize the neuron strongly enough to produce a postsynaptic action potential (blue). If inputs occur on both synapses at about the same time, they sum together and result in an AP. An IPSP reduces the cell's membrane potential and can prevent the generation of an AP. The figure is taken and modified from [ Purves et al., (2004) ].



Die approbierte gedruckte Originalversion dieser Diplomarbeit ist an der TU Wien Bibliothek verfügbar
The approved original version of this thesis is available in print at TU Wien Bibliothek.

Die approbierte gedruckte Originalversion dieser Diplomarbeit ist an der TU Wien Bibliothek verfügbar
The approved original version of this thesis is available in print at TU Wien Bibliothek.

CHAPTER 3

# Hippocampal Activities

The following section presents fundamental hippocampal activities and brings general aspects about their basic mechanisms. Furthermore, it describes the main connections in hippocampal microcircuits which bridge the gap between single, independent cells and large scale networks, as well as elucidates the phenomenon of neuronal cell synchronization. At the end of the chapter, feedback and feedforward connections are introduced and the hybrid neuronal networks for our experiments are shown.

## 3.1 The Agile Hippocampus

The hippocampus is a very entangled structure, where all the cells are highly interconnected, which means that a single hippocampal pyramidal cell interacts with a variety of other neurons from different regions of the hippocampus [ Li et al., (1994) ]. This connectivity can be seen under microscopy observation and, interestingly, this intricate connectivity is believed to lead to different oscillations, such as the mentioned theta, gamma and ripple oscillations. [ Cunningham et al., (2004) ]. Gamma frequency, for example, can emerge in a random network of interconnected fast-spiking basket cells, whereas O-LM interneurons tend to spike in theta frequency. Several electrophysiological experiments on in-vitro preparations have also demonstrated that different cell types in the hippocampus respond to different phases of the population oscillatory activity [ Hájos et al., (2004) ]. During in-vitro gamma oscillations, for example, pyramidal cells signal sparsely whereas some interneurons synchronize and signal phase-locked to each gamma cycle. Other neurons can skip cycles and still manage to phase-lock their activity to the overall oscillations of the network [ Kopell et al., (2010) ].

There are studies showing the interactions and activities of single neurons during oscillations [ Leão et al., (2009) ][ Mann and Paulsen, (2007) ] but due to the large number of cells interacting with each other in different patterns, it is quite difficult to understand all of the mechanisms taking place. These studies suggest that many of the oscillation initiation and transmission

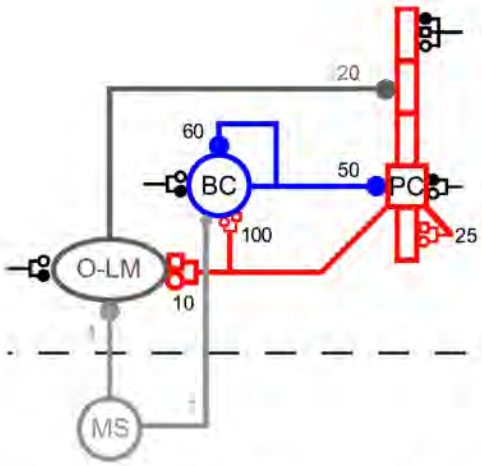



**Figure 3.1:** Hippocampal microcircuit. A network consisting of a pyramidal cell (red), a basket cell (blue) and an O-LM cell (dark gray) is shown. In a recent modeling study 800 PCs, 200 BCs and 200 O-LM cells connected according to this scheme, were simulated. The numbers of inputs for each synapse are shown near the synapses. Inhibitory connections from interneurons using GABA as neurotransmitter are shown as filled circles, excitatory synapses are represented as open circles and open squares. Truncated, black lines show external inputs. MS denotes inputs from the medial septum which is another important brain region and pacing theta rhythms. [ Neymotin et al., (2011) ].

mechanisms are generated by different synchronized neuronal populations. It seems that synchronized cells, spiking together, form the basis for oscillations and subsequently are essential for all types of cognitive functions. Not only this aspect, but also how cells can actually synchronize and then form organized neuronal activities motivates us to investigate synchronization mechanisms at the level of hippocampal microcircuits and record the activities of single units in neuronal networks [ Grillner and Graybiel, (2006) ].

## 3.2 Hippocampal Microcircuits

When referring to the anatomy of the hippocampus, the main subregions CA1 and CA3 are always mentioned as they represent its major input and output region respectively. As mentioned in the chapter 2, the CA3 region gets its main inputs from large pyramidal cells in the layer II of the entorhinal cortex and from other principal cells of the DG, which usually project to the proximal apical dendrites of the CA3 pyramidal cells. Via axon collaterals given off by CA3 pyramidal cells (Schaffer collaterals) CA1 pyramidal cells are activated. CA1 cells finally project to the subiculum which forwards the signals to the entorhinal cortex again. One can imagine that there is a huge number of cells involved performing such a complex structure and their pathways, which makes it challenging to understand the basic mechanisms of neuronal cell synchronization.



Die approbierte gedruckte Originalversion dieser Diplomarbeit ist an der TU Wien Bibliothek verfügbar
The approved original version of this thesis is available in print at TU Wien Bibliothek.

Looking at a smaller scale, for example, a specific microcircuit consisting of the main cells contributing to synchronization and oscillations, enables us to study functions and ongoing mechanisms of specific cell types. Investigating such microcircuits is a powerful approach when studying the activities of specific cells and cell populations. Figure 3.1 contains a schematic representation of a CA3 microcircuit consisting of pyramidal cells, basket cells and O-LM cells. In this network PCs get inhibited by basket cells, which basically connect to the PCs' soma and to other BCs via GABAergic synapses. Furthermore, O-LM cells target to the distal apical dendrites of the PCs via inhibitory GABAergic connections. On the other side, both the O-LM and the basket cells are innervated by the PCs via excitatory connections. This kind of microcircuit is usually used to study questions concerning oscillations, frequency coupling and neuronal synchronization in the hippocampus on a basis of computer simulations. Furthermore, specific connections such as feedback and feedforward connections can easily be studied [ Bartos et al., (2002) ].

## 3.3 Circuit Connectivity

Neuronal networks built from both excitatory and inhibitory neurons are able to self-organize and generate complex properties, depending on their connectivities. Here, we distinguish between *feedforward* and *feedback* configurations. Figure 3.2 shows the basic patterns of microcircuit connectivity.

- In a feedforward network, both the PC and the interneuron receive an excitatory input. Furthermore, the interneuron inhibits the PC. Due to the additional synaptic delay on the path via the interneuron compared to the direct excitation of the PC, this kind of network generates a time-dependent alternation of excitation and inhibition.
- In a feedback network, increased spiking of the PC excites the interneuron. This excitation increases the interneuron's firing, which in turn suppresses the pyramidal cell's activity through its inhibitory connection. This kind of network establishes a feedback loop where increased PC firing triggers its own inhibition.

Both the feedforward and the feedback network are based on the interplay between pyramidal cell depolarization caused by increased excitation and fast repolarization caused by interneuronal inhibition. Therefore, these networks consisting of a simple inhibitory and a single excitatory connection can substantially increase the temporal precision of the cells firing. These mechanisms seem simple but, in fact, they are complex and non-linear. For example, in a network, where two or more interneurons are excited and have synaptic connections to a common pyramidal cell, the PC input is a combination of the interneuronal inhibition underlying a series of complex mechanisms. [ Buzsáki, (1984) ][ Andersen et al., (2006) ]
Other connectivity patterns which describe network activities but consist of only one cell type are *recurrent excitation* and *mutual inhibition*.

- Recurrent excitation defines a circuit where local pyramidal cells connect to other pyramidal cells and increase their firing.



Die approbierte gedruckte Originalversion dieser Diplomarbeit ist an der TU Wien Bibliothek verfügbar
The approved original version of this thesis is available in print at TU Wien Bibliothek.
TU Bibliothek Your knowledge hub WIEN

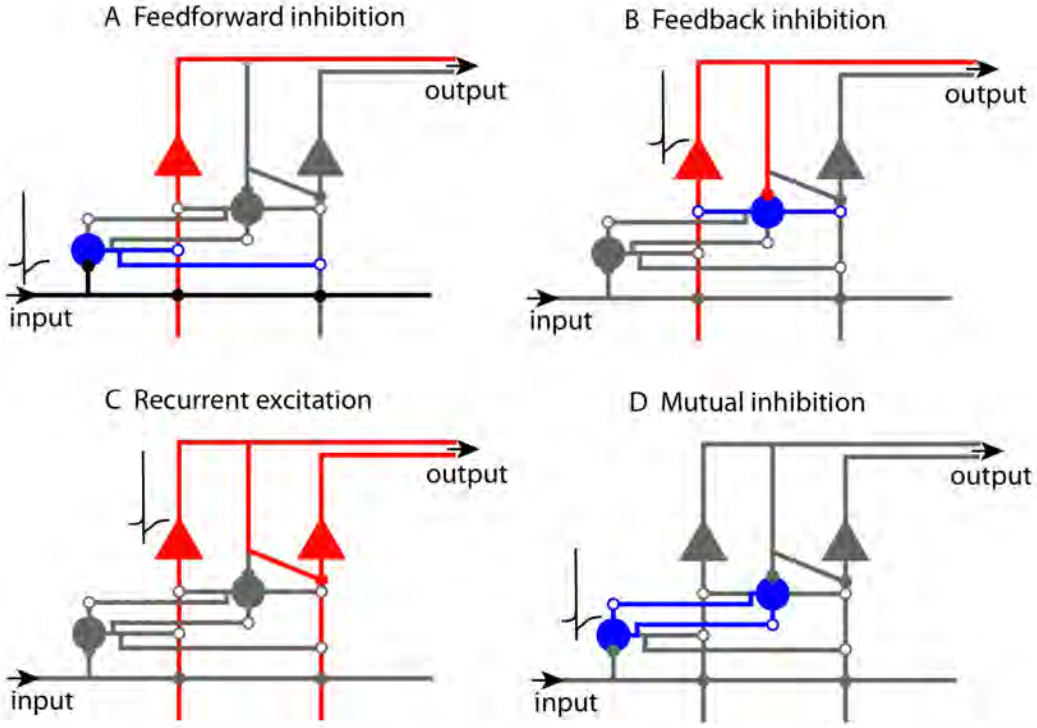



**Figure 3.2:** Circuit connectivity patterns. A: Feedforward inhibition is realized by an interneuron (blue) giving delayed inhibition to a pyramidal cell (red) when both cells receive an excitatory input. B: Feedback inhibition emerges when a pyramidal cell excites an interneuron which in turn provides inhibition to the pyramidal cell in order to slow down its excitation. C: Recurrent excitation describes excitatory connections between pyramidal cells. D: Mutual inhibition arises in networks where interneurons inhibit each other. The figure is taken and modified from [ Andersen et al., (2006) ].

- Mutual inhibition can be found in networks where interneurons form synapses only to other interneurons but not to pyramidal cells. This kind of network is able to generate specific rhythms such as gamma oscillations in interneuronal networks.

Both the recurrent excitation and the mutual inhibition are important mechanisms building cell assemblies and causing synchronous firing of the involved cells.

## 3.4 The Phenomenon of Synchronization

Synchronization of neuronal activities is essential for the operation of brain networks. When observed at the population level, for example through field recordings, networks of the brain appear to be highly synchronized during oscillatory activities, whereas when observed at a level of



Die approbierte gedruckte Originalversion dieser Diplomarbeit ist an der TU Wien Bibliothek verfügbar
The approved original version of this thesis is available in print at TU Wien Bibliothek.
TU Bibliothek Your knowledge hub WIEN

single neurons within a network, they show a less rhythmic firing. This is an indication that neuronal synchronization does not necessarily mean network oscillations. Classically, synchronization describes the adjustment of rhythms in terms of phase-locking and frequency entrainment of a certain population of neurons. Two cells are called *synchronous* if they spike dependently of each other. This can be in-phase, anti-phase or with a certain continuous phase shift. [ Fisahn et al., (1998) ][ Geisler et al., (2005) ][ Fries et al., (2009) ][ LeBeau et al., (2003) ]

Initially, excitation between principal cells was believed to be the main source of rhythmogenesis and neuronal synchronization in specific microcircuits. [ Kuramoto, (1991) ][ Acker et al., (2003) ] But later studies showed that gluamatergic excitation does not synchronize mutually coupled neurons. It makes them fire more unsynchronized instead. It seems that connections between principal cells alone do not synchronize their firings. Investigating inhibition rather than excitation, the work of [ Lytton and Sejnowski, (1991) ] suggests that synchronous rhythmic inhibition by fast-spiking interneurons can make cells fire together. Moreover, a network of interneurons interconnected via GABAergic synapses can generate a coherent output to its targeting cells and is able to synchronize their action potentials. It is believed that so-called long-range inhibition produces best synchrony of both the interneuronal network and targeting PCs in the hippocampus. Besides modeling studies, also in vitro experiments could show that mutual pyramidal cell firing originates from synchronized activity of fast-spiking interneurons. Referring to the divergence of interneurons, thousands of PCs probably share a common interneuron, which is acting as a temporal pacemaker and claiming that synaptic inhibition plays an essential role in synchronization processes. [ Whittington et al., (1995) ][ Sommer and Wennekers, (2001) ][ Bartos et al., (2002) ][ Buzsáki et al., (2004) ][ Traub et al., (2004) ]

Other interneurons like the O-LM cells are also able to control the firing times of PCs but act differently. In contrast to fast-spiking interneurons which tend to spike in gamma frequency, O-LM cells prefer to spike in theta frequency. They can lead to gamma coherence between clusters of both PCs and fast-spiking BCs which is able to make pyramidal cell assemblies synchronized. However, studies showed that these in theta firing O-LM cell clusters are not necessarily needed to see synchronization of PCs. Even with asynchronously firing O-LM cells pyramidal cells are able to synchronize. [ Tort et al., (2007) ][ Csicsvari, (2003) ]

It seems that fast-spiking interneurons are the main source for PC synchronization. They usually fire with higher frequency than O-LM cells and provide IPSCs which are needed to produce synchrony with and between PCs. One of the reasons could be that synchronization between PCs breaks down when their spiking frequency is too low. The coherent output of networks of fast-spiking basket cells is able to control the firing frequency of PCs. Basket cells are not only able to produce gamma, but also amplify theta rhythms. This also supports the theory that fast-spiking interneurons act as pacemakers for pyramidal neurons. [ Cobb et al., (1995) ][ Miles et al., (1996) ][ Wang and Buzsáki, (1996) ][ Pálhalmi et al., (2004) ][ Cardin et al., (2009) ]

Hippocampal pyramidal cells in turn were shown to excite inhibitory neurons via monosynaptic connections. These single synaptic connections provide appropriate excitation to the interneu-



Die approbierte gedruckte Originalversion dieser Diplomarbeit ist an der TU Wien Bibliothek verfügbar
The approved original version of this thesis is available in print at TU Wien Bibliothek.
TU Bibliothek Your knowledge hub WIEN

rons and are able to lead to a synchronized neuronal network. [ Gulyás et al., (1993) ][ Sik et al., (1995) ]

Finally, modeling studies of [ Traub et al., (2000) ] show that hippocampal networks, in particular CA3 networks consisting of both pyramidal cells and inhibitory interneurons connected via feedback connections, are able to generate synchronized activities and oscillations. It turns out that synchronization could occur as an interplay between excitatory principal cells and inhibitory interneurons where PCs drive interneurons through these feedback connections. [ Cunningham et al., (2003) ][ Hájos et al., (2004) ] A similar mechanism was reported in [ Oren and Kullmann, (2012) ] where the interaction of local inhibition with afferent excitation from the entorhinal cortex is encoding spatial information in both the cell's firing rate and the precise timing of its spikes.

## 3.5 Hybrid Neuronal Networks

In order to gain insight into these complex mechanisms contributing to neuronal synchronization, we build different hybrid neuronal networks, connecting two patched, living pyramidal cells with an artificial, modeled interneuron stored on a computer. This gives us the possibility to find a biological realistic network configuration, which is able to synchronize two PCs. Figure 3.3 illustrates eight different configurations which are subsequently run on our dynamic clamp experiments.

The two pyramidal cells (Fig. 3.3, red and black) are patched on their somas and receive interneuronal inhibition according to the different network configurations. The interneuron is simulated on a real-time computer and mimics the behavior of a real interneuron. This hybrid approach gives us the great ability to actively control and investigate the activities of the interneuron in the neuronal network, as well as its influence on the PCs. Hybrid neuronal networks offer a powerful opportunity, when studying interacting objects, such as real, living neurons. The artificial part can be either analog (realized as an electronic circuit) or digital (implemented on a computer). We use a digital approach, since it offers higher flexibility and the simulation of more complex models, i.e. the dynamics of our model interneuron can be described by differential equations and programmed on the computer. Also different connectivity patterns can be simulated very easily. For example, the connections between the different cells can be altered or turned off through some simple modifications in the computer model.

We simulate eight different network configurations consisting of both excitatory and inhibitory connections. Excitatory connections from the patched pyramidal cells to the artificial interneuron represent monosynaptic feedback connections, which can be found between hippocampal pyramidal cells and interneurons. Inhibtitory connections from the interneuron to the PCs simulate GABAergic connections between those cells. In two cases the interneuron is spontaneously active, whereas in the other cases it is driven by the mentioned feedback connections.



Die approbierte gedruckte Originalversion dieser Diplomarbeit ist an der TU Wien Bibliothek verfügbar
The approved original version of this thesis is available in print at TU Wien Bibliothek.
TU Bibliothek Your knowledge hub WIEN

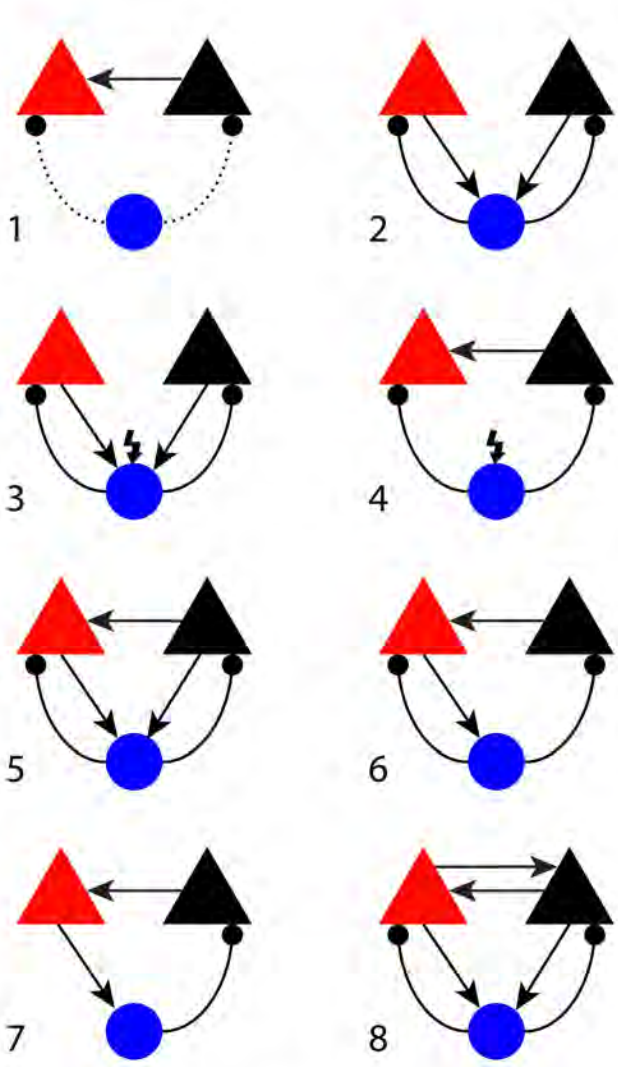



**Figure 3.3:** Schematic compositions of eight different neuronal network configurations. The hybrid microcircuits consist of two patched pyramidal cells (red and black triangle) and a simulated fast-spiking interneuron (blue circle). In network 3 and 4 the simulated interneuron is spontaneously active, indicated by a black flash. Differences in network connectivity are shown by modeled inhibitory (circles) and excitatory (arrows) connections.



Die approbierte gedruckte Originalversion dieser Diplomarbeit ist an der TU Wien Bibliothek verfügbar
The approved original version of this thesis is available in print at TU Wien Bibliothek.

TU WIEN Bibliothek Your knowledge hub
Die approbierte gedruckte Originalversion dieser Diplomarbeit ist an der TU Wien Bibliothek verfügbar
The approved original version of this thesis is available in print at TU Wien Bibliothek.

CHAPTER 4

# The Real-Time System

This chapter introduces the term *real-time* by naming its properties and requirements. Furthermore, it explains how an ordinary computer can be prepared for real-time computation and how fast data acquisition can be realized. On this computer differential equations for a modeled interneuron are stored. To build a hybrid neuronal network, the artificial interneuron is connected to two living pyramidal cells. Therefore, the computer has to provide high speed DAQ and high performance computation.

## 4.1 Fast - Faster - Real Time

As a dynamic clamp system requires that the process of measuring the cells membrane potentials, calculating the modeled equations on the computer and injecting a current back to the neurons has to be finished faster than the fastest dynamic process present in the system, there are some challenges to overcome. One of the bottlenecks is the simulation of the modeled cell which is described by Hodgkin-Huxley equations. The computer has not only to guarantee that its task is finished, it also has to ensure that it is done within a predefined period of time. Such a system is called *real-time system*. It finally turns out that the term *real-time* defines a system that is able to respond within specified time periods to events. This counts for both the computation as well as the data acquisition.

## 4.2 Control and Measurement Device Interface

The Control and Measurement Device Interface (Comedi) project [1] is an open-source software package for Linux operating systems which provides drivers, tools and libraries to provide real-time data acquisition on a computer. This application programming interface (API) enables computers to communicate with DAQ cards of various manufacturers and simplifies writing

[1] http://www.comedi.org



Die approbierte gedruckte Originalversion dieser Diplomarbeit ist an der TU Wien Bibliothek verfügbar
The approved original version of this thesis is available in print at TU Wien Bibliothek.

code for different cards and systems. The comedi project consists of three different software packages:

- Comedi itself is a package of drivers for numerous of commonly used DAQ cards which is implemented as a core Linux kernel module. It enables the computer to read from and write to the DAQ card and get all the information out of it, such as the available digital and analog in- and output ports.
- Comedilib is the library of the project which includes some tutorial programs, documentation and configuration tools in the user space. It enables the user to see how the basic functions for data acquisition work.
- Kcomedilib on the other hand is the kernel space variant of the Comedilib. It is a kernel module and library which is needed for using Comedi out of real-time applications.

Once installed, the DAQ cards of the computer are named from *comedi0* to *comediN* depending on how many cards are used. They are stored in the directory */dev/*. Each device has a specific number of subdevices which are also labeled from *subdevice0* to *subdeviceN*. The subdevices are classified according to their functions, such as *analog Inputs*, *analog Outputs* or *digital In-/Outputs*. The parts of a subdevice are called *channels* which have to be specified for reading and writing. The program *board_info* in the provided demonstration directory of the Comedilib prints all the information about the device.

Besides the preparation of the real-time DAQ card drivers, the computer itself has to be prepared with a special software package in order to operate in real-time.

## 4.3 Real Time Application Interface

The Real Time Application Interface (RTAI) is an open-source project for Linux operating systems which is able to fulfill the requirements for dynamic clamp as it is possible to run programs with defined timing constraints. The RTAI was invented in the Dipartimento di Ingegneria Aerospaziale, Politecnico di Milano from a group of professor Paolo Mantegazza and is a capable alternative to commercial real-time environments such as Lynuxworks, MontaVista Linux, QNX or VxWorks.

It mainly consists of two parts, a patch to the Linux kernel which introduces a hardware abstraction layer and a variety of services for real-time programming such as simulation softwares and a virtual oscilloscope. A conventional computer operating system usually separates virtual memory into kernel space and user space. Kernel space is reserved for running the kernel, i.e. the core of an operating system, which operates between applications and hardware such as CPU, memory or other devices. On the other hand, user space is the set of memory locations in which user processes and user applications are run. The RTAI suite, in particular the Real Time Hardware Abstraction Layer introduces an additional Realtime-Kernel inbetween the computers hardware level and the Linux kernel. The main functions of this sub-kernel are the scheduling and management of the prioritized real-time tasks whereas the normal Linux kernel is still



Die approbierte gedruckte Originalversion dieser Diplomarbeit ist an der TU Wien Bibliothek verfügbar
The approved original version of this thesis is available in print at TU Wien Bibliothek.
TU Bibliothek Your knowledge hub WIEN

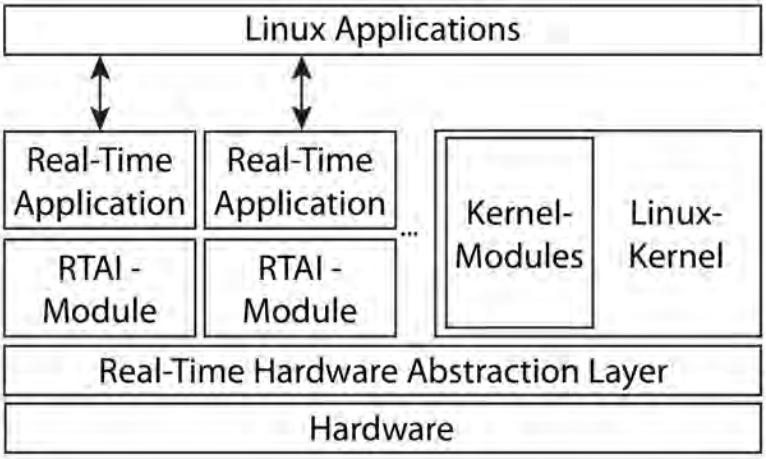



**Figure 4.1:** Structure of RTAI including the newly introduced Real-Time Hardware Abstraction Layer. For the management of the Real-time-Kernel RTAI modules are used. The communication between real-time applications in kernel space and user space applications is done by FIFOs or shared memories.

used for the non-real-time processes. For keeping the system stable, the normal Linux kernel is treated as a real-time task with lowest priority, so that it is only executed if no other real-time task uses the CPU. With this arrangement (Fig. 4.1) the system is able to ensure that processes can be finished before predefined deadlines as it is required for dynamic clamp. For the activation and management of the Real-time-Kernel so-called RTAI modules are used. All RTAI module names usually start with *rtai_*. The command *lsmod* lists all of the loaded modules, the commands *insmod* and *modprobe* are used to load modules, *rmmode* is used to remove loaded modules. For the communication between real-time applications and the user space, FIFOs (first in first out) and shared memories are used. Therefore, the modules *rtai_fifos.ko* and *rtai_shm.ko* have to be loaded. Another important module is *rtai_comedi.ko* which is needed for real-time communication between the real-time interface of the computer and the real-time functions of the Comedi suite.

## 4.4 Hardware

In addition to high performance software a powerful computer and an appropriate DAQ card are needed. The Dell Precision T1500 fulfills our requirements for real-time processing. It has a Quad-Core Intel Core i7 with 2.80 Ghz and 5.8 Gigabyte memory. As our DAQ card the National Instruments PCI-6251 is used. It has 16 analog input and 2 analog output channels which are used to communicate between the computer and the amplifier of our patch clamp rig.



Die approbierte gedruckte Originalversion dieser Diplomarbeit ist an der TU Wien Bibliothek verfügbar
The approved original version of this thesis is available in print at TU Wien Bibliothek.
TU Bibliothek Your knowledge hub WIEN

## 4.5 Installation and Configuration

For the installation of the RTAI and the RTAI-Lab, a software environment for real-time programming, the following software packages are needed:

- the RTAI real-time modules
- the appropriate Linux kernel that will be patched (configured) with the RTAI code: Every RTAI patch lists the Linux kernel versions it can update.
- the Comedi DAQ device modules and drivers
- the EFLTK graphic widgets library [2]: EFLTK is needed by the program *xrtailab*, a virtual oscilloscope which is part of the RTAI-Lab and monitors the real-time applications.
- the Mesa 3D graphical library [3]: This graphical library is needed for visualization and for the program xrtailab.

There are several installation instructions available on the RTAI project website. The following section shows the configuration of our system, using the software packages listed in table 4.1:

| Software package | Version |
|---|---|
| RTAI | rtai-magma.tar.bz2 |
| Linux Kernel | linux-2.6.37.tar.bz2 |
| Comedi | comedi-0.7.70.tar.gz |
| Comedi library | comedilib-0.8.1.tar.gz |
| EFLTK library | efltk-2.0.7.tar.gz |
| Mesa library | MesaLib-7.10.1.tar.bz2 |

**Table 4.1:** The software packages of our real-time computer.

As host operating system the open-source Linux distribution Ubuntu 10.10 (Maverick Meerkat) is used and updated for the latest libraries. The installation of all the required software packages should be done with root privileges. We put all the software packages in the directory *realtime/Downloads/*.

### Mesa library

Ubuntu usually contains the Mesa 3D library, but for a clean install the following commands have to be applied:

```
$ cd /usr/local/src
$ cp /realtime/Downloads/MesaLib-7.10.1.tar.bz2 /usr/local/src
$ tar xjvf MesaLib-7.10.1.tar.bz2
```

[2] http://www.equinox-project.org
[3] http://www.mesa3d.org



Die approbierte gedruckte Originalversion dieser Diplomarbeit ist an der TU Wien Bibliothek verfügbar
The approved original version of this thesis is available in print at TU Wien Bibliothek.

```
$ cd Mesa-7.10.1
$ make realclean
$ make linux-x86-64
$ make install
```

### EFLTK library

For the installation of the EFLTK library the packages *gettext*, *flex*, and *svn* are needed.

```
$ cd /usr/local/src
$ cp /realtime/Downloads/efltk-2.0.7.tar.gz /usr/local/src
$ tar xzf efltk-2.0.7.tar.gz
$ ln -s efltk-2.0.7 efltk
$ cd efltk
$ autoconf
$ ./configure --disable-mysql --disable-unixODBC
$ ./emake
$ ./emake install
$ gedit /etc/ld.so.conf
```

The path */usr/local/lib* must be added to the following file:

```
$ /sbin/ldconfig
```

### Linux kernel and RTAI patch

```
$ cd /usr/src
$ cp /realtime/Downloads/rtai-magma.tar.bz2 /usr/src
$ tar xjvf rtai-magma.tar.bz2
$ ln -s /usr/src/rtai-magma rtai
```

It is important that the RTAI patch and the Linux kernel version match. The supported kernel versions can be found in the directory */usr/src/rtai/base/arch/x86/patches/* after extraction of the downloaded RTAI-Lab. The available patch files have the scheme *hal-linux-<kernel-version>.patch* where *<kernel-version>* is the number of the supported kernel-version including the computer's architecture and a predefined number. We tested a 32-bit variant and a 64-bit version on our system. RTAI supports various architectures and chip designs including x86, x86_64 and PowerPC.

After locating the supported Linux kernel versions in the RTAI directory, the appropriate Kernel can be prepared:

```
$ cp /realtime/Downloads/linux-2.6.37.tar.bz2 /usr/src
$ tar xjvf linux-2.6.37.tar.bz2
$ ln -s /usr/src/linux-2.6.37-rtai linux
```



Die approbierte gedruckte Originalversion dieser Diplomarbeit ist an der TU Wien Bibliothek verfügbar
The approved original version of this thesis is available in print at TU Wien Bibliothek.

The following commands apply the RTAI patch to the Linux kernel:

```
$ cd linux
$ patch -p1 <
  /usr/src/rtai/base/arch/x86/patches/hal-linux-2.6.37-x86-2.9-00.patch
$ make oldconfig
$ make xconfig
```

The kernel is configured as follows:

```
$ make
$ make modules install
$ make install
```

After the Linux kernel is ready, the boot loader has to be updated and configured for the new kernel:

```
$  gedit /boot/grub/menu.lst
```

The following flags must be set and saved:

```
default = 0
howmany = all
memtest86 = false

$ update-grub
```

At this step the computer can be restarted with the newly compiled kernel to be ready for the Comedilib installation.

### Comedilib

The following commands install the Comedilib:

```
$ cd /usr/local/src
$ cp /realtime/Downloads/comedilib-0.8.1.tar.gz /usr/local/src
$ tar xzf comedilib-0.8.1.tar.gz
$ cd comedilib-0.8.1
$ sh autogen.sh
$ ./configure -sysconfdir=/etc -localstatedir=/var
$ make
$ make install
$ make dev
```

After a successful installation the Comedi devices *comedi0* to *comediN* are listed in */dev*.



Die approbierte gedruckte Originalversion dieser Diplomarbeit ist an der TU Wien Bibliothek verfügbar
The approved original version of this thesis is available in print at TU Wien Bibliothek.

### RTAI 1

Because of dependencies between Comedi and RTAI the RTAI package has to installed first without Comedi.

```
$ cd /usr/src/rtai
$ make xconfig
```

This pops up a window. In the menu *General* the installation directory */usr/realtime* and the kernel source directory */usr/src/linux* have to be specified. In the menu *Machine* the number of CPUs should be specified in order to guarantee an optimal usage of the computer.

```
$ make
$ make install
$ gedit /etc/bash.bashrc
```

At the end of the file the command *export PATH=/usr/realtime/bin:$PATH* has to be added. After another reboot, the RTAI system can be used the first time. Therefore, some RTAI-modules have to be loaded with root privileges. The following modules are needed for our purposes:

```
insmod /usr/realtime/modules/rtai_hal.ko
insmod /usr/realtime/modules/rtai_sched.ko
insmod /usr/realtime/modules/rtai_lxrt.ko
insmod /usr/realtime/modules/rtai_fifos.ko
insmod /usr/realtime/modules/rtai_sem.ko
insmod /usr/realtime/modules/rtai_mbx.ko
insmod /usr/realtime/modules/rtai_msg.ko
insmod /usr/realtime/modules/rtai_netrpc.ko ThisNode=''127.0.0.1''
insmod /usr/realtime/modules/rtai_shm.ko
insmod /usr/realtime/modules/rtai_signal.ko
insmod /usr/realtime/modules/rtai_math.ko
insmod /usr/realtime/modules/rtai_tasklets.ko

modprobe comedi
modprobe kcomedilib
modprobe comedi_rt_timer
modprobe ni_pcimio
```

The name *ni_pcimio* is the kernel module name for the Comedi device. The module name for the appropriate hardware is listed in the file *devices.txt* which comes with the Comedi setup. The *insmod* and *modprobe* commands can be saved in a startup file, e.g. *./start_comedi* to avoid retyping of the commands with every reboot of the system. After loading the modules the real-time system's latency can be checked with the following commands:

```
$ cd /usr/realtime/testsuite/kern/latency
$ ./run
```

If the installation was successful, the values for overruns should remain at zero.



Die approbierte gedruckte Originalversion dieser Diplomarbeit ist an der TU Wien Bibliothek verfügbar
The approved original version of this thesis is available in print at TU Wien Bibliothek.
TU Bibliothek Your knowledge hub WIEN

### Comedi

At this step the interface between the DAQ card and the RTAI Linux can be established.

```
$ mkdir /usr/local/src/comedi
$ cd /usr/local/src/comedi
$ cp /realtime/Downloads/comedi.tar.bz2 /usr/local/src/comedi
$ tar xvf comedi.tar.bz2
$ sh autogen.sh
$ ./configure --with-linuxdir=/usr/src/linux --with-rtaidir=/usr/src/rtai
$ gedit /usr/src/linux/.config
```

The command *CONFIG RTHAL=y* has to be inserted to the file before the installation. Also symbolic links to the appropriate header files of the Comedilib need to be created.

```
$ make
$ make install
$ make dev
$ cp include/linux/comedi.h include/linux/comedilib.h /usr/include/
$ cp include/linux/comedi.h include/linux/comedilib.h /usr/local/include/
$ ln -s /usr/include/comedi.h /usr/include/linux/comedi.h
$ ln -s /usr/include/comedilib.h /usr/include/linux/comedilib.h
$ ln -s /usr/include/linux /usr/local/include/linux
```

### RTAI 2

The final step of the installation process is to configure the RTAI for Comedi support.

```
$ cd /usr/local
$ ln -s /src/efltk-2.0.7 efltk
$ ln -s/usr/local/src/comedi comedi
$ cd /usr/src/rtai
$ make xconfig
```

In the menu *Add-ons* the COMEDI support for LXRT has to be set. Furthermore, the COMEDI installation directory must be specified to */usr/local* and in the menu *RTAI Lab* the EFLTK installation directory has to be specified to */usr/local*.

```
$ make
$ make install
```

This concludes the installation of RTAI with Comedi support and enables us to perform dynamic clamp experiments. The system allows us to simulate artificial neurons in real-time and connect them to living cells.



Die approbierte gedruckte Originalversion dieser Diplomarbeit ist an der TU Wien Bibliothek verfügbar
The approved original version of this thesis is available in print at TU Wien Bibliothek.
TU Bibliothek Your knowledge hub WIEN

# CHAPTER 5

# The Artificial Neuron

The following section shows the mathematical modeling of a fast-spiking basket cell which is stored on the real-time computer and connected to living pyramidal cells. The model includes the HH-type equations for the cell's ion channels as well as their synaptic outputs. Furthermore, this chapter includes the model of a pyramidal cell in order to study its synaptic currents which are also simulated on the real-time computer.

## 5.1 Mathematical modeling

Mathematical modeling as a basis of computational neuroscience can be used to simulate a multitude of ongoing activities in human brains and is a powerful technique for studying neurological problems. Models answering questions in neuroscience usually consist of differential equations when describing biological processes, and are simplifications in order to reproduce reality on the computer in a way that the results conform to the reality. They should be as simple as possible and at the same time as exact as necessary.

Since we store our neuronal model on a real-time computer and perform live recordings on living pyramidal cells, which underlies restrictions in computation, we use a biophysically realistic HH-type single compartment model of a basket cell.

## 5.2 Fast-spiking Interneuron

We use the model of [ Wang and Buzsáki, (1996) ] for the simulation of the fast-spiking interneuron:

$$C\frac{dV}{dt} = -g_{Na}m_{\infty}(V)^3h(V - E_{Na}) - g_K n^4(V - E_K) - g_L(V - E_L) - I_{syn} + I_{app} \quad (5.1)$$

with

$$m_{\infty} = \frac{\alpha_m}{\alpha_m + \beta_m} \quad (5.2)$$



Die approbierte gedruckte Originalversion dieser Diplomarbeit ist an der TU Wien Bibliothek verfügbar
The approved original version of this thesis is available in print at TU Wien Bibliothek.
TU Bibliothek Your knowledge hub WIEN

$$\frac{dh}{dt} = (\alpha_h(1-h) - \beta_h h)\phi \tag{5.3}$$

$$\frac{dn}{dt} = (\alpha_n(1-n) - \beta_n n)\phi \tag{5.4}$$

In the equations 5.1, 5.3 and 5.4, the letters *C, V, E, t, $\tau$, g* and *I* denote capacitance density ($\mu F/cm^2$), voltage (*mV*), reversal potential (*mV*), time (*ms*), conductance density ($mS/cm^2$) and current density ($\mu A/cm^2$), respectively. The parameters are C = 1, $g_{Na}$ = 35, $g_K$ = 9, $g_L$ = 0.1, $E_{Na}$ = 55, $E_K$ = -90 and $E_L$ = -65. The rate functions $\alpha_x$ and $\beta_x$ for *x = m, h* and *n* are defined as follows. The three variables m, n, and h are called *gating variables*.

$$\alpha_m = \frac{-0.1(V+35)}{exp(-0.1(V+35)) - 1} \tag{5.5}$$

$$\beta_m = 4\ exp(-(V+60)/18) \tag{5.6}$$

$$\alpha_h = 0.07\ exp(-(V+58)/20) \tag{5.7}$$

$$\beta_h = \frac{1}{exp(-0.1(V+28)) + 1} \tag{5.8}$$

$$\alpha_n = \frac{-0.01(V+34)}{exp(-0.1(V+34)) - 1} \tag{5.9}$$

$$\beta_n = 0.125\ exp(-(V+44)/80) \tag{5.10}$$

With a stimulus of $I_{app}$ = 0.25 $\mu A/cm^2$ and $\phi$ = 3.33 the modeled fast-spiking interneuron fires action potentials as shown in Fig. 5.1.

The cell's synaptic current $I_{syn}$ is described by the equation:

$$I_{syn} = g_{syn} s(V - E_{syn}) \tag{5.11}$$

with

$$\frac{ds}{dt} = \alpha F(V_{pre})(1-h) - \beta s \tag{5.12}$$

In the equations 5.11 and 5.12, $g_{syn}$ denotes the maximal synaptic conductance ($mS/cm^2$), $E_{syn}$ the reversal potential (*mV*), $\alpha$ the channel opening rate ($msec^{-1}$) and $\beta$ the channel closing rate ($msec^{-1}$). The parameters are $g_{syn}$ = 0.1, $E_{syn}$ = -75, $\alpha$ = 12 and $\beta$ = 0.1. The normalized concentration of the postsynaptic transmitter-receptor complex $F(V_{pre})$ is defined as follows:

$$F(V_{pre}) = 1/(1 + \exp(-(V_{pre} - \theta_{syn})/2)) \tag{5.13}$$

with ($\theta_{syn} = 0\ mV$).

The synaptic current of the modeled cell with the parameters above is shown in Fig. 5.2.

For our dynamic clamp experiments, we have to simplify or replace the differential equations of the synaptic current by less computer power consuming methods. Therefore, we simulate the synaptic current amplitudes with a so-called lookup table. The values are taken and extrapolated from [ Maccaferri et al., (2000) ] and [ Losonczy et al., (2003) ]. Figure 5.3 shows the synaptic current prepared for real-time experiments.



Die approbierte gedruckte Originalversion dieser Diplomarbeit ist an der TU Wien Bibliothek verfügbar
The approved original version of this thesis is available in print at TU Wien Bibliothek.

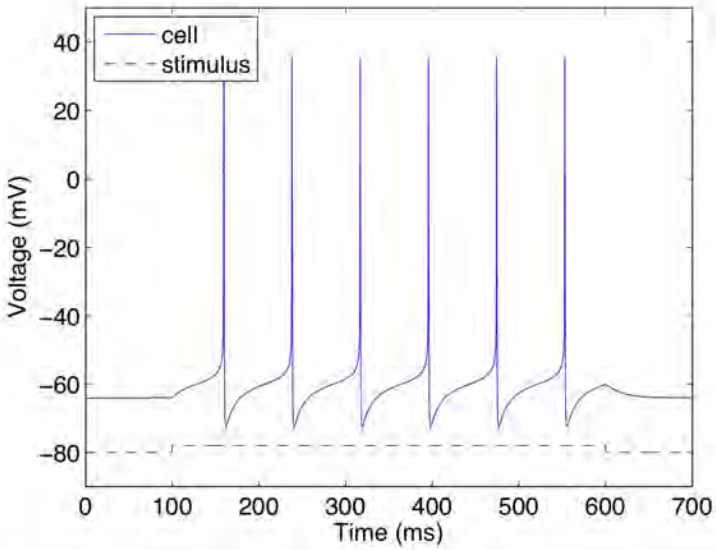



**Figure 5.1:** Simulation of a fast-spiking interneuron. The membrane potential (blue) of a fast-spiking interneuron is shown when a stimulus of $I_{app}$ = 0.25 $\mu A/cm^2$ (black, dashed line) is applied.

## 5.3 Pyramidal Cell

We use the pyramidal cell model of [ Olufsen et al. (2003) ]. The equations 5.1, 5.2, 5.3 and 5.4 are as in the fast-spiking interneuron model. The rate functions $\alpha_x$ and $\beta_x$ for $x = m, h$ and $n$ are defined as follows:

$$\alpha_m = \frac{0.32(V+54)}{1-exp(-(V+54)/4)} \tag{5.14}$$

$$\beta_m = \frac{0.28(V+27)}{exp((V+27)/5)-1} \tag{5.15}$$

$$\alpha_h = 0.128\, exp(-(V+50)/18) \tag{5.16}$$

$$\beta_h = \frac{4}{1+exp(-(V+27)/5)} \tag{5.17}$$

$$\alpha_n = \frac{0.032(V+52)}{1-exp(-(V+52)/5)} \tag{5.18}$$

$$\beta_n = 0.5\, exp(-(V+57)/40) \tag{5.19}$$

A stimulus of $I_{app} = 0.25\ \mu A/cm^2$ gives a cell response as in Fig. 5.4.
Its synaptic current is also realized by a lookup table and shown in Fig. 5.5.



Die approbierte gedruckte Originalversion dieser Diplomarbeit ist an der TU Wien Bibliothek verfügbar
The approved original version of this thesis is available in print at TU Wien Bibliothek.

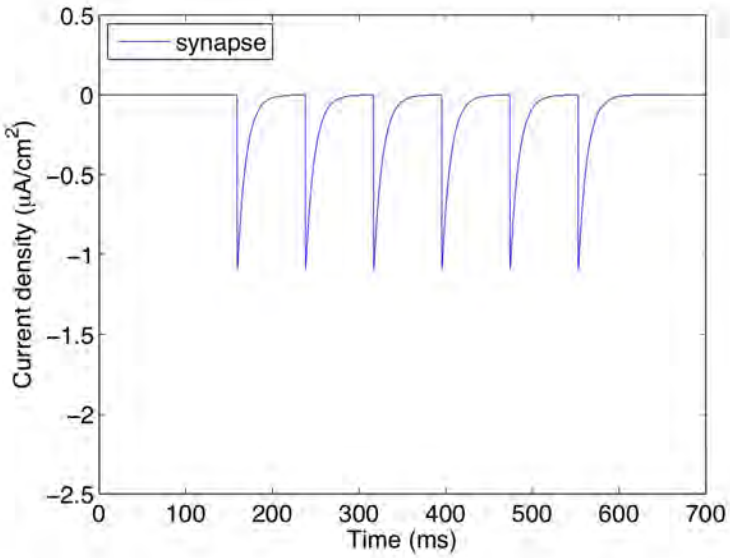



**Figure 5.2:** Simulation of IPSCs. The synaptic output of a fast-spiking interneuron modeled with differential equations [ Wang and Buzsáki, (1996) ] is shown.

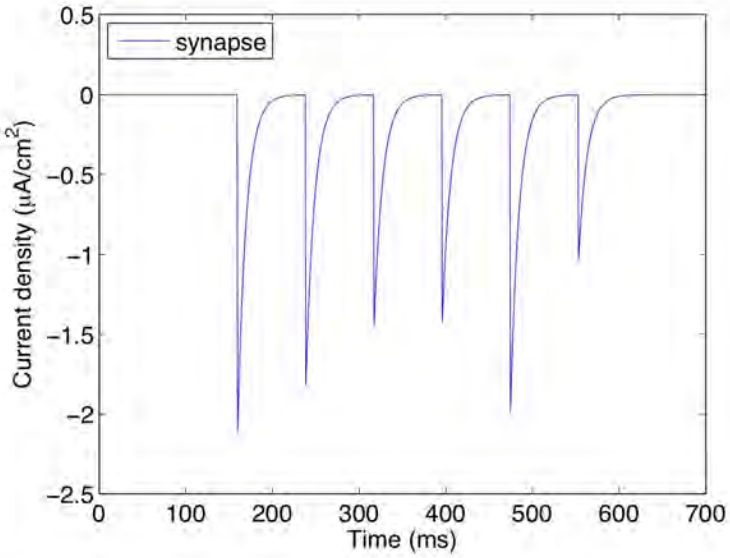



**Figure 5.3:** Simulation of biologically realistic IPSCs. The synaptic output of a fast-spiking interneuron is shown. Synaptic current amplitudes are read from a lookup table which contains experimental data [ Maccaferri et al., (2000) ].



Die approbierte gedruckte Originalversion dieser Diplomarbeit ist an der TU Wien Bibliothek verfügbar
The approved original version of this thesis is available in print at TU Wien Bibliothek.

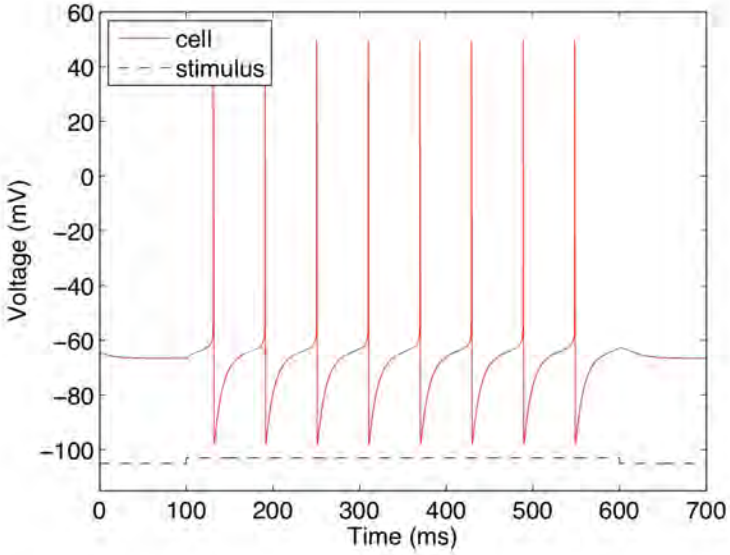



**Figure 5.4:** Simulation of a hippocampal pyramidal cell. The membrane potential (red) of a pyramidal cell is shown for a stimulus of $I_{app} = 0.25\ \mu A/cm^2$ (black, dashed line).

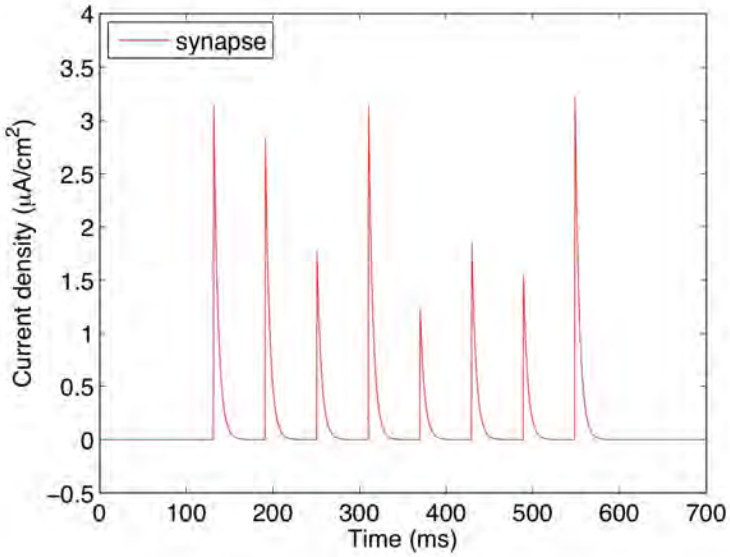



**Figure 5.5:** Simulation of biologically realistic EPSCs. The synaptic current of a pyramidal cell with synaptic current amplitudes taken from [ Losonczy et al., (2003) ] is shown.



Die approbierte gedruckte Originalversion dieser Diplomarbeit ist an der TU Wien Bibliothek verfügbar
The approved original version of this thesis is available in print at TU Wien Bibliothek.

TU WIEN Bibliothek Your knowledge hub
Die approbierte gedruckte Originalversion dieser Diplomarbeit ist an der TU Wien Bibliothek verfügbar
The approved original version of this thesis is available in print at TU Wien Bibliothek.

CHAPTER 6

# The Real-Time Neuron

This chapter explains how the artificial interneuron is realized on the real-time computer and how it processes its inputs and outputs. The computer cell has not only to handle the membrane potentials of the patched cells but also to simulate its synaptic currents according to selected network configurations. Therefore, this section describes the main commands for real-time programming, especially the reading and writing of the simulated excitatory and inhibitory currents.

## 6.1 Real-Time Implementation

We use eight different neuronal network models to study the impact of fast-spiking basket cells and their connectivity patterns on the synchronization of pyramidal cells in the hippocampus. The artificial interneuron and its synaptic connections are simulated in real-time in order to perform live recordings on living cells. The resolution of our real-time system is 50000 $ns$, which means that the values of the artificial cell are recalculated every 0.05 $ms$. The C program for realizing this fast update rate can be found in the appendix section B.5.

Figure 6.1 shows the operating principle of our dynamic clamp setup. The two hippocampal CA1 pyramidal cells are patched on their somas and their measured membrane potentials (Fig. 6.1, red ($V_1$) and black ($V_2$) voltage traces) are sent through an amplifier to the DAQ interface of the real-time computer. The commands for the data acquisition are as follows:

```
comedi_t * comedi_open(const char * filename);

int comedi_data_read(comedi_t * device, unsigned int subdevice,
unsigned int channel, unsigned int range, unsigned int aref,
lsampl_t * data);

value=100*((float)data*10/65536-5);
```



Die approbierte gedruckte Originalversion dieser Diplomarbeit ist an der TU Wien Bibliothek verfügbar
The approved original version of this thesis is available in print at TU Wien Bibliothek.
TU Bibliothek Your knowledge hub WIEN

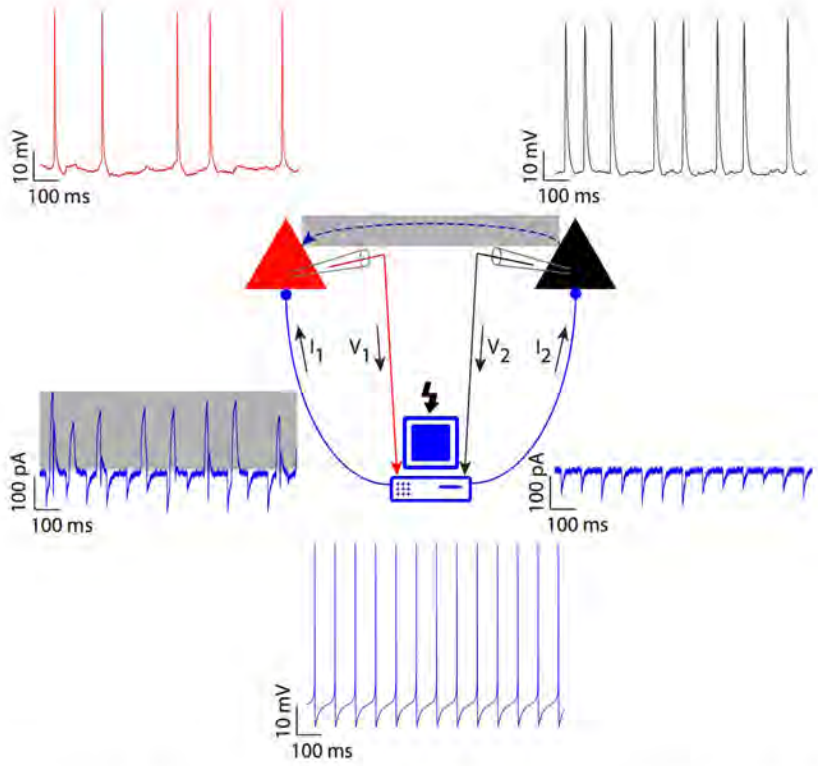



**Figure 6.1:** Dynamic clamp operating principle. Two hippocampal pyramidal cells (red and black triangle) are patched and their membrane potentials ($V_1$ and $V_2$) are read by a real-time computer (blue). The computer simulates a fast-spiking interneuron which can be spontaneously active by getting a stimulus (applied through the keyboard). Synaptic currents ($I_1$ and $I_2$) are fed back to the patched cells including inhibitory (blue current traces) and excitatory currents (gray area).

First the Comedi Device has to be addressed and opened to allow data transfer through the National Instruments card. The command *comedi_data_read* specifies the subdevice, the channel and the range of the Comedi device. Usually it is the device */dev/comedi0* when using only one DAQ card in the computer. All information of the channels can be read out from the program *board_info* located in the example directory of the Comedi library, which is */home/realtime/comedilib-0.8.1/demo* in our case. The parameter *subdevice* specifies which one of the 16 inputs and 2 outputs is used. For reading typically the subdevice 0 is used. The parameter range defines the information how sample values are translated to physical units. The argument *aref* indicates the reference of the device where *AREF_DIFF* is used for differential inputs/outputs. As the range is 16 bits ($2^{16}$=65536) and from -10 $V$ to +10 $V$ the input voltages have to be converted to samples. Therefore, the last line of the code above shifts the range -10 to +10 to the range 0 to +20 and stores the number in the variable *value*.



Die approbierte gedruckte Originalversion dieser Diplomarbeit ist an der TU Wien Bibliothek verfügbar
The approved original version of this thesis is available in print at TU Wien Bibliothek.
TU Bibliothek Your knowledge hub WIEN

These commands are used to read the membrane potentials of the two patched cells ($V_1$ and $V_2$). However, as a hybrid neuronal network with excitatory and inhibitory synapses is simulated, the artificial interneuron should receive synaptic currents of the pyramidal cells and not their membrane potentials. Therefore, the computer program also has to simulate these synaptic currents. This is done by detecting the spike times of the patched cells with a threshold mechanism. The spike times are needed to trigger a program which reads the EPSC amplitudes from a lookup table and inputs them to the artificial neuron. The values of the lookup table are read in user space and passed via FIFOs to the kernel space in order to introduce a current term to the main equation of the modeled interneuron.

Besides synaptic input, the interneuron can also receive a stimulus (Fig. 6.1: black flash) in order to make the initially passive cell spontaneously active. This stimulus can be changed through the computers keyboard. Therefore, the users input is read (user space) and sent via a FIFO to the kernel space where it is introduced to the simulated cell as well. To read values from the user space the following command is used, where the variable *fifo* defines the number of the *first in first out* device to address the right one, *buf* is the parameter for the value coming from the user space and *count* represents its size.

```
int rtf_get(unsigned int fifo, char * buf, int count);
```

With all the information about the input to the cell, the artificial interneuron itself can be computed now. The cell's membrane potential is calculated with the Euler method because of its iterative procedure starting with a given initial value (the membrane potential at time 0) and its easiness to be run on a real-time system where the time step for each iteration corresponds to the clock rate of the computer.

In addition to calculating the synaptic currents from the patched cells to the artificial interneuron, the program also simulates the currents between the artificial cell and the patched cells. These currents are usually inhibitory (Fig. 6.1: $I_1$ and $I_2$, blue traces). Furthermore, it is possible to simulate connections between the patched cells. These typically excitatory currents of the pyramidal cells (Fig. 6.1: dashed line) can easily be added to the currents $I_1$ and $I_2$ which are directly applied to the patched somas [ Robinson and Kawai, (1993) ]. An example excitatory current for this computer-controlled virtual synapse between the two real cells is presented in Fig. 6.1 (gray area).

To apply the simulated synaptic currents to the patched cells the values have to be converted to voltage input values which is done by the following commands, analog to the reading:

```
data=3.2768*value+32768;
```

```
int comedi_data_write(comedi_t * device, unsigned int subdevice,
unsigned int channel, unsigned int range, unsigned int aref,
lsampl_t data);
```



Die approbierte gedruckte Originalversion dieser Diplomarbeit ist an der TU Wien Bibliothek verfügbar
The approved original version of this thesis is available in print at TU Wien Bibliothek.

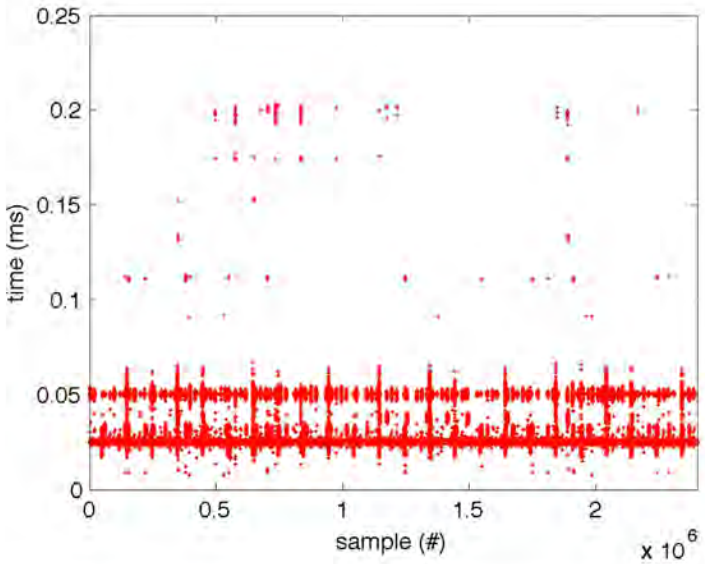



**Figure 6.2:** Duration of real-time periods. The periodic real-time tasks should have a period of 0.05 $ms$. The shown system exhibits deviations up to + 150 $\mu s$ from the expected period.

The functions *init_module()* and *cleanup_module()* in our real-time program are used to initialize and de-initialize the kernel module when it is loaded or stopped. This concludes the programming part of this chapter.

To run the code in real-time, the appropriate kernel modules for the Comedi device have to be loaded. As described in chapter 4 a startup program should be written in order to automatically load and configure the real-time system. Furthermore, the command *comedi_config /dev/comedi0 ni_pcimio* is needed to link the Linux device to the hardware and configure the device. Before running the program a calibration can be performed with *comedi_calibrate /dev/comedi0*. It is also suggested to run a performance test and check if the predefined time constraints for dynamic clamp can be reached.

## 6.2 Performance

Since our real-time program is run and collecting data periodically with *rt_task_make_periodic(&task, rt_get_time() + tick_period, tick_period)* we can measure the time for each period which should be 0.05 $ms$ ideally as the tick rate is set to 50.000 $ns$ (=20 $kHz$). The time is read in each cycle with *rt_get_cpu_time_ns()* and the difference between the previous recorded time is calculated. The result for two minutes of simulation (120 000 ms / 0.05 = 2 400 000 values) of a basket cell is shown in Fig. 6.2.



Die approbierte gedruckte Originalversion dieser Diplomarbeit ist an der TU Wien Bibliothek verfügbar
The approved original version of this thesis is available in print at TU Wien Bibliothek.
TU Bibliothek Your knowledge hub WIEN

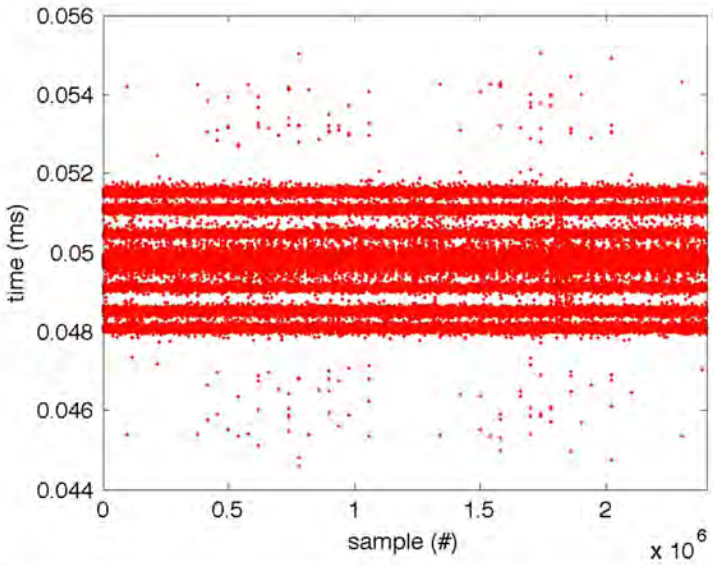



**Figure 6.3:** Duration of real-time periods. The durations of each periodic task when simulating a fast-spiking interneuron and five synaptic connections are shown. The system has a maximal deviation of +/- 6 $\mu s$ from the predefined period duration of 0.05 $ms$.

As there are big deviations between the expected period (0.05 $ms$) and some recorded periods, simplifications in the model can help to improve the real-time system. For example, using look up tables instead of differential equations for calculating synaptic currents or using simpler numerical methods such as the Euler method can change the performance of the system a lot. Our actual system, when running a single basket cell including five simulated synaptic connections (Fig. 6.1), ensures a permanent tick period of 0.05 $ms$ with a maximal deviation of +/- 6 $\mu s$ (Fig. 6.3).



Die approbierte gedruckte Originalversion dieser Diplomarbeit ist an der TU Wien Bibliothek verfügbar
The approved original version of this thesis is available in print at TU Wien Bibliothek.
TU Bibliothek Your knowledge hub WIEN

TU WIEN Bibliothek Your knowledge hub
Die approbierte gedruckte Originalversion dieser Diplomarbeit ist an der TU Wien Bibliothek verfügbar
The approved original version of this thesis is available in print at TU Wien Bibliothek.

CHAPTER 7

# The Experimental Setup

As this work includes both computational as well as experimental approaches based on electrophysiological recordings of hippocampal slices of mice, it is very important to plan such experiments and choose the appropriate materials and methods. This chapter provides the protocols used for the experiments present in this thesis, starting with the slice preparation, continuing with the electrophysiological recordings and concluding with the data analysis of the synchronicity.

## 7.1 Tissue Preparation

P12-P25 (postnatal) hippocampus slices from C57B6 mice are obtained as described in [ Leão et al., (2009) ]. In summary, mouse brains are rapidly removed and placed in ice-cold sucrose/artificial cerebrospinal fluid (ACSF), in mM: KCl, 2.49; $NaH_2PO_4$, 1.43; $NaHCO_3$, 26; glucose, 10; sucrose, 252; $CaCl_2$, 1.0; $MgCl_2$, 4.0. 400 $\mu m$ thick horizontal slices containing the hippocampus are cut using a vibratome (VT1200, Leica, Microsystems) and subsequently moved to a submerged holding chamber containing ACSF (in mM: NaCl, 124; KCl, 3.5; $NaH_2PO_4$, 1.25; $MgCl_2$, 1.5; $CaCl_2$, 1.5; $NaHCO_3$, 30; glucose, 10), constantly bubbled with 95% $O_2$ / 5% $CO_2$ where they are kept at $35°C$ for 1 hour and then maintained at room temperature until they are moved to the microscope stage. There the slices are transferred to a submerged chamber under an upright microscope equiped with DIC optics (Olympus) and perfused with at $30°C$ oxygenated ASCF (Gilson Minipuls 3 pump, 1 – 1.25 $ml/min$). Under the right conditions the hippocampal slices can survive up to six hours under the microscope.

## 7.2 Electrophysiological Recordings

For measuring single cell activity intracellular whole-cell patch clamp is done using borosilicate glass capillaries (GC150F-10 Harvard Apparatus) with a tip resistance around 5 $M\Omega$ pulled on a vertical puller (Narishige, Japan). Pipettes are filled with internal solution containing (in $mM$): KCl, 17.5; K-gluconate, 122.5; NaCl, 9; MgCl2, 1; Mg-ATP (adenosine triphosphat),



Die approbierte gedruckte Originalversion dieser Diplomarbeit ist an der TU Wien Bibliothek verfügbar
The approved original version of this thesis is available in print at TU Wien Bibliothek.
TU Bibliothek Your knowledge hub WIEN

3; GTP-Tris (guanosine triphosphate tris salt), 0.3; HEPES (buffering agent), 1; EGTA (ethylene glycol tetraacetic acid), 0.2; pH is adjusted to 7.2 using KOH. Oscillations are induced by bath application of carbachol which excites hippocampal neurons and increases their activities to study neuronal network synchronization. [ Traub et al., (2001) ][ Pálhalmi et al., (2004) ] Recordings are performed in current clamp mode. To ensure comparability between PC spiking frequency in different recordings, a baseline current is injected to maintain PC potential between -40 $mV$ and -50 $mV$. Therefore, we use the amplifier MultiClamp 700B (Molecular Devices) and WinWCP and WinEDR softwares implemented by Dr. J. Dempster (University of Strathclyde, Glasgow, UK) [1]. Simulations and analysis are done with Matlab (version 2009a and 2011a, The Mathworks, Inc) and custom-made software that reads membrane voltage and generates current commands. The sampling rate of the recording setup is 10 $kHz$. This means the system records a value every 0.1 $ms$. The real-time computer has a sampling rate of 20 $kHz$, thus is writing every 0.05 $ms$ a value to a file which is used for post-analysis.

## 7.3 Data Analysis

Data analysis programs are written in Matlab. To quantify the influence of inhibition and excitation to the phenomenon of synchrony and rhythmicity of pyramidal cells, a synchrony index (SI) is used. The spike times of all neurons are identified by a threshold mechanism (-20 $mV$) and a vector containing series of 0s (no spike) and 1s (spike) for each neuron is created. One vector has a length of 1 200 000 values (= 120 000 milliseconds of recording times 10 for the sampling rate). For the reason of comparability, the first 30 seconds and the last 30 seconds in all recordings are removed. The cross-correlation between individual neurons is inferred using the *coeff* parameter which normalizes between 0 and 1 (it produces correlations identically equal to 1 at zero lag). It is used to compare the peaks of the cross-correlograms (CCG) across groups because it does not depend on the number of spikes as we need for our analysis. Other studies working on synchrony for example use autocorrelograms and calculate a SI which usually includes both metric synchrony and rhythmicity in one value [ Maex and De Schutter, (1998) ]. We further smooth the data in the column vector of the CCG using a moving average filter. The bins for the CCG have a width of 10 $ms$. CCGs of selected spike trains are shown in Fig. 7.1.

To measure synchrony we use the peak of the normalized CCG near 0 $ms$. Spikes within a 100 $ms$ window (+/- 50 $ms$) are defined as synchronous. The variables *t1_spktrain* and *t2_spktrain* in the following formula denote the firing vectors, including 0s for no spike and 1s for detected spikes. The parameter *srate* is the sampling rate in Hertz.

```
srate = 10000;
[CCG lags] = xcorr(t1_spktrain,t2_spktrain,srate,'coeff');
CCG = smooth(CCG,100);
normCCG = CCG/sqrt(length(t1)*length(t2));
I = find(lags > -50 & lags < 50);
synchronyindex = max(normCCG(I));
```

[1] http://spider.science.strath.ac.uk/sipbs/



Die approbierte gedruckte Originalversion dieser Diplomarbeit ist an der TU Wien Bibliothek verfügbar
The approved original version of this thesis is available in print at TU Wien Bibliothek.
TU Bibliothek Your knowledge hub WIEN

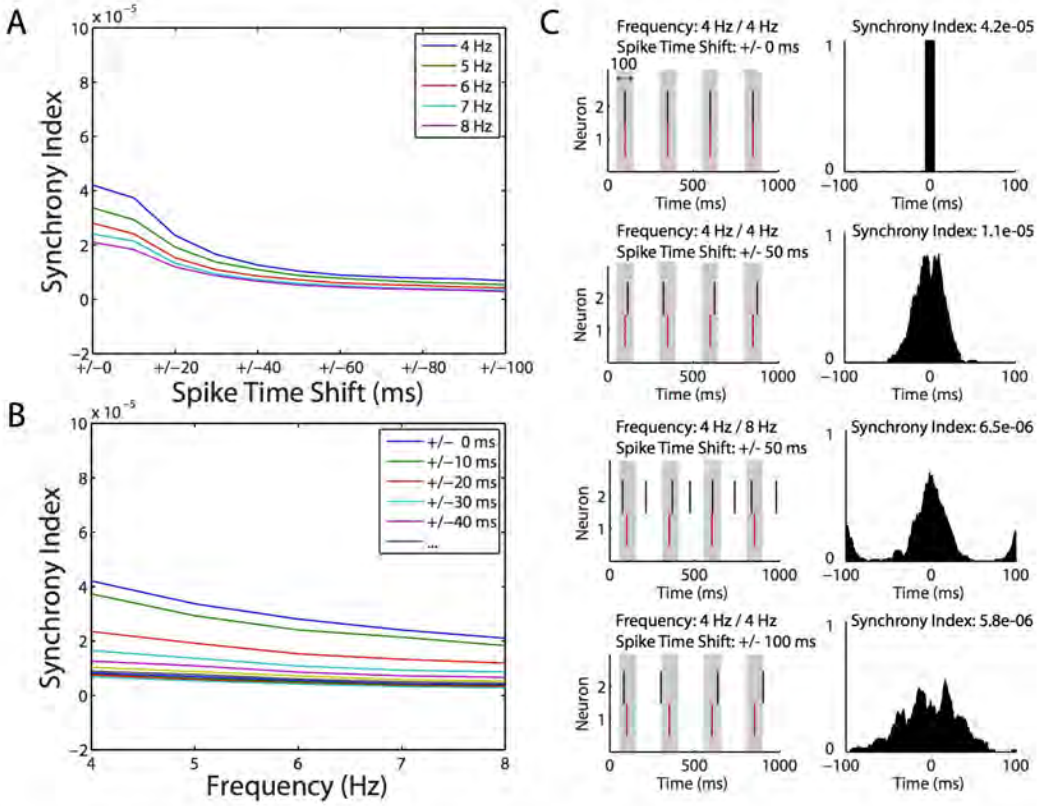



**Figure 7.1:** Synchrony index (SI) ensures comparability across recordings. A: The influence of time shifts of action potentials when spike times of Neuron 2 are moved within a window of +/- 10 $ms$ (and multiples) relative to Neuron 1. The bigger the shift (normally distributed pseudorandom numbers within a certain time window) the lower is the SI independent of the frequency. B: The stability of the SI over frequency tested for selected spike time shifts. C: Four cases of simulated spike trains (60 $sec$) for two neurons represented as rasterplots and cross-correlograms. To quantify synchronization, the synchrony index considers only spike times of Neuron 2 if they are within a window of 100 ms (gray box) relative to a Neuron 1.

Figure 7.1 shows the behavior of the synchrony index when varying the spiking frequency of the two neurons as well as shifting one signal with normally distributed shifts in a certain range. Both the synchrony measure and the CCG are symmetric. Recordings that showed no synchronization with carbachol or outliers (= more than 1.5 times the interquartile distance) were disconsidered. For testing whether differences in the SI are significant a one-tailed student t-test is applied. A p-value of $< 0.05$ shows significant results.



Die approbierte gedruckte Originalversion dieser Diplomarbeit ist an der TU Wien Bibliothek verfügbar
The approved original version of this thesis is available in print at TU Wien Bibliothek.

TU WIEN Bibliothek Your knowledge hub
Die approbierte gedruckte Originalversion dieser Diplomarbeit ist an der TU Wien Bibliothek verfügbar
The approved original version of this thesis is available in print at TU Wien Bibliothek.

Die approbierte gedruckte Originalversion dieser Diplomarbeit ist an der TU Wien Bibliothek verfügbar
The approved original version of this thesis is available in print at TU Wien Bibliothek.

CHAPTER 8

# Results

This chapter shows how different hybrid neuronal network connections are able to synchronize two patched pyramidal cells in the hippocampus. The mechanisms of neuronal synchronization are dependent on a lot of different and complex processes ranging from macro- to microscale activities. We believe that knowing the fundamental mechanisms causing synchronization in microcircuits can help to further understand how larger networks synchronize. Therefore, this chapter puts its focus on the effects of single neurons when behaving in specific hippocampal networks and shows the effects of intrinsic membrane mechanisms such as the HCN channels, when blocking them pharmacologically.

## 8.1 Synchronization in Hybrid Networks

Traditionally it was assumed that the main source of neuronal synchronization are excitatory connections between cells. Common excitation would trigger synchronous actionpotentials in a cell's postsynaptic neurons. But then modeling studies showed quite the opposite, claiming that excitatory connections between pyramidal cells alone do not synchronize their activities. Moreover, inhibition coming from fast-spiking basket cells seems to be the main driver for any kind of cell synchronization [ Whittington et al., (1997) ][ Börgers and Kopell, (2003) ]. This sounds conflicting because the effects of inhibition and excitation are fairly different. The best way to investigate this uncertainty would probably be to record the activities of a multitude of neurons simultaneously. However, since there are limitations when trying to record from larger numbers of neurons at the same time, studying the main principles causing synchronization on single cells in defined microcircuits is the most promising approach. Therefore, we studied eight different biological realistic hippocampal microcircuits in order to prove their ability to synchronize pyramidal cells.

## 8.2 Synchronization Depends on the Network Connectivity

Testing the effects of various anatomically realistic hybrid microcircuits in the hippocampus, we found out that network connectivity plays a very important role in pyramidal cell synchronization. Figure 8.1 and 8.2 show that already the modification of a single connection can dramatically disrupt the PC synchronization.

When patching two unconnected CA1 pyramidal cells in the hippocampus and applying 10 $\mu M$ carbachol extracellularly to evoke oscillations, it seems intuitive that the PCs spike independently from each other. Figure 8.1 C (upper panel) shows an example recording of two ordinary PCs. Looking at the times of their action potentials no dependencies of their spike times can be detected. Sometimes these neurons fire almost at the same time, sometimes they spike antiphase, but most of the time their APs seem to occur at unpredictable points in time. In our experiments, a typical PC spikes with about 4 $Hz$ to 8 $Hz$. Compared to fast-spiking interneurons which tend to spike in gamma, i.e. with at least 30 $Hz$ and therefore approximately every 30 $ms$, the spiking frequency of PCs is quite low. Assuming that both PCs fire with about 4 $Hz$, this means that one PC has a window of approximately 250 $ms$ to generate its spike. Theoretically it can occur at the same time as the AP of the second PC, but also up to 250 $ms$ delayed. Therefore, it is quite likely that two unconnected PCs fire at different times. Based on this typical interspike interval of approximately 250 $ms$ for PCs, we defined two spikes as synchronous if the actionpotential of neuron 1 occurs within +/- 50 $ms$ relative to the actionpotential of neuron 2 (for details see chapter 7).

Since real pyramidal cells do not necessarily spike with exactly the same frequency or even can skip cycles we calculated the cross-correlation of their spike times in order to detect similarities and synchronous events. Figure 8.1 D (upper panel) shows the mean cross-correlogram for two unconnected PCs. The flat distribution of the time delays between the spikes is a clear indication that there is no relationship between the cells. This means that randomly patched pyramidal cells tend to spike asynchronously.

However, the goal of this study was to connect these two pyramidal cells artificially in order to find a network configuration which is able to synchronize these cells. It turned out that connecting the two living PCs with a fast-spiking interneuron (Figure 8.1 A) caused the PCs to synchronize their actionpotentials. The network which is able to generate stable synchronization between the two PCs consists of both excitatory and inhibitory connections. Thereby the interneuron functions as a rhythmic pacemaker in the network. It seems that the inhibitory connections of the spontaneously active interneuron slow down the activities of both PCs, whereas the excitatory connection between the PCs causes the red pyramidal cell to spike if the black one has fired. This can also be seen from the mean cross-correlogram. The mean time delay of a spike of neuron 1 (red) compared to a spike of neuron 2 (black) is about 10 $ms$ to 15 $ms$. Also looking at the voltage and current traces in Figure 8.1 C, one can see that the action potentials of neuron 1 are slightly delayed compared to the APs of neuron 2. Note, that not every excitation of neuron 2 causes an AP in neuron 1.



Die approbierte gedruckte Originalversion dieser Diplomarbeit ist an der TU Wien Bibliothek verfügbar
The approved original version of this thesis is available in print at TU Wien Bibliothek.
TU Bibliothek Your knowledge hub WIEN

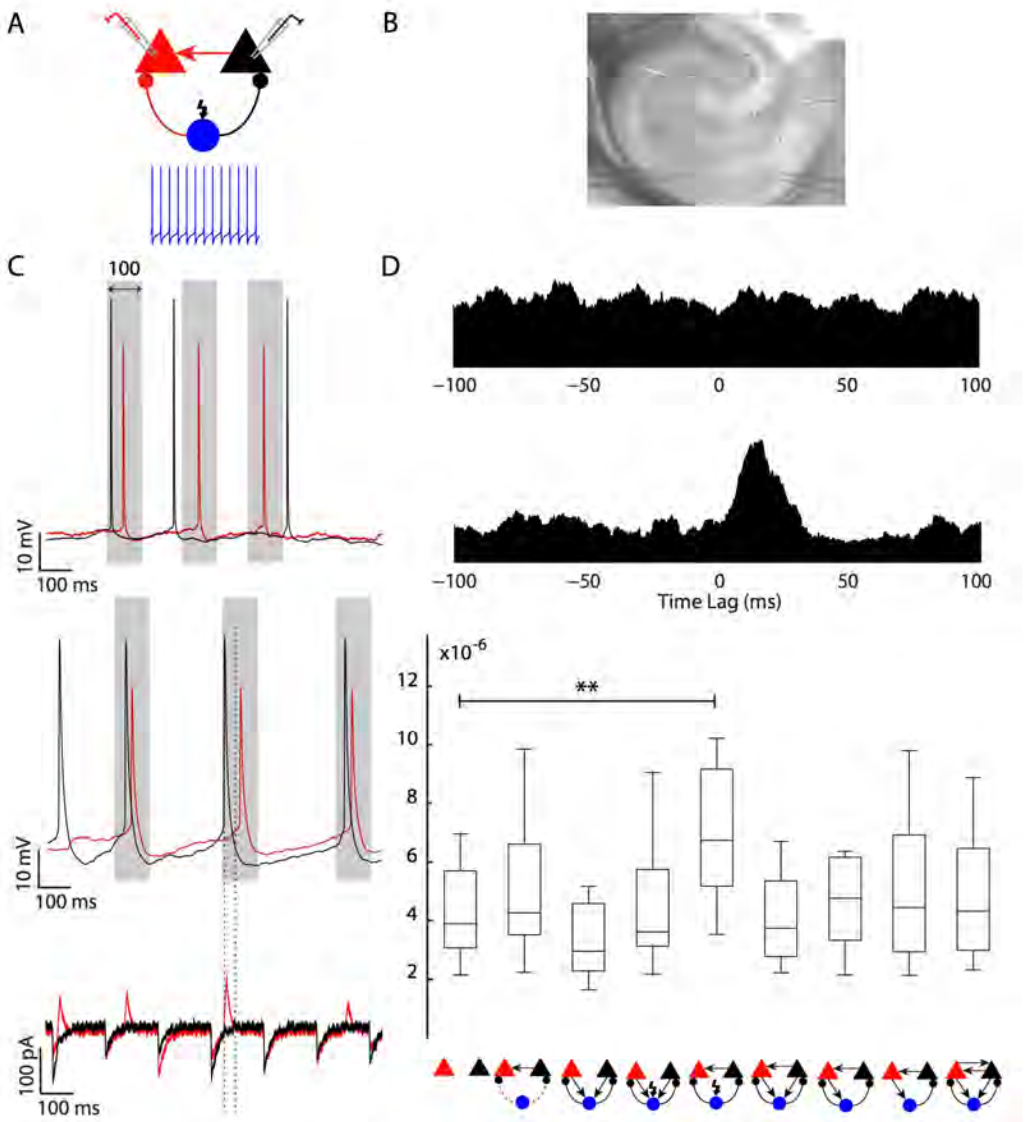



**Figure 8.1:** Synchronization depends on the network connectivity. A: Schematic representation of a hybrid neuronal network causing stable synchrony between two CA1 pyramidal cells (red and black triangle). B: Bright field microscopy image of the hippocampal formation including two patched CA1 pyramidal cells. C: Selected spike trains of the control case (top panel) and the synchronizing hybrid neuronal network from A (middle panel) are shown. The synaptic currents (bottom panel) are simulated by the real-time computer and fed back to the patched cells. D: Mean cross-correlogram (CCG) of two unconnected CA1 pyramidal cells (top panel). The two cells spike independently from each other. Bottom panel: Mean CCG of two pyramidal cells connected to a fast-spiking interneuron as shown in A. The mean CCG exhibits a clear peak around 0 $ms$ meaning that the two PCs are synchronized. E: Box plots of the synchrony indices of all eight network configurations (insets) and the control case. ** p-value < 0.01, n = 12.



Die approbierte gedruckte Originalversion dieser Diplomarbeit ist an der TU Wien Bibliothek verfügbar
The approved original version of this thesis is available in print at TU Wien Bibliothek.
TU Bibliothek Your knowledge hub WIEN

## 8.3 Excitatory Connections Mobilize Neurons

Depending on their type of connections, different cell types are capable to synchronize their firing times. Figure 8.1 suggests that excitation can play an important role in synchronizing specific cells. The group of Netoff studied glutamatergic stellate cells of the medial entorhinal cortex and GABAergic oriens-lacunosum-moleculare interneurons of the CA1 region in the hippocampus using the dynamic clamp technique. When coupling a real, patched stellate cell with a modeled one they found out that excitatory networks can generate stable synchrony between these two cells. The neurons clearly synchronized better with excitation than with inhibition. When studying the influence of excitatory and inhibitory connections on the synchronization of two O-LM interneurons (one real and one modeled), they could also see that excitatory connections were able to synchronize their spike times whereas when coupling them by inhibitory connections, the cells phase-locked in anti-synchrony. [ Netoff et al., (2005) ] These findings suggest that excitation indeed is able to synchronize the spike times of specific neurons. On the other hand, connecting two real stellate cells (instead of one real and one modeled) showed a slightly different behavior. The two cells fired still together but with bigger time delays between their synchronous spikes. The synchronization became noisier and the cross-correlograms flatter. This uncertainty and moderate difference in synchronization seems to arise from the fact of using living, biological cells which can differ a bit in certain properties.

Because of the findings above, we also investigated the effects of excitatory connections between two principal cells which are known to form excitatory synapses. Therefore, we coupled the two living pyramidal cells by a computer-controlled excitatory connection (Fig. 8.2, network 1). It turned out that this type of connection was not able to synchronize the two patched PCs. The mean CCG of network 1 shows no clear peak. Note, the artificial interneuron in the figure is not active (dashed lines for non active inhibitory connections) but denotes the computer which simulates the connection between the two patched cells. However, looking at the synchrony indices of network 1 (Fig. 8.1 E), one can see that there is a big variation of their values over the different recordings, meaning that no stable synchronization occurred.

## 8.4 Feedback Connections in the Network

Our experiments suggest that a network configuration such as shown in Fig. 8.1 A causes stable synchronization between two real pyramidal cells. This network consists of both excitatory and inhibitory connections. Since excitation alone does not necessarily synchronize the PCs firing times, there is probably an essential influence of interneuronal inhibition. [ Whittington et al., (1995) ][ Kopell et al., (2010) ] As fast-spiking basket cells are believed to be the pacemakers in neuronal networks, we further investigated their influence on the synchronization of PCs. Therefore, we built a network in which the interneuron was not spontaneously active, but received excitation from a feedback connection (Fig. 8.2, network 6). Although the mean CCG shows a small peak, the synchrony indices of network 6 (Fig. 8.1 E) do not show higher synchronization of the PCs.



Die approbierte gedruckte Originalversion dieser Diplomarbeit ist an der TU Wien Bibliothek verfügbar
The approved original version of this thesis is available in print at TU Wien Bibliothek.
TU Bibliothek Your knowledge hub WIEN

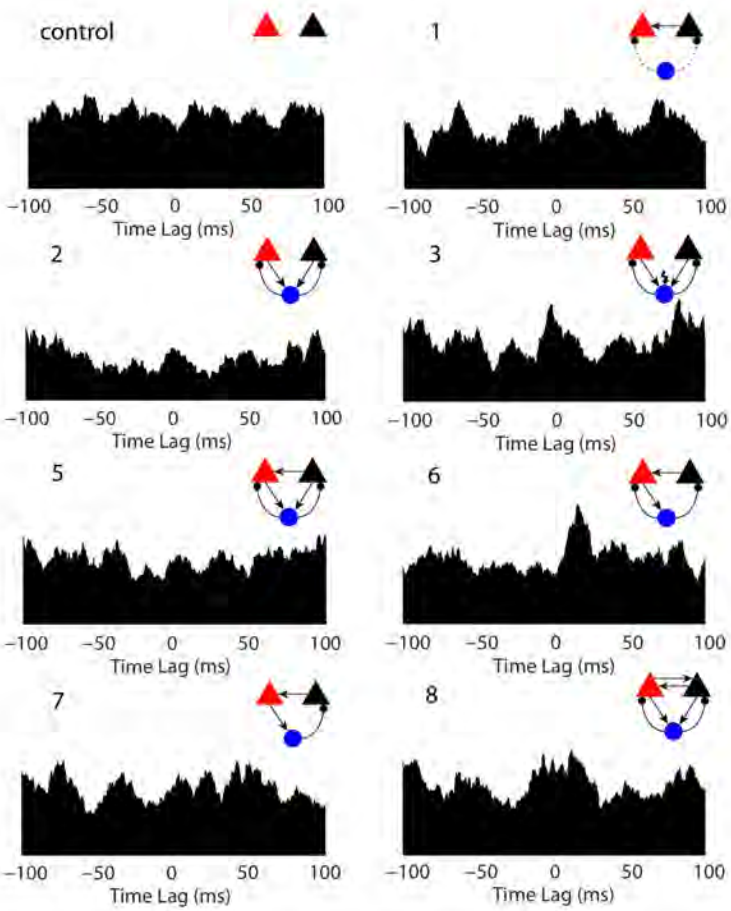



**Figure 8.2:** Mean cross-correlograms of eight neuronal networks. Two pyramidal cells (red and black triangle) are connected to a fast-spiking interneuron (blue circle) according to the connection scheme shown in the inset. In the control, pyramidal cells spike independently from each other in the presence of 10 $\mu M$ carbachol. None of the seven hybrid neuronal networks causes stable synchronization of the pyramidal cells. n = 12.

Investigating the feedback connections alone, we removed the excitatory connection between the PCs and connected both PCs with the interneuron (Fig. 8.2, network 2 and 3). Although the PCs do not seem to synchronize, one can see that the variation of the synchrony indices of network 2 (Fig. 8.1 E) decreases over the different recordings. Thus, the feedback connections made our recordings more stable. In network 3 we introduced a stimulus to the basket cell in order to study the effects of a spontaneously active interneuron and its ability to synchronize PCs. The interneuron was spiking with about 15 $Hz$. However, it was not able to cause the PCs to fire together. Moreover, the stabilizing effect of the feedback connections was gone. In some recordings high synchronization was measured, whereas in other less synchronization was seen.



Die approbierte gedruckte Originalversion dieser Diplomarbeit ist an der TU Wien Bibliothek verfügbar
The approved original version of this thesis is available in print at TU Wien Bibliothek.
TU Bibliothek Your knowledge hub WIEN

## 8.5 Membrane Mechanisms of a Neuron

Besides neuronal connectivity, specific channel characteristics of a cell can change its excitability. In fact, neurons are electrically excitable because of differences in concentration of certain ions inside and outside the cell. Neurons usually consist of a multitude of different ion channels in their membranes which are used to let ions pass in order to compensate these differences in ion concentration. Some ion channels are voltage gated, meaning that they can be opened and closed by changing the potential difference across the cell's membrane. Others are chemically gated, meaning that they can be opened and closed by chemical interactions. However, most of these ion channels are only permeable to specific types of ions, such as sodium ($Na^+$), potassium ($K^+$), chloride ($Cl^-$) and calcium ($Ca^{2+}$) which are the most important ions for neurological processes. Already small differences in concentration can lead to notable differences in the firing characteristics of a cell and therefore can change its synchronization properties. Also changes in a channel's conductance has a considerable influence on the cell's firing activities.

For most currents, especially the ones taking part in the gating mechanisms of sodium or potassium channels, increasing voltage increases their conductances. But for the hyperpolarization-activated cyclic-nucleotide cation channel current Ih increasing voltage decreases its channel conductance. Ih is a mixed $Na^+$ and $K^+$, depolarizing current that is activated by hyperpolarization and influences the cells resting membrane potential. It is able to modulate a cell's excitability and therefore plays an important role in pacing rhythms of neurons. As inhibition hyperpolarizes a cell, it activates Ih which in turn raises the cell's voltage and may cause APs.

There are four different subtypes of HCN channels (HCN1-4) [ Santoro and Tibbs, (1999) ]. The different subtypes are characterized by the membrane potential at which Ih is 50% activated ($V_{1/2}$) and by their sensitivity to the nucleotide *cyclic adenosine monophosphate* (cAMP). HCN1 channels are the fastest because they are activated with a relatively depolarized membrane voltage and have a low sensitivity to cAMP. HCN4 channels on the other side are slowly activated because of a more hyperpolarized $V_{1/2}$ and they are strongly sensitive to cAMP. Studies showed that the HCN channels are non-uniformly expressed throughout the central nervous system of mice. The hippocampus has a high density of HCN1 channels whereas other brain regions contain fewer HCN1 channels. The expression of HCN channels also differs between pyramidal cells and interneurons as well as their subtypes. It even differs between parts of a single cell. Distal dendrites of PCs were shown to contain more HCN channels than perisomatic regions of the same cell. [ Santoro, (2000) ][ Leão et al., (2005) ]

## 8.6 The Effects of Ih

It is believed that Ih has a stabilizing effect on the subthreshold activity of a cell by causing its channels to generate a depolarizing current [ Santoro and Tibbs, (1999) ]. This depolarizing influence can increase the cell's resting membrane potential by approximately 10 $mV$. Furthermore Ih is able to influence oscillatory activities by shifting the theta rhythm in the hippocampus. [ Magee, (2001) ][ Chen et al., (2002) ][ Shah et al., (2004) ][ Rotstein et al., (2005) ]



Die approbierte gedruckte Originalversion dieser Diplomarbeit ist an der TU Wien Bibliothek verfügbar
The approved original version of this thesis is available in print at TU Wien Bibliothek.
TU Bibliothek Your knowledge hub WIEN

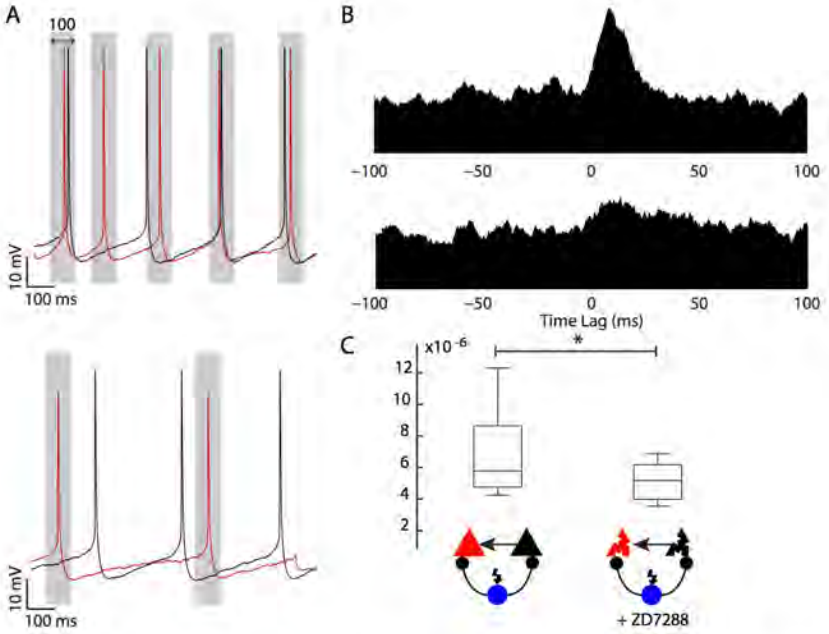



**Figure 8.3:** ZD7288 disrupts synchronization in neuronal networks. A: Selected spike trains from two pyramidal cells in the synchronizing hybrid neuronal network without (top panel) and with application of 10 $\mu M$ ZD7288 (bottom panel) are shown. B: Mean cross-correlograms (CCG) for the hybrid neuronal network without (top panel) and with application of ZD7288 (bottom panel) are shown. There is a clear peak around 0 $ms$ in the top mean CCG, meaning that the two pyramidal cells tend to spike synchronously. ZD7288 disrupts this synchronization, indicated by a flat mean CCG (bottom). C: Box plots of the synchrony indices of the two networks. * p-value < 0.05, n = 12.

Since Ih seems to have an essential influence on the rhythmic firing of cells, we investigated its ability of synchronizing neurons. Therefore, we built the same hybrid neuronal network as before consisting of two patched CA1 PCs and an artificial real-time interneuron. The schematic representation of the connectivity can be seen in Fig. 8.3 C. It is the same network which was shown to cause stable synchronization between the two patched pyramidal cells. For the pharmacological blocking of the HCN channels we applied the organic antagonist ZD7288 (10 $\mu M$) extracellularly. This downregulation of Ih should increase EPSPs and as a consequence increase the cell's firing. [ George et al., (2009) ] showed that Ih is able to enhance spike firing in response to an EPSP when the spike threshold is low. On the other side it inhibits firing when the spike threshold is high. This could be one reason why the spiking frequency of the PCs in our hybrid neuronal network decreased, since the strong interneuronal inhibition hyperpolarized the cells and inhibited their firing. It finally turned out that these low firing PCs lost their ability to synchronize. Figure 8.3 shows selected spike trains and the mean CCGs of our hybrid neuronal network with and without application of ZD7288.



Die approbierte gedruckte Originalversion dieser Diplomarbeit ist an der TU Wien Bibliothek verfügbar
The approved original version of this thesis is available in print at TU Wien Bibliothek.
TU Bibliothek Your knowledge hub WIEN

TU WIEN Bibliothek Your knowledge hub
Die approbierte gedruckte Originalversion dieser Diplomarbeit ist an der TU Wien Bibliothek verfügbar
The approved original version of this thesis is available in print at TU Wien Bibliothek.

# CHAPTER 9

# Discussion

This study presents a novel approach for investigating ongoing phenomena concerning synchronization in hippocampal microcircuits. Since the ability to record from large numbers of cells simultaneously and in single-cell-precision is limited, we use a hybrid method to study neuronal network dynamics caused by the activities of single neurons within this network. This technique, which allows us to introduce to specific neurons the synaptic response from other cells during network activity, is called *dynamic clamp*. It gives us the possibility to couple single cells and build different neuronal networks [ Sharp et al., (1993a) ]. Living cells can be connected to a real-time computer, which is used to simulate neuronal processes, ranging from simple synaptic conductances to more complex models of whole cells.

Our initial purpose of using the dynamic clamp technique was to study the role of fast-spiking basket cells and how they influence the synchronization of pyramidal cells. This hybrid approach allows us to better understand several aspects of interneuronal inhibition and its importance for neuronal synchronization. Furthermore, we can investigate a variety of other network connectivity patterns and the role of excitatory and inhibitory currents. The ultimate goal was to understand how pyramidal cells should be coupled in order to cause them to spike in synchrony. Our results, showing specific connectivity patterns for two pyramidal cells and one basket cell, are promising indications of how larger neuronal networks in the hippocampus synchronize. We show network configurations, which enable the involved cells to fire together.

In this study, we have investigated pyramidal cells in the CA1 region of the hippocampus and fast-spiking basket cells to determine the role of inhibitory and excitatory postsynaptic currents. Our results of recording from two hippocampal pyramidal cells, when connecting them to an artificial interneuron on a real-time computer, indicate that both excitatory as well as inhibitory connections play an essential role in pyramidal cell synchronization. Modeling studies on layer II stellate cells of the medial entorhinal cortex [ Acker et al., (2003) ] showed that these cells are able to synchronize when receiving excitation and not with inhibition. Furthermore, recent studies using a hybrid approach could show that these excitatory stellate cells synchronize in



Die approbierte gedruckte Originalversion dieser Diplomarbeit ist an der TU Wien Bibliothek verfügbar
The approved original version of this thesis is available in print at TU Wien Bibliothek.
TU Bibliothek Your knowledge hub WIEN

phase via monosynaptic connections [ Netoff et al., (2005) ] and that conduction delays can cause stable synchronization in hybrid neuronal networks of the entorhinal cortex [ Wang et al., (2012) ]. Following these studies, we investigated the effects of excitatory connections between the principal cells in the hippocampus and their ability to synchronize these type of neurons. In accordance with our studies, we could see that CA1 pyramidal cells in the hippocampus are not able to synchronize their spike times by single excitation. The two PCs still tend to spike independently of each other. Unidirectional excitation, from one cell to the other but not back, seems to be too weak or too little for causing the cells to spike together.

Instead, pyramidal cell synchronization occurs if the PCs are driven by fast-spiking basket cells. In that regard, the basket cells were shown to be the pacemakers of hippocampal network activities and therefore the main source for synchronization [ Wang and Buzsáki, (1996) ]. Our results show that the introduction of a fast-spiking interneuron increased the level of synchrony. Simulations of cortical pyramidal neurons showed that these cells can be synchronized by inhibitory interneurons [ Lytton and Sejnowski, (1991) ]. These type of neurons seem to control the rhythm in the network. Indeed, they are able to synchronize themselves [ Wang and Buzsáki, (1996) ]. A synchronized network of basket cells provides its postsynaptic neurons with correlated inputs, which makes it comprehensible to accept the importance of this interneuronal inhibition.

Our results that the greatest level of pyramidal cell synchronization was produced when eliminating the feedback connections from PCs to the interneuron seems contradictory to some modeling studies [ Van Vreeswijk et al., (1994) ][ Hansel et al., (1995) ]. However, we could observe that interneurons are essential to synchronize the firing times of PCs in the hippocampus by their inhibitory connections. A spontaneously active interneuron was needed to synchronize two pyramidal cells when one PC was exciting the other. But how stable is this synchronization and what could disrupt simultaneously spiking pyramidal cells?

Besides synaptic inputs, intrinsic membrane mechanisms can also influence the firing properties of cells and in consequence their ability to synchronize. Pyramidal cells are known to express hyperpolarization activated currents that are believed to contribute to network oscillations. The h-current (Ih) plays an important role in regulating neuronal excitability, particularly in hippocampal and neocortical pyramidal neurons. It has a stabilizing effect on the subthreshold activity of a cell by causing its channels to generate a depolarizing current. This current was shown to actively shift the theta rhythm in the hippocampus and influence a cell's synchronization properties. Pathologically, ih contributes to epileptiform activity [ Magee, (2001) ][ Chen et al., (2002) ]. Therefore, we pharmacologically blocked the HCN channels by extracellular application of the antagonist ZD7288 in order to study changes in synchronization properties of PCs. We could observe, that blocking of the HCN channels dramatically impaired pyramidal cell synchronization. The spiking frequency of the pyramidal cells decreased leading to less synchronized activities of the two patched cells. Both the blockage of Ih and the interneuronal inhibition together lowered the PCs spiking frequency which in turn could cause the disruption of the synchronization.



Die approbierte gedruckte Originalversion dieser Diplomarbeit ist an der TU Wien Bibliothek verfügbar
The approved original version of this thesis is available in print at TU Wien Bibliothek.
TU Bibliothek Your knowledge hub WIEN

Summing up, our results show that both intrinsic membrane mechanisms as well as specific connectivity patterns determine how pyramidal cells in the hippocampus synchronize their action potentials. We investigated CA1 pyramidal cells which are shown to form fewer synapses to neighboring PCs, compared to CA3 pyramidal cells. This missing excitatory connection could also be a reason why CA3 usually shows higher synchrony between its pyramidal cells than CA1. [ Andersen et al., (2006) ]. We could observe in our experiments that an excitatory connection between the CA1 pyramidal cells is needed to cause their synchronization. Therefore, it will be interesting to also investigate several connectivity patterns in the CA3 region in order to find further explanations for the involved processes in the synchronization of neurons.

One reason could be the contribution of other cells and their signals. Since we are patching two living pyramidal cells in a 400 $\mu m$ thick horizontal slice, there are still a lot of other active neurons present in the tissue. These neurons are alive and can have an essential influence on our hybrid network by sending synaptic inputs to the patched cells. Future experiments will include the pharmacological blocking of excitatory and inhibitory inputs. The application of three specific receptor antagonists is planned. To prevent the patched cells from receiving excitatory inputs, we are planning to block the main glutamatergic receptors, namely NMDA receptors by application of dAP5 and AMPA receptors by application of CNQX. We are also planning to block GABA receptors with picrotoxin (PTX) in order to turn off inhibitory inputs from connected basket cells. With this experiments we hope to further gain insight into the complex mechanisms taking place in the hippocampus in order to decode the phenomenon of neuronal synchronization.



Die approbierte gedruckte Originalversion dieser Diplomarbeit ist an der TU Wien Bibliothek verfügbar
The approved original version of this thesis is available in print at TU Wien Bibliothek.
TU Bibliothek Your knowledge hub WIEN

TU WIEN Bibliothek Your knowledge hub
Die approbierte gedruckte Originalversion dieser Diplomarbeit ist an der TU Wien Bibliothek verfügbar
The approved original version of this thesis is available in print at TU Wien Bibliothek.

APPENDIX A

# Abbreviations

**ACSF** artificial cerebrospinal fluid

**AP** action potential

**API** application programming interface

**BC** basket cell

**CA** cornu ammonis

**cAMP** cyclic adenosine monophosphate

**CCG** cross-correlogram

**Comedi** Control and Measurement Device Interface

**DAQ** data acquisition

**DG** dentate gyrus

**EC** entorhinal cortex

**EPSC** excitatory postsynaptic current

**EPSP** excitatory postsynaptic potential

**FIFO** first in first out

**GABA** gamma-aminobutyric acid

**HCN** Hyperpolarization-activated cyclic-nucleotide

**HH** Hodgkin–Huxley



Die approbierte gedruckte Originalversion dieser Diplomarbeit ist an der TU Wien Bibliothek verfügbar
The approved original version of this thesis is available in print at TU Wien Bibliothek.
TU Bibliothek Your knowledge hub WIEN

**Ih** HCN cation channel current

**IPSC** inhibitory postsynaptic current

**IPSP** inhibitory postsynaptic potential

**O-LM** oriens-lacunosum-moleculare

**P-LM** pyramidale-lacunosum-moleculare

**PC** pyramidal cell

**PTX** picrotoxin

**R-LM** radiatum-lacunosum-moleculare

**REM sleep** rapid eye movement sleep

**RTAI** Real Time Application Interface

**SI** synchrony index

**Sub** subiculum



Die approbierte gedruckte Originalversion dieser Diplomarbeit ist an der TU Wien Bibliothek verfügbar
The approved original version of this thesis is available in print at TU Wien Bibliothek.
TU Bibliothek Your knowledge hub WIEN

# APPENDIX B

# Source Code

**Listing B.1:** Host Code: Basket.m

```
% Markus Michael Hilscher – 0727932
% Basket.m
% Model of a fast–spiking interneuron

clear;
tic

%% User Input
EndOfSimulation = 700; % Simulation time in ms
dt = 0.05; % step for Euler
phi = 3.33; % Wang and Buszaki (1996) show phi = 5, 3.33 and 2
            % smaller phi -> IK is slower, AHP amplitude more negative
Stimulus = 0.25; % Wang and Buszaki (1996) show Stimulus = 1, 1.2 and 1.4 uA/cm^2
Starttime = 100; % starting time of the stimulus in ms
Endtime = 600; % ending time of the stimulus in ms
V = -64; % membrane voltage at the beginning in mV
Isyn = 0; % synaptic current in uA/cm^2

%% Constants
ENa = 55; % reversal potential of the Na+ current in mV
EK = -90; % reversal potential of the K+ current in mV
EL = -65; % reversal potential of the leak current in mV

gNa = 35; % conductance of the Na+ current in mS/cm^2
gK = 9; % conductance of the K+ current in mS/cm^2
gL = 0.1; % conductance of the leak current in mS/cm^2
```



Die approbierte gedruckte Originalversion dieser Diplomarbeit ist an der TU Wien Bibliothek verfügbar
The approved original version of this thesis is available in print at TU Wien Bibliothek.
TU Bibliothek Your knowledge hub WIEN

```
27
28  Cmem = 1; % membrane capacitance density in uF/cm^2
29
30  xh = 0; % inactivation variable h
31  xn = 0; % activation variable n
32  xs = 0; % gating variable s of open synaptic ion channels
33
34  gsyn = 0; % synaptic conductance in mS/cm^2
35  value = load( 'Basket.dat' ) / 10000; % load weights for the synapse
36  cntAMP = 999; % counter for the ampitude
37  spkCNT = 1; % counter for file reading
38  Isynpost = 0; % post synaptic current density in uA/cm^2
39
40  t_rec = 0;
41  x_plot = zeros(1,EndOfSimulation/dt+1);
42  y_plot = zeros(1,EndOfSimulation/dt+1);
43  y_plot_syn = zeros(1,EndOfSimulation/dt+1);
44
45  %% Program
46  for t=0:dt:EndOfSimulation
47
48      if t>=Starttime;
49          Iapp = Stimulus;
50      else
51          Iapp = 0;
52      end
53      if t>Endtime;
54          Iapp = 0;
55      end
56
57      alpham = -0.1*(V+35)/(exp(-0.1*(V+35))-1); % alpha m
58      alphah = 0.07*exp(-(V+58)/20); % alpha h
59      alphan = -0.01*(V+34)/(exp(-0.1*(V+34))-1); % alpha n
60
61      betam = 4*exp(-(V+60)/18); % beta m
62      betah = 1/(exp(-0.1*(V+28))+1); % beta h
63      betan = 0.125*exp(-(V+44)/80); % beta n
64
65      taum = 1/(alpham+betam); % taum
66      x_0m = alpham*taum; % minf
67
68      xh = xh + dt* phi*(alphah*(1-xh) - betah*xh); % dh/dt
69      xn = xn + dt* phi*(alphan*(1-xn) - betan*xn); % dn/dt
```



Die approbierte gedruckte Originalversion dieser Diplomarbeit ist an der TU Wien Bibliothek verfügbar
The approved original version of this thesis is available in print at TU Wien Bibliothek.
TU Bibliothek Your knowledge hub WIEN

```
70
71      INa = gNa*x_0m^3*xh*(V-ENa); % Na+ current
72      IK = gK*xn^4*(V-EK); % K+ current
73      IL = gL*(V-EL); % leak current
74
75      Iion = INa + IK + IL; % ionic current
76
77      V = V + dt*(-Iion -Isyn + Iapp) / Cmem; % membrane voltage
78
79      Vpre = V;
80
81      [ Isynpost, xs ] = Basket_syn(Vpre, dt, xs); % calculates the synaptic current
82      % [ Isynpost, gsyn, cntAMP, spkCNT ] = Basket_syn_dat( Vpre, dt, gsyn, value, cntAMP, spkCNT );
83      % calculates the synaptic current with lookup table
84
85      t_rec = t_rec+1;
86      x_plot(t_rec) = t;
87      y_plot(t_rec) = V;
88      y_plot_syn(t_rec) = -Isynpost;
89
90  end
91
92  toc
93
94  %% Plotting
95  figure()
96  set(gcf,'color','white')
97  set(gca,'fontsize',14)
98  cell = plot(x_plot,y_plot,'b');
99  legend('cell',2);
100 hold on;
101 y_plot_stim(1:Starttime/dt) = -80;
102 y_plot_stim(Starttime/dt+1:Endtime/dt+1) = -78;
103 y_plot_stim(Endtime/dt+2:EndOfSimulation/dt+1) = -80;
104 stimulus = plot(x_plot,y_plot_stim,'--k');
105 hold off;
106 legend([cell,stimulus],'cell','stimulus',2);
107 axis([0 EndOfSimulation -90 50]);
108 xlabel('Time (ms)');
109 ylabel('Voltage (mV)');
110
111 figure()
112 set(gcf,'color','white')
```



Die approbierte gedruckte Originalversion dieser Diplomarbeit ist an der TU Wien Bibliothek verfügbar
The approved original version of this thesis is available in print at TU Wien Bibliothek.
TU Bibliothek Your knowledge hub WIEN

```
113 set(gca,'fontsize',14)
114 synapse = plot(x_plot,y_plot_syn,'b');
115 legend(synapse,'synapse',2);
116 axis([0 EndOfSimulation -2.5 0.5]);
117 xlabel('Time (ms)');
118 ylabel('Current density (\muA/cm^2)');
```

**Listing B.2:** Host Code: Basket_syn.m

```
1  % Markus Michael Hilscher - 0727932
2  % Basket_syn.m
3  % Model of a fast-spiking interneuron
4
5  % function [ Isynpost ] = Basket_syn( Vpre, dt, xs )
6  %
7  % Contains the equations to calculate the synaptic current of a fast-spiking
8  % interneuron
9  %
10 % Input:
11 % scalar "Vpre"
12 % contains the value of the membrane potential of the simulated cell
13 %
14 % scalar "dt"
15 % contains the Euler step
16 %
17 % scalar "xs"
18 % contains the value of the gating variable s of open synaptic ion
19 % channels from the previous Euler step
20 %
21 % Output:
22 % scalar "Isynpost"
23 % contains the value of the post synaptic current density in uA/cm^2
24 %
25 % scalar "xs"
26 % contains the value of the gating variable s of open synaptic ion
27 % channels from the actual Euler step
28
29 function [ Isynpost, xs ] = Basket_syn( Vpre, dt, xs )
30
31     %% Constants
32     Esyn = -75; % synaptic reversal potential in mV
33     gsyn = 0.1; % synaptic conductance in mS/cm^2
34     thetasyn = 0; % mV
35     alphas = 12; % channel opening rate in msec^-1
```



Die approbierte gedruckte Originalversion dieser Diplomarbeit ist an der TU Wien Bibliothek verfügbar
The approved original version of this thesis is available in print at TU Wien Bibliothek.
TU Bibliothek Your knowledge hub WIEN

```
36      betas = 0.1; % channel closing rate in msec^-1
37      Vpost = -64; % post membrane potential in mV
38
39      %% Program
40      FVpre = 1/(1+exp(-(Vpre-thetasyn)/2)); % transmitter-receptor complex
41      xs = xs + dt* (alphas*FVpre*(1-xs)-betas*xs); % ds/dt
42      Isynpost = gsyn*xs*(Vpost-Esyn); % synaptic current at the postsynaptic cell
43
44  end
```

**Listing B.3:** Host Code: Basket_syn_dat.m

```
1   % Markus Michael Hilscher - 0727932
2   % Basket_syn_dat.m
3   % Model of a fast-spiking interneuron
4
5   % function [ Isynpost ] = Basket_syn( Vpre, dt, xs )
6   %
7   % Contains the equations to calculate the synaptic current of a fast-spiking
8   % interneuron
9   %
10  % Input:
11  % scalar "Vpre"
12  % contains the value of the membrane potential of the simulated cell
13  %
14  % scalar "dt"
15  % contains the Euler step
16  %
17  % scalar "gsyn"
18  % contains the value of the synaptic conductance in mS/cm^2 from the
19  % previous Euler step
20  %
21  % scalar "value"
22  % contains the weights for the synapse
23  %
24  % scalar "cntAMP"
25  % contains the counter for the ampitude from the previous Euler step
26  %
27  % scalar "spkCNT"
28  % contains the counter for file reading from the previous Euler step
29  %
30  % Output:
31  % scalar "Isynpost"
32  % contains the value of the post synaptic current density in uA/cm^2
```



Die approbierte gedruckte Originalversion dieser Diplomarbeit ist an der TU Wien Bibliothek verfügbar
The approved original version of this thesis is available in print at TU Wien Bibliothek.
TU Bibliothek Your knowledge hub WIEN

```
33 %
34 % scalar "gsyn"
35 % contains the value of the synaptic conductance in mS/cm^2 from the
36 % actual Euler step
37 %
38 % scalar "cntAMP"
39 % contains the counter for the ampitude from the actual Euler step
40 %
41 % scalar "spkCNT"
42 % contains the counter for file reading from the actual Euler step
43
44 function [ Isynpost, gsyn, cntAMP, spkCNT ] = Basket_syn_dat( Vpre, dt, gsyn, value, cntAMP, spkCNT )
45
46     %% Constants
47     Esyn = -75; % synaptic reversal potential in mV
48     Vthres = -20; % threshold potential in mV
49     Vpost = -64; % post membrane potential in mV
50     taui = 10; % tau for inhibitory synapse in msec
51
52     %% Program
53     gsyn = gsyn*(1-dt/taui); % model of inhibitory synapse
54     w=value(cntAMP+1); % weight of the synapse
55
56     if (Vpre > Vthres) % firing of fast-spiking interneuron
57         gsyn = gsyn + w; % updating synaptic weight
58         if (spkCNT==1) % interneuron starts spiking
59             if (cntAMP<1) % Isyn via synapse accoring to file from line 1000 to 1
60                 cntAMP=1000;
61             end
62             cntAMP = cntAMP - 1; % decreasing counter for reading from file
63             spkCNT=0;
64         end
65     elseif (spkCNT==0) % mv <= Vthres (not spiking) -> ready for spiking
66         spkCNT=1;
67     end
68
69     Isynpost = gsyn*(Vpost-Esyn); % synaptic current at the postsynaptic cell
70 end
```

**Listing B.4:** Host Code: Pyr_syn_dat_005.m

```
1 % Markus Michael Hilscher - 0727932
2 % Pyr_syn_dat_005.m
3 % Model of a pyramidal cell
```



Die approbierte gedruckte Originalversion dieser Diplomarbeit ist an der TU Wien Bibliothek verfügbar
The approved original version of this thesis is available in print at TU Wien Bibliothek.
TU Bibliothek Your knowledge hub WIEN

```
4
5  clear;
6  tic
7
8  %% User Input
9  EndOfSimulation = 700; % Simulation time in ms
10 dt = 0.01; % step for Euler
11 Stimulus = 0.25; % stimulus in uA/cm^2
12 Starttime = 100; % starting time of the stimulus in ms
13 Endtime = 600; % ending time of the stimulus in ms
14 V = -64; % membrane voltage at the beginning in mV
15 Isyn = 0; % synaptic current in uA/cm^2
16
17 %% Constants
18 ENa = 50; % reversal potential of the Na+ current in mV
19 EK = -100; % reversal potential of the K+ current in mV
20 EL = -67; % reversal potential of the leak current in mV
21
22 gNa = 100; % conductance of the Na+ current in mS/cm^2
23 gK = 80; % conductance of the K+ current in mS/cm^2
24 gL = 0.1; % conductance of the leak current in mS/cm^2
25
26 Cmem = 1; % membrane capacitance density in uF/cm^2
27
28 gsyn = 0; % synaptic conductance in mS/cm^2
29 gsyn_005 = 0; % synaptic conductance in mS/cm^2
30 Vthres = -20; % threshold potential in mV
31 Isynpost = 0; % post synaptic current density in uA/cm^2
32 Isynpost_005 = 0; % post synaptic current density in uA/cm^2
33 Vpost = -64; % post membrane potential in mV
34
35 value = load( 'PyrCell.dat' ) / 5; % load weights for the synapse
36 taue = 5; % tau for excitatory synapse in msec
37 cntAMP = 999; % counter for the ampitude
38 cntAMP_005 = 999; % counter for the ampitude
39 spkCNT = 1; % counter for file reading
40 spkCNT_005 = 1; % counter for file reading
41
42 xh = 0; % inactivation variable h
43 xn = 0; % activation variable n
44
45 t_rec = 0;
46 t_rec_005 = 0;
```



Die approbierte gedruckte Originalversion dieser Diplomarbeit ist an der TU Wien Bibliothek verfügbar
The approved original version of this thesis is available in print at TU Wien Bibliothek.
TU Bibliothek Your knowledge hub WIEN

```
x_plot = zeros(1,EndOfSimulation/dt+1);
y_plot = zeros(1,EndOfSimulation/dt+1);
y_plot_syn = zeros(1,EndOfSimulation/dt+1);

x_plot_005 = zeros(1,EndOfSimulation/dt/5+1);
y_plot_syn_005 = zeros(1,EndOfSimulation/dt/5+1);

EulerCounter = 0;

%% Program
for t=0:dt:EndOfSimulation

    if t>=Starttime;
        Iapp = Stimulus;
    else
        Iapp = 0;
    end
    if t>Endtime;
        Iapp = 0;
    end

    alpham = 0.32*(V+54)/(1-exp(-(V+54)/4)); % alpha m
    alphah = 0.128*exp(-(V+50)/18); % alpha h
    alphan = 0.032*(V+52)/(1-exp(-(V+52)/5)); % alpha n

    betam = 0.28*(V+27)/(exp((V+27)/5)-1); % beta m
    betah = 4/(1+exp(-(V+27)/5)); % beta h
    betan = 0.5*exp(-(V+57)/40); % beta n

    taum = 1/(alpham+betam); % taum
    x_0m = alpham*taum; % minf

    xh = xh + dt* (alphah*(1-xh) - betah*xh); % dh/dt
    xn = xn + dt* (alphan*(1-xn) - betan*xn); % dn/dt

    INa = gNa*x_0m^3*xh*(V-ENa); % Na+ current
    IK = gK*xn^4*(V-EK); % K+ current
    IL = gL*(V-EL); % leak current

    Iion = INa + IK + IL; % ionic current

    V = V+dt*(-Iion -Isyn + Iapp) / Cmem; % membrane voltage

```



Die approbierte gedruckte Originalversion dieser Diplomarbeit ist an der TU Wien Bibliothek verfügbar
The approved original version of this thesis is available in print at TU Wien Bibliothek.
TU Bibliothek Your knowledge hub WIEN

```
90      Vpre = V;
91
92      gsyn = gsyn*(1-dt/taue); % model of excitatory synapse
93      w=value(cntAMP+1);
94
95      if (Vpre > Vthres) % firing of pyramidal cell
96          gsyn = gsyn + w; % updating synaptic weight
97          if (spkCNT==1) % interneuron starts spiking
98              if (cntAMP<1) % Isyn via synapse accoring to file from line 1000 to 1
99                  cntAMP=1000;
100             end
101             cntAMP = cntAMP - 1; % decreasing counter for reading from file
102             spkCNT=0;
103         end
104     elseif (spkCNT==0) % mv <= Vthres (not spiking) -->  ready for spiking
105         spkCNT=1;
106     end
107
108     Isynpost = gsyn*(Vpost);  % no Esyn (the reversal potential for excitation is generally 0mV)
109
110     if (EulerCounter == 5 || t==0)
111         EulerCounter = 0;
112
113         Vpre_005 = V;
114
115         gsyn_005 = gsyn_005*(1-(dt*5)/taue); % model of excitatory synapse
116         w_005=value(cntAMP_005+1)*5; % *5 to get original value
117
118         if (Vpre_005 > Vthres) % firing of pyramidal cell
119             gsyn_005 = gsyn_005 + w_005; % updating synaptic weight
120             if (spkCNT_005==1) % interneuron starts spiking
121                 if (cntAMP_005<1) % Isyn via synapse accoring to file from line 1000 to 1
122                     cntAMP_005=1000;
123                 end
124                 cntAMP_005 = cntAMP_005 - 1; % decreasing counter for reading from file
125                 spkCNT_005=0;
126             end
127         elseif (spkCNT_005==0) % mv <= Vthres (not spiking) -->  ready for spiking
128             spkCNT_005=1;
129         end
130
131         Isynpost_005 = gsyn_005*(Vpost); % no Esyn
132
```



Die approbierte gedruckte Originalversion dieser Diplomarbeit ist an der TU Wien Bibliothek verfügbar
The approved original version of this thesis is available in print at TU Wien Bibliothek.
TU Bibliothek Your knowledge hub WIEN

```
133             t_rec_005 = t_rec_005+1;
134             x_plot_005(t_rec_005) = t;
135             y_plot_syn_005(t_rec_005) = -Isynpost_005;
136         end
137
138         t_rec = t_rec+1;
139         x_plot(t_rec) = t;
140         y_plot(t_rec) = V;
141         y_plot_syn(t_rec) = -Isynpost;
142
143         EulerCounter = EulerCounter + 1;
144     end
145
146     toc
147
148     %% Plotting
149     figure()
150     set(gcf,'color','white')
151     set(gca,'fontsize',14)
152     cell = plot(x_plot,y_plot,'r');
153     legend('cell',2);
154     hold on;
155     y_plot_stim(1:Starttime/dt) = -105;
156     y_plot_stim(Starttime/dt+1:Endtime/dt+1) = -103;
157     y_plot_stim(Endtime/dt+2:EndOfSimulation/dt+1) = -105;
158     stimulus = plot(x_plot,y_plot_stim,'--k');
159     hold off;
160     legend([cell,stimulus],'cell','stimulus',2);
161     axis([0 EndOfSimulation -115 60]);
162     xlabel('Time (ms)');
163     ylabel('Voltage (mV)');
164
165     figure()
166     set(gcf,'color','white')
167     set(gca,'fontsize',14)
168     synapse = plot(x_plot,y_plot_syn,'r');
169     legend(synapse,'synapse',2);
170     axis([0 EndOfSimulation -0.5 4]);
171     xlabel('Time (ms)');
172     ylabel('Current density (\muA/cm^2)');
173
174     figure()
175     set(gcf,'color','white')
```



Die approbierte gedruckte Originalversion dieser Diplomarbeit ist an der TU Wien Bibliothek verfügbar
The approved original version of this thesis is available in print at TU Wien Bibliothek.
TU Bibliothek Your knowledge hub WIEN

```
176 set(gca,'fontsize',14)
177 synapse = plot(x_plot_005,y_plot_syn_005,'r');
178 legend(synapse,'synapse',2);
179 axis([0 EndOfSimulation -0.5 4]);
180 xlabel('Time (ms)');
181 ylabel('Current density (\muA/cm^2)');
```

**Listing B.5:** Host Code: myrt_process.c

```
1  #include <linux/module.h> // header files for RTAI calculation
2  #include <asm/io.h> // and user space - kernel space communication
3  #include <math.h>
4  #include <rtai.h>
5  #include <rtai_sched.h>
6  #include <rtai_fifos.h>
7  #include <linux/comedi.h> // header files for data acquistion with the
8  #include <linux/comedilib.h> // complete interface of Comedi
9
10 #define TICK_PERIOD 50000 // tickrate: 50000 ns = 0.050 ms -> 20 kHz
11 #define TASK_PRIORITY 1 // priority to be given to the task, highest priority is 0
12 #define STACK_SIZE 10000 // size of the stack to e used by the new task
13 #define FIFO 0  // first in first out data structure
14 #define FIFO1 1  // for communication with user space
15 #define FIFO2 2
16 #define FIFO3 3
17 #define FIFO4 4
18 #define FACTOR 10/65536 // factor for the voltage output
19 #define TIMESTEP 0.05 // Euler step
20
21 static RT_TASK task; // real-time task
22 int subdevice = 0; // input subdevice
23 int chan = 0; // channel
24 int chan1 = 1;
25 int range = 1; // input range
26 int range1 = 2; // output range
27 int aref = AREF_DIFF; // reference of the device; differential inputs/outputs
28 comedi_t *device; // represent an open Comedi device
29 lsampl_t datab; // represent data values in libcomedi
30 lsampl_t datab1;
31 int pdatab;  // data buffer for writing
32 int pdatab1;
33
34 // Model of a fast-spiking interneuron
35 float mv;  // membrane voltage in mV
```



Die approbierte gedruckte Originalversion dieser Diplomarbeit ist an der TU Wien Bibliothek verfügbar
The approved original version of this thesis is available in print at TU Wien Bibliothek.
TU Bibliothek Your knowledge hub WIEN

```
36 float mvpreA; // presynaptic membrane potential in mV
37 float mvpreB;
38
39 float Iapp; // stimulus in uA/cm^2
40 float INa; // Na+ current
41 float IK; // K+ current
42 float IL; // leak current
43 float Iion; // ionic current
44 float Isyn = 0; // synaptic current
45
46 float ENa = 55; // reversal potential of the Na+ current in mV
47 float EK = -90; // reversal potential of the K+ current in mV
48 float EL = -65; // reversal potential of the leak current in mV
49
50 float gNa = 35; // conductance of the Na+ current in mS/cm^2
51 float gK = 9; // conductance of the K+ current in mS/cm^2
52 float gL = 0.1; // conductance of the leak current in mS/cm^2
53
54 float phi = 3.33; // smaller phi -> IK is slower -> AHP amplitude more negative
55 float Cmem = 1; // membrane capacitance density in uF/cm^2
56
57 float h; // inactivation varible h
58 float n; // activation varible n
59 float minf;
60 float alpham;
61 float alphah;
62 float alphan;
63 float betam;
64 float betah;
65 float betan;
66
67 float value[1000]; // load weights for the synapse
68 float value_pyr[1000];
69 float isyn_pyrA; // synaptic current in uA/cm^2
70 float isyn_pyrB;
71
72 int esyn = 75; // synaptic reversal potential in mV
73 int Vthres = -20; // threshold potential in mV
74 int taui = 10; // tau for inhibitory synapse in msec
75 int taue = 5; // tau for excitatory synapse in msec
76
77 float w_pyrA = 0.01; // weight of the synapse
78 float w_pyrB = 0.01;
```



Die approbierte gedruckte Originalversion dieser Diplomarbeit ist an der TU Wien Bibliothek verfügbar
The approved original version of this thesis is available in print at TU Wien Bibliothek.
TU Bibliothek Your knowledge hub WIEN

```
79  float w_A = 0.01;
80  float w_B = 0.01;
81  float w_BA=0.01;
82  float w_AB=0.01;
83  //wPyr of 0.01 produces 100pA when the input is 2nA/V
84
85  float gsyn_A = 0; // synaptic conductance in mS/cm^2
86  float gsyn_B = 0;
87  float gsyn_pyrA = 0;
88  float gsyn_pyrB = 0;
89  float gsyn_BA = 0;
90  float gsyn_AB = 0;
91
92  int cntAMP_B = 0;  // counter for the amplitude
93  int cntAMP_A = 999;
94  int cntAMP_pyrB = 0;
95  int cntAMP_pyrA = 999;
96  int spkCNT = 1;  // counter for file reading
97  int spkCNT_pyrA = 1;
98  int spkCNT_pyrB = 1;
99
100 float time;  // time stamp
101
102 // Program
103 static void fun(int t)
104 {
105     while (1) {
106         rtf_get(FIFO1, &value, sizeof(value));
107         rtf_get(FIFO2, &value_pyr, sizeof(value_pyr));
108         // get the weights for the synapses from the userspace
109         rtf_get(FIFO3, &Iapp, sizeof(Iapp));
110         // get the stimulus value from the userspace
111         comedi_data_read(device,subdevice,chan1,range,aref,&datab);
112         // read single sample from channel
113         // Comedi device, subdevice, channel, range, analog reference type, data
114         mvpreB=100*((float)datab*FACTOR-5);
115         // converting voltages to samples
116         comedi_data_read(device,subdevice,chan,range,aref,&datab1);
117         mvpreA=100*((float)datab1*FACTOR-5);
118
119         alpham = -0.1*(mv+35)/(exp(-0.1*(mv+35))-1);  // alpha m
120         alphah = 0.07*exp(-(mv+58)/20);  // alpha h
121         alphan = -0.01*(mv+34)/(exp(-0.1*(mv+34))-1);  // alpha n
```



Die approbierte gedruckte Originalversion dieser Diplomarbeit ist an der TU Wien Bibliothek verfügbar
The approved original version of this thesis is available in print at TU Wien Bibliothek.
TU Bibliothek Your knowledge hub WIEN

```
122
123         betam = 4*exp(-(mv+60)/18);   // beta m
124         betah = 1/(exp(-0.1*(mv+28))+1);  // beta h
125         betan = 0.125*exp(-(mv+44)/80);   // beta n
126
127         minf = alpham/( alpham + betam );  // minf
128         h = h + TIMESTEP* phi*(alphah*(1-h) - betah*h); // dh/dt
129         n = n + TIMESTEP* phi*(alphan*(1-n) - betan*n); // dn/dt
130
131         INa = gNa*minf*minf*minf*h*(mv-ENa);  // Na+ current
132         IK = gK*n*n*n*n*(mv-EK);   // K+ current
133         IL = gL*(mv-EL);    // leak current
134
135         Iion = INa + IK + IL;    // ionic current
136
137         //synaptic input to interneuron
138         gsyn_A = gsyn_A*(1-TIMESTEP/taue);  // model of excitatory synapse
139         gsyn_B = gsyn_B*(1-TIMESTEP/taue);
140         gsyn_BA = gsyn_BA*(1-TIMESTEP/taue);  // synaptic current inbetween pyramidal cells
141         gsyn_AB = gsyn_AB*(1-TIMESTEP/taue);
142         w_A=value_pyr[cntAMP_pyrA];   // get synaptic weight
143         w_B=value_pyr[cntAMP_pyrB];
144
145         if (mvpreA > Vthres)    // firing of pyramidal cell A
146         {
147             gsyn_A = gsyn_A + w_A;   // updating synaptic conductance
148             gsyn_AB = gsyn_AB + w_AB;
149             if (spkCNT_pyrA==1) {   // pyramidal cell starts spiking
150                 if (cntAMP_pyrA<1) { cntAMP_pyrA=1000; } // start reading file from beginning
151                 cntAMP_pyrA--;   // reading pyramidal cell file descending
152                 spkCNT_pyrA=0;   // set spike ready to 0
153             }
154         } else if (spkCNT_pyrA==0) { spkCNT_pyrA=1; } // ready for spiking
155
156         if (mvpreB > Vthres)    // firing of pyramidal cell B
157         {
158             gsyn_B = gsyn_B + w_B;
159             gsyn_BA = gsyn_BA + w_BA;
160             if (spkCNT_pyrB==1) {
161                 if (cntAMP_pyrB>999) { cntAMP_pyrB=-1; } // start reading file from the beginning
162                 cntAMP_pyrB++;
163                 spkCNT_pyrB=0;
164             }
```



Die approbierte gedruckte Originalversion dieser Diplomarbeit ist an der TU Wien Bibliothek verfügbar
The approved original version of this thesis is available in print at TU Wien Bibliothek.
TU Bibliothek Your knowledge hub WIEN

```
165         } else if (spkCNT_pyrB==0) { spkCNT_pyrB=1; }
166
167         //-- Cases 1, 2, 3, 8 ----------------------------------------//
168             Isyn = gsyn_A*(mv) + gsyn_B*(mv); //
169         //----------------------------------------------------------//
170
171         //-- Cases 4, 5 ----------------------------------------------//
172         // Isyn = gsyn_A*(mv);   //
173         //----------------------------------------------------------//
174
175         //-- Cases 6, 7 ----------------------------------------------//
176         // Isyn = 0;    //
177         //----------------------------------------------------------//
178
179         // no Esyn (the reversal potential for excitation is generally 0mV)
180         mv = mv + TIMESTEP*(-Iion -Isyn + Iapp);
181         // membrane potential of the fast-spiking interneuron
182
183         //synaptic input to pyramidal cells
184         gsyn_pyrA = gsyn_pyrA*(1-TIMESTEP/taui); // model of inhibitory synapse
185         gsyn_pyrB = gsyn_pyrB*(1-TIMESTEP/taui);
186         w_pyrA=value[cntAMP_A];
187         w_pyrB=value[cntAMP_B];
188         w_BA=value[cntAMP_pyrB];
189         w_AB=value[cntAMP_pyrA];
190
191         if (mv > Vthres)    // firing of fast-spiking interneuron
192         {
193             gsyn_pyrA = gsyn_pyrA + w_pyrA;   // updating synaptic conductance
194             gsyn_pyrB = gsyn_pyrB + w_pyrB;
195             if (spkCNT==1) {    // interneuron starts spiking
196                 if (cntAMP_B>999) { cntAMP_B=-1; }  // Isyn via synapse B
197                 if (cntAMP_A<1) { cntAMP_A=1000; } // Isyn via synapse A
198                 cntAMP_B++;
199                 cntAMP_A--;
200                 spkCNT=0;
201             }
202         } else if (spkCNT==0) { spkCNT=1; }   // ready for spiking
203
204         //-- Cases 1, 2 ----------------------------------------------//
205           isyn_pyrA = gsyn_pyrA*(mvpreA-esyn);   // synaptic current to pyramidal cell A
206           isyn_pyrB = gsyn_pyrB*(mvpreB-esyn);   // synaptic current to pyramidal cell B
207         //----------------------------------------------------------//
```



Die approbierte gedruckte Originalversion dieser Diplomarbeit ist an der TU Wien Bibliothek verfügbar
The approved original version of this thesis is available in print at TU Wien Bibliothek.
TU Bibliothek Your knowledge hub WIEN

```
208
209         //-- Cases 3, 4, 6, 7 ------------------------------------------//
210         // isyn_pyrA = gsyn_pyrA*(mvpreA-esyn) - gsyn_BA*(mvpreA); //
211         // isyn_pyrB = gsyn_pyrB*(mvpreB-esyn);  //
212         //-----------------------------------------------------------------//
213
214         //-- Case 5 ----------------------------------------------------//
215         // isyn_pyrA = -gsyn_BA*(mvpreA);  //
216         // isyn_pyrB = gsyn_pyrB*(mvpreB-esyn);  //
217         //-----------------------------------------------------------------//
218
219         //-- Case 8 ----------------------------------------------------//
220         // isyn_pyrA = gsyn_pyrA*(mvpreA-esyn) - gsyn_BA*(mvpreA); //
221         // isyn_pyrB = gsyn_pyrB*(mvpreB-esyn) - gsyn_AB*(mvpreB); //
222         //-----------------------------------------------------------------//
223
224         pdatab=3.2768*isyn_pyrA+32768;    // converting samples to voltages
225         comedi_data_write(device,1,chan,range1,aref,pdatab); // write single sample to channel
226         // device, subdevice, channel, range, analog reference type, data
227         pdatab1=3.2768*isyn_pyrB+32768;
228         comedi_data_write(device,1,chan1,2,aref,pdatab1);
229
230         rtf_put(FIFO, &mv, sizeof(mv));
231         // put the membrane voltage of the FS interneuron to the userspace
232         time = rt_get_cpu_time_ns();    // get the current time
233         rtf_put(FIFO4, &time, sizeof(time));    // put the time stamp to the userspace
234         rt_task_wait_period();    // wait until next period
235     }
236 }
237
238 int init_module(void)
239 {
240     RTIME tick_period;    // period timer
241     rt_set_periodic_mode();    // set timer mode
242     rt_task_init(&task, fun, 1, STACK_SIZE, TASK_PRIORITY, 1, 0); // create a periodic task
243     // task, task function, pass single integer value data, stack size, task priority, flag, signal
244     rtf_create(FIFO, 8000);    // create a real-time FIFO in kernel space
245     rtf_create(FIFO1, 8000);
246     rtf_create(FIFO2, 8000);
247     rtf_create(FIFO3, 8000);
248     rtf_create(FIFO4, 20000);
249     // start timer and periodic task
250     tick_period = start_rt_timer(nano2count(TICK_PERIOD));
```



Die approbierte gedruckte Originalversion dieser Diplomarbeit ist an der TU Wien Bibliothek verfügbar
The approved original version of this thesis is available in print at TU Wien Bibliothek.
TU Bibliothek Your knowledge hub WIEN

```
251     // convert nanoseconds to internal count units and start timer
252     rt_task_make_periodic(&task, rt_get_time() + tick_period, tick_period);
253     // task gets suitable for periodic execution; task, start time (get the current time), period
254     mv = -64;       // membrane voltage at the beginning in mV
255     h = 0;        // inactivation varible h
256     n = 0;        // activation varible n
257     device=comedi_open("/dev/comedi0");     // open a Comedi device
258     comedi_data_read_hint(device,subdevice,chan,range,aref); // tell driver which channel is the next
259     // device, subdevice, channel, range, analog reference type
260     return 0;
261 }
262
263 void cleanup_module(void)
264 {
265     comedi_data_write(device,1,chan,0,aref,32768);
266     comedi_close(device);      // close a Comedi device
267     stop_rt_timer();       // stop timer
268     rtf_destroy(FIFO);       // close a real-time FIFO in kernel space
269     rtf_destroy(FIFO1);
270     rtf_destroy(FIFO2);
271     rtf_destroy(FIFO3);
272     rtf_destroy(FIFO4);
273     rt_task_delete(&task);      // delete a real-time task
274     return;
275 }
```

Die approbierte gedruckte Originalversion dieser Diplomarbeit ist an der TU Wien Bibliothek verfügbar
The approved original version of this thesis is available in print at TU Wien Bibliothek.

TU WIEN Bibliothek Your knowledge hub
Die approbierte gedruckte Originalversion dieser Diplomarbeit ist an der TU Wien Bibliothek verfügbar
The approved original version of this thesis is available in print at TU Wien Bibliothek.

# Bibliography


Acker, C. D., Kopell, N. and White, J. A. 2003. Synchronization of strongly coupled excitatory neurons: relating network behavior to biophysics. *J. Comput. Neurosci.* 15:71-90.

Andersen, P., Morris, R., Amaral, D., Bliss, T. and O'Keefe, J. 2006. The Hippocampus Book. *Oxford University Press.*

Axmacher, N., Mormann, F., Fernández, G., Elger, C. E. and Fell, J. 2006. Memory formation by neuronal synchronization. *Brain Res.* 52:170-182.

Bartos, M., Vida, I., Frotscher, M., Meyer, A., Monyer, H., Geiger, J. R. P. and Jonas, P. 2002. Fast Synaptic Inhibition Promotes Synchronized Gamma Oscillations in Hippocampal Interneuron Networks. *PNAS.* 99:13222-13227.

Bland, B. H. and Oddie, S. D. 2001. Theta band oscillation and synchrony in the hippocampal formation and associated structures: the case for its role in sensorimotor integration. *Behavioural Brain Research.* 127:119-136.

Börgers, C. and Kopell, N. 2003. Synchronization in networks of excitatory and inhibitory Neurons with sparse, random connectivity. *Neural Comput.* 15:509-538.

Buzsáki, G. 1984. Feed-forward inhibition in the hippocampal formation. *Prog. Neurobiol.* 22:131-153.

Buzsáki, G. 1989. Two-stage model of memory trace formation: a role for „noisy"brain states. *Neuroscience.* 31:551-570.

Buzsáki, G., Geisler, C., Henze, D. A. and Wang, X.-J. 2004. Interneuron Diversity series: Circuit complexity and axon wiring economy of cortical interneurons. *Trends Neurosci.* 27:186-193.

Cardin, J. A., Carlén, M., Meletis, K., Knoblich, U., Zhang, F., Deisseroth, K., Tsai, L. H. and Moore, C. I. 2009. Driving fast-spiking cells induces gamma rhythm and controls sensory responses. *Nature.* 459:663-667.

Chen, K., Aradi, I., Santhakumar, V. and Soltesz, I. 2002. H-channels in epilepsy: new targets for seizure control? *Trends Pharmacol. Sci.* 23:552-557.




Die approbierte gedruckte Originalversion dieser Diplomarbeit ist an der TU Wien Bibliothek verfügbar
The approved original version of this thesis is available in print at TU Wien Bibliothek.
TU Bibliothek Your knowledge hub WIEN

Cobb, S. R., Buhl, E. H., Halasy, K., Paulsen, O. and Somogyi, P. 1995. Synchronization of neuronal activity in hippocampus by individual GABAergic interneurons. *Nature.* 378:75-78.

Csicsvari, J., Jamieson, B., Wise, K. D. and Buzsáki, G. 2003. Mechanisms of gamma oscillations in the hippocampus of the behaving rat. *Neuron.* 37:311-322.

Cunningham, M. O., Davies, C. H., Buhl, E. H., Kopell, N. and Whittington, M. A. 2003. Gamma oscillations induced by kainate receptor activation in the entorhinal cortex in vitro. *J. Neurosci.* 23:9761-9769.

Cunningham, M. O., Halliday, D. M., Davies, C. H., Traub, R. D., Buhl, E. H. and Whittington, M. A. 2004. Coexistence of gamma and high-frequency oscillations in rat medial entorhinal cortex in vitro. *J. Physiol.* 559:347-353.

Cutsuridis, V., Graham, B., Cobb, S. and Vida, I. 2010. Hippocampal Microcircuits - A Computational Modeler's Resource Book. *Springer.*

Deuchars, J. and Thomson, A. M. 2001. CA1 pyramid-pyramid connections in rat hippocampus in vitro: dual intracellular recordings with biocytin filling. *Neuroscience.* 74:1009-1018.

Dorval, A. D., Christini, D. J. and White, J. A. 2001. Real-Time linux dynamic clamp: a fast and flexible way to construct virtual ion channels in living cells. *Ann. Biomed. Eng.* 29:897-907.

Fisahn, A., Pike, F. G., Buhl, E. H. and Paulsen, O. 1998. Cholinergic induction of network oscillations at 40 Hz in the hippocampus in vitro. *Nature.* 394:186-189.

Fisahn, A., Heinemann, S. F. and McBain, C. J. 2005. The Kainate Receptor Subunit GluR6 Mediates Metabotropic Regulation of the Slow and Medium AHP Currents in Mouse Hippocampal Neurones. *J. Physiol.* 562:199-203.

Freund, T. F. and Buzsáki, G. 1996. Interneurons of the hippocampus. *Hippocampus.* 6:347-470.

Fries, P., Nikolić, D. and Singer, W. 2007. The gamma cycle. *Trends in Neurosciences.* 30:309-316.

Fries, P. 2009. The Model- and the Data-Gamma. *Neuron.* 64:601-602.

Geisler, C., Brunel, N. and Wang, X.-J. 2005. Contributions of intrinsic membrane dynamics to fast network oscillations with irregular neuronal discharges. *J. Neurophysiol.* 94:4344-4361.

George, M. S., Abbott, L. F. and Siegelbaum, S. A. 2009. HCN hyperpolarization-activated cation channels inhibit EPSPs by interactions with M-type K+ channels. *Nat. Neurosci.* 12:577-584.

Grillner, S. and Graybiel, A. M. 2006. Microcircuits: The interface between neurons and the global brain function. *MIT Press.* 2006



Die approbierte gedruckte Originalversion dieser Diplomarbeit ist an der TU Wien Bibliothek verfügbar
The approved original version of this thesis is available in print at TU Wien Bibliothek.
TU Bibliothek Your knowledge hub WIEN

Gulyás, A. I., Miles, R., Sík, A., Tóth, K., Tamamaki, N. and Freund, T. F. 1993. Hippocampal pyramidal cells excite inhibitory neurons through a single release site. *Nature.* 366:683-687.

Hájos, N., Pálhalmi, J., Mann, E. O., Németh, B., Paulsen, O. and Freund, T. F. 2004. Spike Timing of Distinct Types of GABAergic Interneuron During Hippocampal Gamma Oscillations In Vitro. *J. Neurosci.* 24: 9127-9137.

Hansel, D., Mato, G. and Meunier, C. 1995. Synchrony in Excitatory Neural Networks. *Neural Computation.* 7:307-337.

Hodgkin, A. L. and Huxley, A. F. 1952. A quantitative description of membrane current and its application to conduction and excitation in nerve. *J. Physiol.* 117:500-544.

Klausberger, T. and Somogyi, P. 2008. Neuronal diversity and temporal dynamics: the unity of hippocampal circuit operations. *Science.* 321:53-57.

Kopell, N., Ermentrout, G. B., Whittington, M. A. and Traub, R. D. 2000. Gamma Rhythms and Beta Rhythms Have Different Synchronization Properties. *PNAS.* 97:1867-1872.

Kopell, N., Börgers, C., Pervouchine, D., Malerba, P. and Tort, A. 2010. Gamma and Theta Rhythms in Biophysical Models of Hippocampal Circuits. *Hippocampal Microcircuits.* 423-457.

Kuramoto, Y. 1991. Collective synchronization of pulse-coupled oscillators and excitable units. *Nonlinear Phenomena.* 50:15-30.

Leão, R. N., Svahn, K., Berntson, A. and Walmsley, B. 2005. Hyperpolarization-activated (I) currents in auditory brainstem neurons of normal and congenitally deaf mice. *Eur. J. Neurosci.* 22:147-157.

Leão, R. N., Tan, H. M. and Fisahn, A. 2009. Kv7/KCNQ Channels Control Action Potential Phasing of Pyramidal Neurons During Hippocampal Gamma Oscillations In Vitro. *J. Neurosci.* 29:13353-13364.

LeBeau, F. E. N., Traub, R. D., Monyer, H., Whittington, M. A. and Buhl, E. H. 2003. The role of electrical signaling via gap junctions in the generation of fast network oscillations. *Brain Research Bulletin.* 62:3-13.

Li, X. G., Somogyi, P., Ylinen, A. and Buzsáki, G. 1994. The hippocampal CA3 network: an in vivo intracellular labeling study. *J. Comp. Neurol.* 339:181-208.

Losonczy, A., Somogyi, P. and Nusser, Z. 2003. Reduction of excitatory postsynaptic responses by persistently active metabotropic glutamate receptors in the hippocampus. *J. Neurophysiol.* 89:1910-1919.

Lytton, W. W. and Sejnowski, T. J. 1991. Simulations of cortical pyramidal neurons synchronized by inhibitory interneurons. *J. Neurophysiol.* 66:1059–1079.



Die approbierte gedruckte Originalversion dieser Diplomarbeit ist an der TU Wien Bibliothek verfügbar
The approved original version of this thesis is available in print at TU Wien Bibliothek.
TU Bibliothek Your knowledge hub WIEN

Maccaferri, G., David, J., Roberts, B., Szucs, P., Cottingham, C. A. and Somogyi, P. 2000. Cell surface domain specific postsynaptic currents evoked by identified GABAergic neurones in rat hippocampus in vitro. *J. Physiol.* 524.1:91-116.

Maex, R. and De Schutter, E. 1998. Synchronization of Golgi and Granule Cell Firing in a Detailed Network Model of the Cerebellar Granule Cell Layer. *J Neurophysiol.* 80:2521-2537.

Magee, J. C. 2001. Dendritic mechanisms of phase precession in hippocampal CA1 pyramidal neurons. *J. Neurophysiol.* 86:528-532.

Mann, E. O. and Paulsen, O. 2007. Role of GABAergic inhibition in hippocampal network oscillations. *Trends in Neurosciences.* 30:343-349.

Marín-Padilla M. 1998. Cajal–Retzius cells and the development of the neocortex. *Trends in Neurosciences.* 21:64-71.

Megías, M., Emri, Z., Freund, T. F. and Gulyás, A. I. 2001. Total number and distribution of inhibitory and excitatory synapses on hippocampal CA1 pyramidal cells. *Neurosciences.* 102:527-540 .

Mehta, M. R. 2005. Role of rhythms in facilitating short-term memory. *Neuron.* 45:7-9.

Miles, R., Tóth, K., Gulyás, A. I., Hájos, N. and Freund, T. F. 1996. Differences between somatic and dendritic inhibition in the hippocampus. *Neuron.* 16:815–823 .

Netoff, T. I., Banks, M. I., Dorval, A. D., Acker, C. D., Haas, J. S., Kopell, N. and White, J. A. 2005. Synchronization in Hybrid Neuronal Networks of the Hippocampal Formation. *J. Neurophysiol.* 93:1197-1208.

Neymotin, S. A., Lazarewicz, M. T., Sherif, M., Contreras, D., Finkel, L. H. and Lytton, W. W. 2011. Ketamine Disrupts Theta Modulation of Gamma in a Computer Model of Hippocampus. *J. Neurosci.* 31:11733-11743.

Olufsen, M. S., Whittington, M. A., Camperi, M. and Kopell, N. 2003. New roles for the gamma rhythm: population tuning and preprocessing for the Beta rhythm. *J. Comput. Neurosci.* 14:33-54.

Oren, I. and Kullmann, D. M. 2012. Mapping out hippocampal inhibition. Nature Neuroscience. *Journal.* 15:346-347.

Pálhalmi, J., Paulsen, O., Freund, T. F. and Hájos, N. 2004. Distinct properties of carbachol- and DHPG-induced network oscillations in hippocampal slices. *Neuropharmacology.* 47:381-389.

Purves, D., Augustine, G. J., Fitzpatrick, D., Hall, W. C., LaMantia, A.-S., McNamara, J. O., and White L. E. 2004. Neuroscience, Fourth Edition. *Sinauer Associates.*

Robinson, H. P. and Kawai, N. 1993. Injection of digitally synthesized synaptic conductance transients to measure the integrative properties of neurons. *J. Neurosci. Methods.* 49:157-165.



Die approbierte gedruckte Originalversion dieser Diplomarbeit ist an der TU Wien Bibliothek verfügbar
The approved original version of this thesis is available in print at TU Wien Bibliothek.
TU Bibliothek Your knowledge hub WIEN

Rotstein, H. G., Pervouchine, D. D., Acker, C. D., Gillies, M. J., White, J. A., Buhl, E. H., Whittington, M. A. and Kopell, N. 2005. Slow and fast inhibition and an H-current interact to create a theta rhythm in a model of CA1 interneuron network. *J. Neurophysiol.* 94:1509-1518.

Santoro, B. and Tibbs, G. R. 1999. The HCN gene family: molecular basis of the hyperpolarization-activated pacemaker channels. *Ann. N. Y. Acad. Sci.* 868:741-764.

Santoro, B., Chen, S., Luthi, A., Pavlidis, P., Shumyatsky, G. P., Tibbs, G. R. and Siegelbaum, S. A. 2000. Molecular and functional heterogeneity of hyperpolarization-activated pacemaker channels in the mouse CNS. *J. Neurosci.* 20:5264-5275.

Shah, M. M., Anderson, A. E., Leung, V., Lin, X. and Johnston, D. 2004. Seizure-induced plasticity of h channels in entorhinal cortical layer III pyramidal neurons. *Neuron.* 44:495-508.

Sharp, A. A., O'Neil, M. B., Abbott, L. F. and Marder, E. 1993. The dynamic clamp: artificial conductances in biological neurons. *Trends Neurosci.* 16:389-394.

Sharp, A. A., O'Neil, M. B., Abbott, L. F. and Marder, E. 1993. Dynamic Clamp: Computer-Generated Conductances in Real Neurons. *J. Neurophysiol.* 69:992-995.

Sik, A., Penttonen, M., Ylinen, A. and Buzsáki, G. 1995. Hippocampal CA1 Interneurons: An in Vivo Intracellular Labeling Study. *J. Neurosci.* 15:6651-6665.

Sommer, F. T. and Wennekers, T. 2001. Associative memory in networks of spiking neurons. *Neural Networks.* 14:825-834.

Somogyi, P. and Klausberger, T. 2005. Defined Types of Cortical Interneurone Structure Space and Spike Timing in the Hippocampus. *J. Physiol.* 562:9-26.

Spruston, N. 2008. Pyramidal neurons: dendritic structure and synaptic integration. *Nature Reviews Neuroscience.* 9:206-221.

Tort, A. B. L., Rotstein, H. G., Dugladze, T., Gloveli, T. and Kopell, N. J. 2007. On the Formation of Gamma-Coherent Cell Assemblies by Oriens Lacunosum-Moleculare Interneurons in the Hippocampus. *PNAS.* 104:13490-13495.

Traub, R. D., Bibbig, A., Fisahn, A., LeBeau, F. E., Whittington, M.A. and Buhl, E.H. 2000. A model of gamma-frequency network oscillations induced in the rat CA3 region by carbachol in vitro. *Eur. J. Neurosci.* 12:4093-4106.

Traub, R. D., Whittington, M. A., Buhl, E. H., LeBeau, F. E., Bibbig, A., Boyd, S., Cross, H. and Baldeweg. T. 2001. A possible role for gap junctions in generation of very fast EEG oscillations preceding the onset of, and perhaps initiating, seizures. *Epilepsia.* 42:153-170.

Traub, R. D., Bibbig, A., LeBeau, F. E. N., Buhl, E. H. and Whittington, M. A. 2004. Cellular mechanisms of neuronal population oscillations in the hippocampus in vitro. *Annu. Rev. Neurosci.* 27:247-278.



Die approbierte gedruckte Originalversion dieser Diplomarbeit ist an der TU Wien Bibliothek verfügbar
The approved original version of this thesis is available in print at TU Wien Bibliothek.
TU Bibliothek Your knowledge hub WIEN

Van Vreeswijk, C., Abbott, L. F. and Ermentrout, G. B. Traub, R. D., Bibbig, A., LeBeau, F. E. N., Buhl, E. H. and Whittington, M. A. 1994. When inhibition not excitation synchronizes neural firing. *J. Comput. Neurosci.* 1:313-321.

Wang, S., Chandrasekaran, L., Fernandez, F. R., White, J. R. and Canavier, C. C. 2012. Short Conduction Delays Cause Inhibition Rather than Excitation to Favor Synchrony in Hybrid Neuronal Networks of the Entorhinal Cortex. *PLoS Comput. Biol.* 1:e1002306.

Wang, X.-J. and Buzsáki, G. 1996. Gamma Oscillation by Synaptic Inhibition in a Hippocampal Interneuronal Network Model. *J. Neurosci.* 16:6402-6413.

Whittington, M. A., Traub, R. D. and Jefferys, J. G. R. 1995. Synchronized oscillations in interneuron networks driven by metabotropic glutamate receptor activation. *Nature.* 373:612-615.

Whittington, M. A., Traub, R. D., Faulkner, H. J., Stanford, I. M. and Jefferys, J. G. 1997. Recurrent excitatory postsynaptic potentials induced by synchronized fast cortical oscillations. *Proc. Natl. Acad. Sci. U.S.A.* 94:12198-12203.

Allen Institute for Brain Science. http://www.brain-map.org/. Accessed: 2012-05-20

Comparative Mammalian Brain Collections. http://www.brainmuseum.org/. Accessed: 2012-05-20



Die approbierte gedruckte Originalversion dieser Diplomarbeit ist an der TU Wien Bibliothek verfügbar
The approved original version of this thesis is available in print at TU Wien Bibliothek.
TU Bibliothek Your knowledge hub WIEN